E. WOLF, PROGRESS IN OPTICS XXIX

II

ENHANCED BACKSCATTERING IN OPTICS

BY

YU. N. BARABANENKOV

Center for Surface and Vacuum Studies
117313 Moscow, USSR

YU. A. KRAVTSOV

Academy of Sciences of the USSR
General Physics Institute, GROT
Vavilov St. 38
117942 Moscow, USSR

V. D. OZRIN

Academy of Sciences of the USSR
Nuclear Safety Institute
B. Tulskaya 52
113191 Moscow, USSR

A. I. SAICHEV

Lobachevski State University
603600 Nizhni Novgorod, USSR

CONTENTS

PAGE

§ 1. INTRODUCTION 67

§ 2. ENHANCED BACKSCATTER FROM SOLIDS IMMERSED IN A TURBULENT MEDIUM 69

§ 3. ENHANCED BACKSCATTERING BY A RANDOM MEDIUM 123

§ 4. MULTIPATH COHERENT EFFECTS IN SCATTERING FROM A LIMITED CLUSTER OF SCATTERERS 168

§ 5. ENHANCED BACKSCATTERING BY ROUGH SURFACES 183

§ 6. RELATED EFFECTS IN ALLIED FIELDS OF PHYSICS . 186

§ 7. CONCLUSION 189

ACKNOWLEDGEMENT 190

REFERENCES 190

§ 1. Introduction

Propagation of light in a turbulent atmosphere or another random medium gives rise to a variety of fluctuation effects caused by the random inhomogeneities in the medium. As a rule, these effects degrade the radiation by corrupting its coherence, broadening the beam, and decreasing the intensity.

In the last two decades, a qualitatively new class of fluctuation effects has been observed, caused by the fine coherence effects that arise in a double passage of waves through the same inhomogeneities of the medium. These effects result in some ordering of the scattered radiation rather than its degradation.

The manifestation of coherent effects in multiple scattering has been suggested by WATSON [1969] with reference to a private communication from Ruffine. The Ruffine–Watson coherence effects arise in the multiple scattering of a wave from a large number of discrete scatterers. We shall refer to this class of phenomena as (multipath) coherent effects. According to Watson and Ruffine, to any closed scattering path ($Os_1s_2, \ldots s_nO$ in fig. 1.1a) connecting the source at point O with the receiver placed at the same point O there corresponds an opposite path $Os_n \ldots s_2s_1O$, such that the fields in the direct path, $u_{O12\ldots nO}$, and reverse path, $u_{On\ldots 21O}$, are coherent for arbitrarily located scattering centers $s_1, s_2, \ldots, s_n$. When the source O and the receiver O′ are separated (fig. 1.1b), the fields $u_{O12\ldots nO'}$ and $u_{On\ldots 21O'}$ are no longer identical and lose coherence for sufficiently distant O and O′.

Watson treats points $s_1s_2 \ldots s_n$ as centers of infinitesimal elements of the random medium, which are summarized in integrating over the entire volume of the medium. This line of reasoning has been continued by DE WOLF [1971], who applied it to the description of waves backscattered from small-scale inhomogeneities of a turbulent medium. Although this effect proved to be exceedingly weak in a turbulent medium, de Wolfs' theory has served as a jumping-off place for considering a more realistic problem of backscattering from solids embedded in such media (BELENKII and MIRONOV [1972], VINOGRADOV, KRAVTSOV and TATARSKII [1973]).

This effect is observed as a higher intensity of a wave scattered strictly backwards in a turbulent medium rather than that of a wave backscattered in

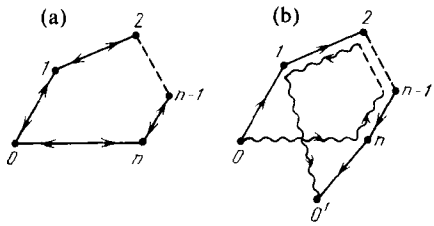

Fig. 1.1. (a) When the locations of the transmitter and receiver coincide, the forward and reverse scattering paths are identical and the respective fields are coherent. (b) Separation of the transmitter and receiver breaks down the coherence between the paths $Os_1s_2 \dots s_nO'$ and $Os_n \dots s_2s_1O'$.

a homogeneous medium. This was the first of a series of effects in which a random medium produced an enhanced rather than a degraded intensity.

BARABANENKOV [1973, 1975] has interpreted the coherent paths in a medium with small-scale inhomogeneities by means of scattering diagrams. When the point of observation, O′, is brought into the location O of the source, the contribution of cyclic diagrams becomes equal to that of ladder diagrams; therefore, the intensity peak scattered backwards by a random inhomogeneous medium is about twice as large as the intensity of backscatter. Cyclic diagrams have proved to be a very useful interpretation tool that has been widely accepted for the analysis of enhancement in multiple scattering of waves.

More recently, the effect of backscatter enhancement has been observed experimently by KUGA and ISHIMARU [1984], WOLF and MARET [1985], and some other workers. It has been reported under the name of weak localization, borrowed from the theory of electron scattering in metals. It is worth noting that in metals the weak-localization effect has a very small magnitude because of the strong Coulomb interaction of electrons. This effect is stronger for photons, which do not interact with one another, and it leads to a marked enhancement of backscattering.

In one-dimensional, random-inhomogeneous media, coherent effects are of major importance for propagation of waves and lead to phenomena similar to the strong-localization regime of electrons in solids predicted by ANDERSON [1958]. Specifically, GAZARYAN [1969] and other workers (see, e.g., KLYATSKIN [1975]) have found that the transparency of a one-dimensional, randomly inhomogeneous slab falls off exponentially with thickness in much the same way as the wave function of electrons does under strong localization, whereas the phenomenological transport theory predicts a much weaker power law.

The effects of backscatter enhancement and weak localization head the list of phenomena in which coherent paths of the Watson–Ruffine type are essential. In this survey we intend to describe multiple new manifestations of coherent effects in backscattering. These include the effects of long-distance correlations, the partial reversal of the phase front in a random medium, the magic cap effect, antispecular scattering by very rough random surfaces, and backscattering involving surface waves.

This survey will replace our previous review papers (KRAVTSOV and SAICHEV [1982b, 1985]) and a recent monograph by BANAKH and MIRONOV [1987] on lidar sounding of a turbulent atmosphere, which unfortunately have become obsolete and need to be updated. We hope that this publication will be useful not only for researchers in optics but also for workers in other fields of wave physics. We would like to use it to acquaint researchers in the West with relevant studies made in the Soviet Union and not known to our western colleagues. We became aware of the need for updated information on the subject during the Tallinn workshop in 1988, which was organized by V. I. Tatarskii and A. Ishimaru. Personal contacts in this workshop stimulated us to prepare this review.

§ 2. Enhanced Backscatter from Solids Immersed in a Turbulent Medium

2.1. ABSOLUTE EFFECT OF ENHANCED BACKSCATTER: A POINT TRANSMITTER AND A POINT SCATTERER IN A TURBULENT MEDIUM

2.1.1. *Pure effect of enhanced backscatter*

Consider monochromatic waves propagating in a medium with dielectric constant $\varepsilon = 1 + \tilde{\varepsilon}$. Assume that the inhomogeneities are weak enough, i.e., $|\tilde{\varepsilon}| \ll 1$, statistically uniform and isotropic, and the characteristic scale l_ε of inhomogeneities is large compared with the wavelength λ, i.e., $l_\varepsilon \gg \lambda$. These conditions are typical of light waves propagating in a turbulent atmosphere. In such a medium, scattering occurs predominantly in the direction of propagation. Therefore, a description of such waves may be based on a scalar approximation.

An optical wave backscattered from solids immersed in a medium with large-scale inhomogeneities passes through the same inhomogeneities which it has passed through in the forward direction (fig. 2.1). The double passage of a wave through the same inhomogeneities gives rise to the effect of backscatter enhancement (BSE). This effect occurs in media whose inhomogeneities

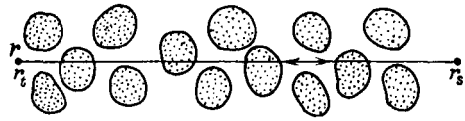

Fig. 2.1. For a point of observation r placed near the transmitter r_t, the scattered radiation travels back through the same inhomogeneities through which the forward wave has passed.

remain virtually unchanged during the wave travelling from the transmitter to the scatterer and back. The effect of time-dependent variations of the inhomogeneities upon the field of the reflected wave will be discussed here; at the moment we shall assume that they are time-invariant, i.e., $\tilde{\varepsilon} = \tilde{\varepsilon}(r)$. In this case the Green function $G(r_1, r_2)$ describing the field of a scalar monochromatic wave obeys the path reciprocity theorem

$$G(r_1, r_2) = G(r_2, r_1)\,. \tag{2.1}$$

This relationship is of principal significance in describing the BSE and other effects of double passage of waves.

Let a point transmitter at point $r = r_t$ produce a primary field $u(r) = G(r_t, r)$. When this wave is incident on a point scatterer at point r_s, it gives rise to the scattered field

$$u_s(r) = fG(r_t, r_s)\, G(r_s, r)\,,$$

where f is the amplitude of scattering. Thus, from eq. (2.1),

$$u_s(r) = fG(r_s, r_t)\, G(r_s, r)\,.$$

At an arbitrary point r the intensity of the scattered field is

$$I_s(r) = \sigma I(r_s, r_t)\, I(r_s, r)\,, \tag{2.2}$$

where $\sigma = |f|^2$ is the scattering cross section in vacuum, and $I(r_s, r)$ is the intensity of a point source at r_s observed at point r,

$$I(r_s, r) = |G(r_s, r)|^2\,.$$

We normalize the intensity $I_s(r)$ to the intensity $I_s^0(r)$ of the scattered wave in a homogeneous medium,

$$I_s^0(r) = \sigma I_0(|r_t - r_s|)\, I_0(|r - r_s|)\,,$$

and obtain

$$\begin{aligned} J_s(r) &= I_s(r)/I_s^0(r) \\ &= J(r_s, r_t)\, J(r_s, r)\,, \end{aligned} \tag{2.3}$$

where $J(\boldsymbol{r}_s, \boldsymbol{r}) = I(\boldsymbol{r}_s, \boldsymbol{r})/I_0(|\boldsymbol{r} - \boldsymbol{r}_s|)$ is the relative intensity of the wave emitted from the location of the scatterer.

The effect of enhanced backscattering can be derived from elementary considerations. We note that from the conservation of full flux of energy for the average intensity of a wave emitted by a point isotropic source, it follows that $\langle I(\boldsymbol{r}_s, \boldsymbol{r})\rangle = I_0(|\boldsymbol{r} - \boldsymbol{r}_s|)$, so that

$$\langle J(\boldsymbol{r}_s, \boldsymbol{r})\rangle = 1 . \tag{2.4}$$

From eq. (2.3) the average relative intensity of a backscattered wave observed at the location of the transmitter, $\boldsymbol{r} = \boldsymbol{r}_t$, is

$$\langle J_s(\boldsymbol{r}_t)\rangle = \langle J^2(\boldsymbol{r}_s, \boldsymbol{r}_t)\rangle .$$

The mean square, i.e., $\langle J^2(\boldsymbol{r}_s, \boldsymbol{r}_t)\rangle$, always exceeds the square of the mean, i.e., $\langle J(\boldsymbol{r}_s, \boldsymbol{r}_t)\rangle^2$, which is unity in view of eq. (2.4). Therefore, the backscatter enhancement factor K_{bsc} is always larger than unity,

$$\begin{aligned} K_{bsc} &= I_s(\boldsymbol{r}_t)/I_s^0(\boldsymbol{r}_t) \\ &= \langle J_s(\boldsymbol{r}_t)\rangle = \langle J^2(\boldsymbol{r}_s, \boldsymbol{r}_t)\rangle > \langle J(\boldsymbol{r}_s, \boldsymbol{r}_t)\rangle^2 = 1 . \end{aligned} \tag{2.5}$$

For a turbulent medium the BSE effect was first predicted by BELENKII and MIRONOV [1972] and VINOGRADOV, KRAVTSOV and TATARSKII [1973]. A typical dependence of K upon the distance between the transmitter and scatterer in a turbulent medium is given in fig. 2.2 with three regions indicated for weak, strong, and saturated fluctuations of intensity. Mechanisms leading to these regions have been discussed by ISHIMARU [1978], RYTOV, KRAVTSOV and TATARSKII [1989a,b], YAKUSHKIN [1985], BANAKH and MIRONOV [1987], and MARTIN and FLATTE [1988]. As $L = |\boldsymbol{r}_s - \boldsymbol{r}_t|$ tends to infinity, the enhancement factor asymptotically approaches $K(\infty) = 2$, and in the region of focusing K can somewhat exceed this value.

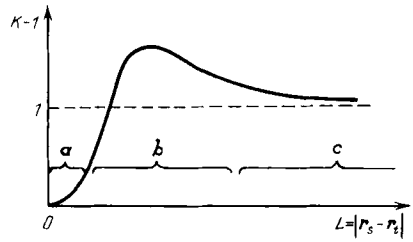

Fig. 2.2. Dependence of the backscattering enhancement factor $K_{bsc} = K(\boldsymbol{r}_t, \boldsymbol{r}_s)$ on the distance between the transmitter and scatterer in a turbulent medium. (a) Region of weak fluctuations of intensity; (b) region of strong fluctuations caused by random focusings; (c) region of saturated fluctuations.

2.1.2. *A phase screen*

Random inhomogeneities of a medium inducing the fluctuations in intensity should not necessarily fill all the path from source to scatterer. They may fill, e.g., a narrow layer in this path. The effect of this layer on a wave can be described by the phase-screen approximation (VINOGRADOV, KRAVTSOV and TATARSKII [1973]). Fluctuations in the intensity of plane waves having passed through a random phase screen distorting the phase of a passing wave have been studied by SALPETER [1967], ALIMOV and ERUKHIMOV [1973], and SHISHOV [1974]. A recalculation of these results for the case of spherical waves is straightforward (ISHIMARU [1978]). If a point scatterer is in the focusing region of a wave passing through the screen, the enhancement factor is calculated to be considerably above the asymptotic value $K = 2$ characteristic of a medium with three-dimensional inhomogeneities. A rough estimate for this case may be obtained as $K \approx \ln \sigma_\varphi^2$, where σ_φ^2 is the variance of the phase distortions caused by the screen.

2.1.3. *Spatial redistribution of the scattered intensity*

Enhancement of average backscatter intensity does not contradict the conservation laws because it is accompanied by the reduction of scattering sideways. In other words, a spatial redistribution of the average intensity takes place.

Consider the average relative intensity $\langle J_s(\boldsymbol{r}) \rangle$ of a scattered wave at points $\boldsymbol{r} = \boldsymbol{r}_t + \boldsymbol{\rho}$ of a sphere with radius $L = |\boldsymbol{r}_t - \boldsymbol{r}_s|$ centered on a scatterer, as shown in fig. 2.3a. By definition, $\langle J_s(\boldsymbol{r}) \rangle$ represents the enhancement factor en route $\boldsymbol{r}_t \to \boldsymbol{r}_s \to \boldsymbol{r} = \boldsymbol{r}_t + \boldsymbol{\rho}$, so that on the sphere we have

$$K(\boldsymbol{\rho}, L) = \langle J_s(\boldsymbol{r}) \rangle$$
$$= \langle J(\boldsymbol{r}_s, \boldsymbol{r}_t) J(\boldsymbol{r}_s, \boldsymbol{r}) \rangle . \tag{2.6}$$

From the conservation of the full flux of energy of the scattered wave it follows that the average of $\langle J_s \rangle = K$ over the sphere is

$$(4\pi L^2)^{-1} \oint K(\boldsymbol{\rho}, L)\, \mathrm{d}s = 1 . \tag{2.7}$$

For a wave scattered strictly in the backward direction, $K(0, L) = K_{bsc} > 1$; therefore, at some distance from the transmitter $K - 1$ must be negative. A typical plot of $K(\boldsymbol{\rho}, L)$ as a function of the angle θ reckoned from the specular direction is shown in fig. 2.3b.

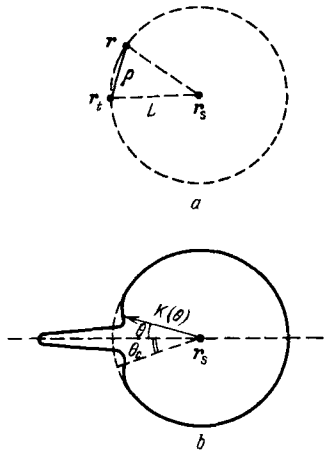

Fig. 2.3. (a) Placing a point of observation r on the sphere of radius $L = |r_t - r_s|$; (b) profile of the enhancement factor K as a function of the angle θ.

This redistribution of intensity of scattered radiation is no longer evident for $\rho > \rho_c$, where $\rho_c \approx \theta_c L$ is the distance from source to detector at which the emitted and scattered waves actually propagate through different, statistically independent inhomogeneities of the medium. In fact, ρ_c is the intensity transverse correlation radius of a wave that has travelled a distance from r_s to r_t in one direction. This can be readily verified by representing the "single-passage" relative intensity J in the form $\langle J \rangle + \Delta J = 1 + \Delta J$, where $\Delta J = J - \langle J \rangle$ represents fluctuations of the relative intensity. Now, the enhancement factor (2.6) can be written as

$$K(\rho, L) = 1 + B_{\Delta J}(\rho, L), \tag{2.8}$$

where

$$B_{\Delta J}(\rho, L) = \langle \Delta J(r_s, r_t)\, \Delta J(r_s, r_t + \rho) \rangle$$

is the correlation function of fluctuations ΔJ at the adjacent points r_t and $r_t + \rho$ for a single passage of a wave from r_s to r_t.

Because of the small angular dimensions of the backscatter cone, the photodetector that will record the backscatter-enhancement effect should be of small angular dimensions. If the detector aperture is larger than ρ_c, the intensity averaged over the aperture will be almost equal to the intensity that would be obtained in the absence of inhomogeneities. This averaging effect of the detector aperture has been noted by VINOGRADOV, KRAVTSOV and TATARSKII [1973].

2.1.4. *Backscatter enhancement under weak fluctuations of intensity*

If the scatterer is in the region of weak fluctuations of the intensity of the emitted wave, Rytov's approximation may be used for analysis of backscattering enhancement (see, e.g., TATARSKII [1967], ISHIMARU [1978], RYTOV, KRAVTSOV and TATARSKII [1989a,b]). In this approximation,

$$B_{\Delta J}(\boldsymbol{\rho}, L) = 4\pi^2 k^2 L \int_0^1 \eta^2 \, \mathrm{d}\eta \int_0^\infty \varkappa \, \mathrm{d}\varkappa J_0(\varkappa\rho) \times \sin^2[L(1-\eta)\varkappa^2/2k\eta] \, \Phi_\varepsilon(\kappa\eta), \tag{2.9}$$

where $k = 2\pi/\lambda$ is the wavenumber and $\Phi_\varepsilon(\varkappa)$ the spatial spectrum of permittivity fluctuations.

In media with single-scale inhomogeneities the correlation of the intensity fluctuations breaks down at $\rho_c \approx \theta_c L \sim l_\varepsilon$. Therefore, a redistribution of the average backscatter intensity occurs within a cone with half-included angle $\theta_c \approx l_\varepsilon/L$. In a turbulent medium the correlation radius of level fluctuations is given by the Fresnel scale $\rho_f \approx (\lambda L)^{1/2}$. Quantitative data on enhanced backscattering under various illuminating conditions and for different scatterers may be found in the monograph by BANAKH and MIRONOV [1987].

2.1.5. *Saturated fluctuations of intensity*

If we assume that the scatterer is in the region of saturated fluctuations of the intensity of an emitted wave, the field of a wave incident on the scatterer is the sum of a large number of statistically independent waves passing from transmitter to scatterer through different paths. In light of the central limit theorem, near the scatterer the field of the emitted wave will be asymptotically Gaussian (ZAVOROTNYI, KLYATSKIN and TATARSKII [1977], DASHEN [1979], YAKUSHKIN [1978]). Its statistical properties are completely defined by the average $\langle G(\boldsymbol{r}_s, \boldsymbol{r})\rangle = 0$ and the coherence function $\Gamma(\boldsymbol{\rho}, L) = \langle G(\boldsymbol{r}_s, \boldsymbol{r}) G^*(\boldsymbol{r}_s, \boldsymbol{r}_t)\rangle$ with $\Gamma(0, L) = \Gamma_0(L)$.

The principal physical characteristic of a wave in the saturation regime is the radius of coherence $\rho_c(L)$ of the spherical wave, which is defined by $|\Gamma(\rho_c, L)|/I_0(L) \approx 1/e$. A saturability condition of intensity fluctuations of a wave that has travelled a distance L (ZAVOROTNYI, KLYATSKIN and TATARSKII [1977]) has the form

$$\gamma(L) \equiv L/k\rho_c^2(L) \gg 1, \tag{2.10}$$

which allows for a simple geometrical interpretation. The quantity $\gamma(L)$ is the

ratio of the characteristic side shift of rays (in the random inhomogeneous medium and in the homogeneous medium)

$$\sigma_\rho(L) = L/k\rho_c(L) \tag{2.11}$$

to the coherence radius $\rho_c(L)$. In agreement with eq. (2.10) the intensity fluctuations become saturated when the side shift of the rays exceeds ρ_c.

Applying the laws of Gaussian statistics to the complex amplitude of the emitted wave yields for the average in eq. (2.6)

$$K(\boldsymbol{\rho}, L) = 1 + |\Gamma^2(\boldsymbol{\rho}, L)|/I_0^2(L)\,. \tag{2.12}$$

This expression suggests in particular that, in the saturation regime, $K = K(0, L) = 2$. Backscatter enhancement can be observed in a small neighborhood of the transmitter confined by the radius $\rho_c(L)$. The Gaussian approximation used in deriving eq. (2.12) fails to observe that for $\rho \gtrsim \rho_c(L)$ enhancement gives way to reduction. However, there are reasons to believe that in the regime of saturated fluctuations of intensity the reduction is small, $|1 - K(\boldsymbol{\rho}, L)| \ll 1$ is valid in the wide angular region $\rho_c < \rho < \sigma_\rho$. Useful results on backscatter enhancement under the conditions of saturated fluctuations are given in the book by BANAKH and MIRONOV [1987].

2.1.6. *A lens interpretation of backscatter enhancement*

An easily tractable lens model of the backscatter-enhancement effect is based on representing a random medium as a collection of focusing and defocusing lenses, i.e., biconvex and biconcave lenses shown in fig. 2.4. Assume that the scatterer is a sphere of radius a. In the geometric optics approximation the scattering cross section of the sphere is $\sigma = \pi a^2$. If the sphere is in the focus of a lens of radius $R \gg a$ which is placed between the source and the sphere, the effective cross section of this system, $\sigma_{foc} = \pi R^2$, is many times the scattering cross section of the sphere alone, $\sigma_{foc}/\sigma = (R/a)^2 \gg 1$. If the lens defocuses the incident radiation, then, assuming the same focal length as that for the biconvex lens, the effective scattering cross section will be only $\frac{1}{4}$ of σ, namely, $\sigma_{defoc}/\sigma \approx (F/2F)^2 = \frac{1}{4}$.

If we assume that the probability of encountering a focusing or defocusing element is the same, than for $R/a \gg 1$ the mean effective cross section

$$\sigma_{eff} = \tfrac{1}{2}(\sigma_{foc} + \sigma_{defoc}) \approx \frac{1}{2}\left(\frac{R^2}{a^2} + \frac{1}{4}\right)\sigma$$

will exceed the "vacuum" value σ. Thus, the backscatter-enhancement effect

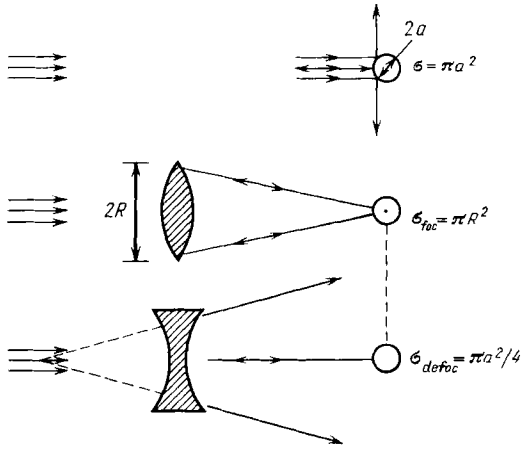

Fig. 2.4. Scattering by a sphere of radius a in a homogeneous medium (top), scattering after passing through a focusing lens (middle), and defocusing lens (bottom).

may be treated as a result of a strong asymmetry in the action of the focusing and defocusing inhomogeneities.

2.1.7. *Backscatter-enhancement relying on multipath coherent effects*

The effect of backscattering enhancement allows an interpretation with the aid of multipath coherent effects of Watson–Ruffine that suggests a common cause for a wide variety of phenomena.

Imagine an opaque screen with two widely spaced pinholes placed midway between the transmitter and scatterer, as shown in fig. 2.5. A wave arrives at the scatterer along two different paths, so that we can separate the Green function accordingly, i.e.,

$$u(\boldsymbol{r}_s) \approx G(\boldsymbol{r}_t, \boldsymbol{r}_s) = G_1(\boldsymbol{r}_t, \boldsymbol{r}_s) + G_2(\boldsymbol{r}_t, \boldsymbol{r}_s) .$$

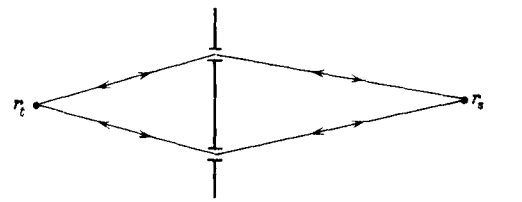

Fig. 2.5. Coherent effects occur when radiation from a source arrives at a scatterer through a few paths.

Assume that random inhomogeneities in front of and behind the screen give rise to strong phase fluctuations so that the two waves incident on the scatterer are mutually incoherent; i.e., $\langle G_1 G_2^* \rangle = 0$.

The field of the scattered wave at the point of the transmitter is proportional to

$$u_s(\boldsymbol{r}_t) = f(G_1 + G_2)^2 .$$

This field may also be represented as the sum of two waves reaching the transmitter through different pinholes

$$u_s = u_s^1 + u_s^2 = fGG_1 + fGG_2 .$$

Unlike the waves of G_1 and G_2 incident upon the scatterer, the terms u_s^1 and u_s^2 always contain identical (coherent) components, $G_2 G_1$ and $G_1 G_2$, corresponding to the scattered waves that have passed the same route, transmitter – hole 1 – and scatterer – hole 2, but in opposite directions. Because of the mutually coherent addends, the average intensity of the scattered wave at the transmitter is

$$\langle I_s(\boldsymbol{r}_t) \rangle = I_{11} + I_{22} + 4I_{12} ,$$

which exceeds by $2I_{12}$ the average intensity corresponding to the wave intensities u_s^1 and u_s^2 added incoherently, viz.,

$$\langle I_s \rangle_{\text{incoh}} = I_{11} + I_{22} + 2I_{12} ,$$

where

$$I_{11,22} = \sigma \langle |G^4| \rangle ,$$

$$I_{12} = \sigma \langle |G_1^2| \rangle \langle |G_2^2| \rangle .$$

It is worth noting that $\langle I_s \rangle_{\text{incoh}}$ equals the average intensity of the scattered wave measured at a point $\boldsymbol{r}$, at a distance from the transmitter where u_s^1 and u_s^2 are no longer coherent.

We introduce a coefficient

$$K = \langle I_s(\boldsymbol{r}_t) \rangle / \langle I_s \rangle_{\text{incoh}} \equiv \langle I_{\text{bsc}} \rangle / \langle I_{\text{sep}} \rangle$$

that characterizes the enhancement of a backscattered wave over the intensity at points far separated from the transmitter. If $I_{11,22} \approx I_{12}$, then $K \approx \frac{3}{2}$. It should be evident that as the number of pinholes M in the screen increases, the enhancement factor grows as $K \approx 2 - 1/M$ and approaches two as M tends to infinity.

In this imaginary experiment the effect of enhanced backscattering is caused

by the artificially provided multipath (two-path for the two-pinhole case) coherent effects of the Watson–Ruffine type. In other words the effect near the transmitter is caused by the interference of waves that have passed in opposite directions through the same random inhomogeneities of the medium. A similar process takes place in propagation of waves in a turbulent medium. However, unlike the preceding experiment with the screen, here the multipath propagation of a wave incident upon a scatterer occurs as a result of random walk and entanglement of rays in a turbulent medium.

In what follows we picture a ray pattern of backscatter enhancement in a turbulent medium, which although rough, yields correct quantitative estimates of the effects of double passage. We begin with estimating the distance between two rays emanated from a source at an angle θ_0. In a turbulent medium, at a distance x from the source, each of the rays experiences fluctuations of the angle of propagation in the order of $\tilde{\theta} = 1/k\rho_c(x)$. If the rays pass through different random inhomogeneities, the distance between them will be

$$\int_0^L [\theta_0 + \tilde{\theta}(x)]\, \mathrm{d}x \approx \rho_0(L) + \sigma_\rho(L),$$

where $\sigma_\rho(L)$ is given by eq. (2.11) and $\rho_0(L) = \theta_0 L$ is the distance between the rays in vacuum. The smallest angle θ_0 at which the rays may still be thought of independent random walks compares with the coherence angle $\theta_c(L) = \rho_c(L)/L$. The dimensionless ratio of $\sigma_\rho(L)$ and $\rho_0(L) \approx \theta_c L = \rho_c$, denoted by $\gamma(L)$ in eq. (2.10), characterizes the degree of random broadening of ray tubes in the turbulent medium.

As long as $\gamma(L) < 1$, the ray tubes emerge almost undistorted and the fluctuations of intensity $\delta I \sim \gamma^2$ caused by random compression and expansion of the ray tubes are small and may be treated with Rytov's approximation. At $\gamma \sim 1$, random focusing phenomena appear (random caustics) that are responsible for the strong fluctuations of the wave intensity (KRAVTSOV [1968]).

Further away from the transmitter, where $\gamma(L) \gg 1$, rays are entangled in a random manner and many almost independent rays meet at every point, as shown in fig. 2.6; the number of such rays may be estimated as $M \approx \gamma^2 \gg 1$. The stochastic interference of independent waves arriving through various rays now becomes the principal mechanism of intensity fluctuations, rather than the compression and expansion of ray tubes as is the case for $\gamma \ll 1$. Accordingly, the field of a wave incident upon a scatterer may be represented as a sum of a large number M, of statistically independent components, namely,

$$G(\boldsymbol{r}_t, \boldsymbol{r}_s) = \sum_{m=1}^{M} G_m(\boldsymbol{r}_t, \boldsymbol{r}_s).$$

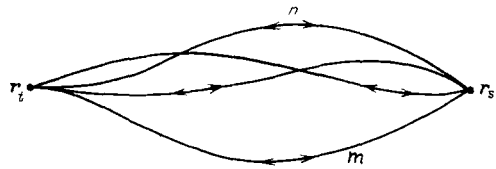

Fig. 2.6. Multipath coherent effects in the range of saturated fluctuations in a turbulent medium.

From the reciprocity theorem it follows that the scattered waves return to the transmitter through the same M rays (paths). The fields of all rays incident upon the source will be partially coherent, because to every pair of rays incident on the scatterer, say m and n in fig. 2.6, there correspond a pair of scattered waves propagating along these rays in an opposite direction.

Multiple coherent scattering paths that occur in a turbulent medium result, as in the preceding experiment with a screen, in an enhancement of the average backscattered intensity, the enhancement factor K approaching two. When the point of observation is shifted a distance $\rho \gtrsim \rho_c(L)$ from the transmitter–scatterer line, the coherence paths break down and the mutual coherence of waves scattered in various rays disappears.

The coherence paths also break down when the observation point moves along the transmitter–scatterer line over a distance of the order of the longitudinal radius of coherence estimated as $l_\parallel \approx \rho_c/\theta_c = k\rho_c^2(L)$ (VINOGRADOV [1974]). The domain of observability of enhanced backscattering is illustrated in fig. 2.7.

2.1.8. *Experimental evidence*

GURVICH and KASHKAROV [1977] were the first to observe the "pure" effect of enhanced backscattering in optics. A point source of light was simulated by a laser beam focused with a lens system (fig. 2.8). The receiving aperture was a small opening in a blackened face of a prism, enabling the point of observation of the scattered field $\boldsymbol{r}$ to be brought to within 0.5 mm of the effective trans-

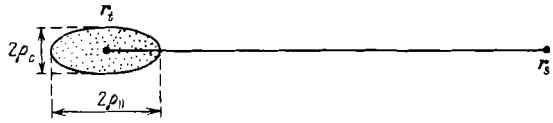

Fig. 2.7. Region of observation of enhanced backscattering is defined by the transverse (ρ_c) and longitudinal ($\rho_\parallel$) radii of correlation of the spherical wave reflected by the scatterer.

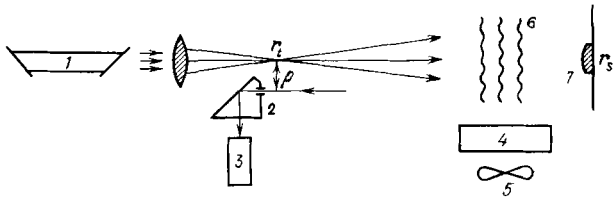

Fig. 2.8. Schematic diagram of a laboratory set-up for observation of backscatter enhancement (GURVICH and KASHKAROV [1977]). 1, Laser; 2, receiver prism; 3, photomultiplying tube; 4, heater; 5, fan; 6, turbulent air flow; 7, scatterer (spherical mirror).

mitter, $\boldsymbol{r}_t$. A fan and heater produced a turbulent flow of air. The scatterer was a sheet of paper or a 1 cm diameter spherical mirror with curvature radius $a \approx 0.5$ m. The Fresnel spot of radius $\sqrt{\lambda a}$ was larger than the coherence radius $\rho_c \approx 5$ mm, so that the convex mirror actually played the role of a point scatterer.

Figure 2.9 shows the experimental dependence of the enhancement factor K upon the distance $\rho = |\boldsymbol{r}_t - \boldsymbol{r}|$ from transmitter to receiver. Enhancement is of the order of 1.4 near the source with a gradual decrease at a distance of about 3 mm, which is comparable with the coherence radius ρ_c.

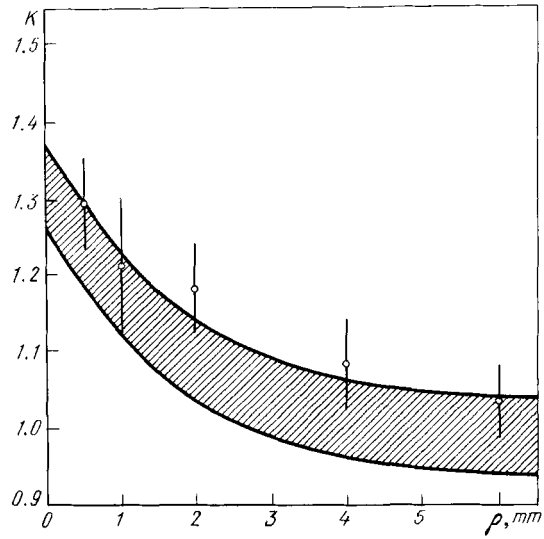

Fig. 2.9. Enhancement factor K versus distance between the transmitter and receiver in a laboratory experiment. Experimental points are shown as open circles with bars representing standard deviation. The cross-hatched area corresponds to the values of $K(\rho)$ calculated through the measured values of $B_{\Delta J}(\rho)$.

A field experiment was carried out in a 1300 m long route (KASHKAROV [1983]). The source and receiver were the same as in the laboratory experiment. To increase the intensity of backscattered light, the scatterer was made as a set of 4000 spherical scatterers placed over 1 m^2 of a screen. In addition to the average backscattered intensity, the correlation function of the field intensity $B_{\Delta J}$ in the rectilinear path was measured. The plot of $K(\rho, L) - 1$ as a function of $B_{\Delta J}(\rho)$ is represented in fig. 2.10. The experimental points lie fairly close to the bisector, in agreement with the theoretical predictions (see § 2.1.3).

The value of these experiments has been not only that they confirmed the theoretical predictions but also that they tested a new technique for monitoring turbulent media. Instead of a correlation function, this method measures the average backscattered intensity, which is much easier to do. Another practical advantage of the method is that the transmitter and detector can be placed in the immediate vicinity of one another rather than being separated by a considerable distance, as with the traditional monitoring techniques.

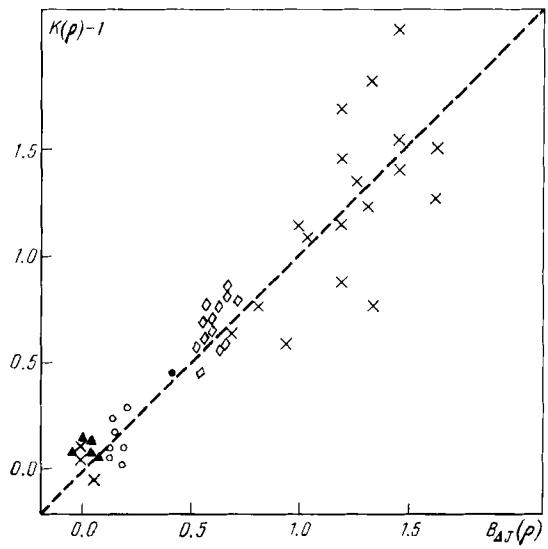

Fig. 2.10. Enhancement $K(\rho) - 1$ plotted versus measured values of the intensity correlation coefficient $B_{\Delta J}(\rho)$ for several experimental runs shows small deviations from the bisector (dashed line).

2.1.9. *Enhancement of backscattered intensity fluctuations: Residual correlation of the intensity*

An enhancement of the average intensity of a backscattered wave detected near the transmitter is accompanied by an enhancement of fluctuations of the intensity compared with the intensity scattered sideways (VINOGRADOV, KRAVTSOV and TATARSKII [1973], BELENKII and MIRONOV [1974] and BANAKH and MIRONOV [1987]). The variance of the relative intensity fluctuations of a scattered wave is

$$\langle(\Delta J)^2\rangle = \langle J_s^2(\boldsymbol{r})\rangle - \langle J_s(\boldsymbol{r})\rangle^2$$
$$= \langle J^2(\boldsymbol{r}_t)\, J^2(\boldsymbol{r})\rangle - \langle J(\boldsymbol{r}_t)\, J(\boldsymbol{r})\rangle^2 . \tag{2.13}$$

Here we assume, as before, that the observation point $\boldsymbol{r}$ is at a distance $\rho = |\boldsymbol{r} - \boldsymbol{r}_t|$ from the transmitter (see fig. 2.3). For the wave scattered strictly backwards the variance of the relative intensity fluctuations is

$$\langle(\Delta J_{bsc})^2\rangle = \langle J^4\rangle - \langle J^2\rangle^2 . \tag{2.14}$$

It would be natural to compare this quantity with the variance of relative intensity fluctuations for a wave scattered sideways, i.e., at a distance $\rho \gg \rho_c$, where it may be safely taken that the inhomogeneities encountered by the emitted and scattered waves were almost independent. The average terms in eq. (2.13) break down into the products of the means to give

$$\langle(\Delta J_{sep})^2\rangle \equiv \langle J^2\rangle^2 - 1 .$$

We introduce the enhancement factor of intensity fluctuations as the ratio of intensity variances for waves scattered backwards and sideways, i.e.,

$$K_{\Delta J} = \langle(\Delta J_{bsc})^2\rangle / \langle(\Delta J_{sep})^2\rangle$$
$$= [\langle J^4\rangle - \langle J^2\rangle^2]/[\langle J^2\rangle^2 - 1] . \tag{2.15}$$

If the fluctuations are weak, the averages in eq. (2.15) may be computed in Rytov's approximation. In this approximation $J = \exp(2\chi)$, where χ is the level of amplitude obeying a Gaussian distribution with variance $\sigma_\chi^2 = B_\chi(0, L)$ of eq. (2.9) and mean $\langle\chi\rangle = -\sigma_\chi^2$. From the normal distribution of χ it follows that

$$\langle J^n\rangle = \exp[2n(n-1)\sigma_\chi^2] ,$$

so that the enhancement factor of the fluctuations of backscattered intensity

is

$$K_{\Delta J} = \frac{\exp(24\sigma_\chi^2) - \exp(8\sigma_\chi^2)}{\exp(8\sigma_\chi^2) - 1} > 2 .$$

For the case of saturated fluctuations of intensity, it follows from the fact that the field of the forward wave is asymptotically Gaussian, that the probability density of the normalized intensity $J(\boldsymbol{r})$ asymptotically approaches the exponential law ($J > 0$)

$$W(J) = \exp(-J) .$$

The moments of intensity are then $\langle J^n \rangle = n!$, so that from eq. (2.15) we obtain

$$K_{\Delta J} = [4! - (2!)^2]/[(2!)^2 - 1] = 6.67 .$$

Experimental studies into fluctuation effects have been reported by BELENKII, MAKAROV, MIRONOV and POKASOV [1978], PATRUSHEV, PETROV and POKASOV [1983], and KASHKAROV, NESTEROVA and SMIRNOV [1984]. Specifically, KASHKAROV, NESTEROVA and SMIRNOV [1984] measured the intensity moments of the forward wave, $\langle J^2 \rangle$ and $\langle J^4 \rangle$, and the variances of intensity fluctuations of a wave scattered backwards and sideways. Results of these experiments agree satisfactory with the theory outlined above. Detailed discussions of intensity fluctuations for scattered waves may be found in the monographs by MIRONOV [1981], BANAKH and MIRONOV [1987] and ZUEV, BANAKH and POKASOV [1988].

One more effect is noteworthy for fluctuations of intensity of scattered waves, namely, the effect of a residual correlation of intensity for arbitrarily separated points of observation. According to eq. (2.3) the correlation function of the relative intensity of a scattered wave J_s is given by

$$B_s(\boldsymbol{\rho}_1, \boldsymbol{\rho}_2, L) = \langle J_s(\boldsymbol{r}_1) J_s(\boldsymbol{r}_2) \rangle$$
$$= \langle J^2(\boldsymbol{r}_t, \boldsymbol{r}_s) J(\boldsymbol{r}_1, \boldsymbol{r}_s) J(\boldsymbol{r}_2, \boldsymbol{r}_s) \rangle ,$$

where $\boldsymbol{\rho}_{12} = \boldsymbol{r}_{1,2} - \boldsymbol{r}_t$. If the points of transmission and observation are sufficiently far from one another so that $\rho_{1,2} \gg \rho_c$, then

$$B_s(\rho_{1,2} \gg \rho_c, L) = \langle J^2 \rangle \langle J \rangle^2 = \langle J^2 \rangle . \tag{2.16}$$

This quantity exceeds unity, since $\langle J^2 \rangle = K_{bsc} > 1$. If $J_s(\boldsymbol{r}_1)$ and $J_s(\boldsymbol{r}_2)$ were uncorrelated, then for B_s we should obtain $(\langle J_s \rangle)^2 = (\langle J \rangle)^4 = 1$. The differ-

ence

$$B_s(\rho_{1,2} \gg \rho_c, L) - 1 = \langle J^2 \rangle - 1 = K_{bsc} - 1 > 0$$

is exactly the quantity that characterizes the residual correlation of the backscattered intensity for distant points. This difference is caused by the fact that the wave incident upon the scatterer is amplitude modulated because of the fluctuations in between the transmitter and the scatterer. This modulation, identical for all points of observation, is responsible for the residual correlation effects, which was discussed first by BELENKII and MIRONOV [1974].

2.1.10. *Scattering from small inhomogeneities in a turbulent medium: A hybrid approach*

An enhanced backscattering may be obtained not only for bodies embedded in a turbulent medium, but also for the small-scale component of the spectrum of inhomogeneities. DE WOLF [1971] has analyzed this problem on the basis of a selective summation of series in perturbation theory, and VINOGRADOV and KRAVTSOV [1973] have tackled it in the framework of a hybrid approach. In this approach the zeroth order approximation is the field that has been distorted already by large inhomogeneities and the effect of the small-scale component is taken into account with the aid of perturbation theory. This is essentially a statistical version of the distorted wave Born approximation (DWBA) method.

The hybrid approach has advantages over the selective summation technique in that it leads to an objective faster and, what is more important, in a more consistent manner. Indeed, whereas de Wolf has taken small inhomogeneities into account twice (in the propagator and inhomogeneity spectrum), the hybrid approach handles small-scale and large-scale inhomogeneities independently.

Let $B_\varepsilon(\rho) = \langle \tilde{\varepsilon}(\boldsymbol{r} + \boldsymbol{\rho})\, \tilde{\varepsilon}(\boldsymbol{r}) \rangle$ be the correlation function and $\Phi_\varepsilon(\boldsymbol{\varkappa})$ the spectrum of random and isotropic fluctuations of medium permittivity. Represent the spectrum $\Phi_\varepsilon(\boldsymbol{\varkappa})$ as a sum of two nonnegative components, i.e.,

$$\Phi_\varepsilon(\boldsymbol{\varkappa}) = \Phi_\mu(\boldsymbol{\varkappa}) + \Phi_\nu(\boldsymbol{\varkappa}), \tag{2.17}$$

then the correlation function $B_\varepsilon(\rho)$ is

$$B_\varepsilon(\rho) = B_\mu(\rho) + B_\nu(\rho). \tag{2.18}$$

We think of $\nu(\boldsymbol{r})$ as the large-scale component and $\mu(\boldsymbol{r})$ as the small-scale component, the spectrum $\Phi_\varepsilon(\boldsymbol{\varkappa})$ being divided by the boundary wavenumber $\boldsymbol{\varkappa}^*$, as shown in fig. 2.11.

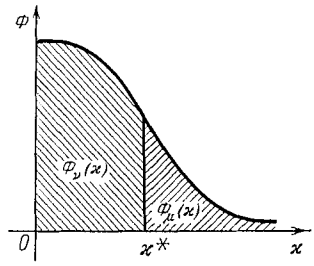

Fig. 2.11. One version of dividing the spectrum of fluctuations of permittivity into small-scale ($\varkappa > \varkappa^*$) and large-scale ($\varkappa < \varkappa^*$) components.

Partitioning the fluctuations of ε into two parts ν and μ, we observe that in view of eqs. (2.17) and (2.18) these parts are uncorrelated, i.e., $B_{\mu\nu} = 0$. Now, we write the wave equation as

$$\Delta u + k^2(1 + \nu)u = -k^2\mu u\,, \tag{2.19}$$

and as a zeroth approximation we take the solution u_ν caused by the passage of the wave through large inhomogeneities and satisfying

$$\Delta u_\nu + k^2(1 + \nu)u_\nu = 0\,. \tag{2.20}$$

The respective Green function will be G_ν.

To a first approximation, from eq. (2.19) we obtain the once-scattered field

$$u_\mu^{(1)} = -k^2 \int_v \mu(\boldsymbol{r}')\, u_\nu(\boldsymbol{r}')\, G_\nu(\boldsymbol{r}, \boldsymbol{r}')\, \mathrm{d}^3 r'\,. \tag{2.21}$$

The average intensity of this field, $I_\mu^{(1)}$, can be calculated by carrying out independent averaging over ν and μ, namely

$$\bar{I}_\mu^{(1)}(r) = k^4 \int\int B_\mu(\boldsymbol{r}' - \boldsymbol{r}'') \times \langle G_\nu(\boldsymbol{r}, \boldsymbol{r}')\, G_\nu^*(\boldsymbol{r}, \boldsymbol{r}'')\, u_\nu(\boldsymbol{r}')\, u_\mu(\boldsymbol{r}'')\, \mathrm{d}^3 r'\, \mathrm{d}^3 r''\,.$$

Assume that the coherence radius ρ_c of the fields u_ν and G_ν is large compared with the correlation radius of the small-scale component l_μ, and that the fields u_ν and G_ν differ from the respective values in vacuum, $u_0(\boldsymbol{r}')$ and $G_0(\boldsymbol{r}, \boldsymbol{r}') = -\exp(ik|\boldsymbol{r} - \boldsymbol{r}'|)/4\pi|\boldsymbol{r} - \boldsymbol{r}'|$, by random factors whose squared moduli equal, respectively, $J(\boldsymbol{r}', \boldsymbol{r}_t)$ and $J(\boldsymbol{r}, \boldsymbol{r}')$ with $\boldsymbol{r}_t$ being the emanation point of the primary wave. Then the mixed moment in the integrand for $\bar{I}_\mu^{(1)}$

can be replaced with a simpler expression

$$\langle G_\nu G_\nu^* u_\nu u_\nu^* \rangle \approx \frac{I_0(\boldsymbol{R})\, K(\boldsymbol{\rho}, \boldsymbol{R})}{16\pi^2 |\boldsymbol{R} - \boldsymbol{r}|^2} \exp[i\boldsymbol{q}\cdot(\boldsymbol{r}' - \boldsymbol{r}'')],$$

where $I_0(\boldsymbol{R})$ is the primary field intensity at the point $\boldsymbol{R} = \frac{1}{2}(\boldsymbol{r}' + \boldsymbol{r}'')$, $\boldsymbol{q} = k(\boldsymbol{n}_i - \boldsymbol{n}_s) = k[(\boldsymbol{R} - \boldsymbol{r}_0)/|\boldsymbol{R} - \boldsymbol{r}_0| - (\boldsymbol{R} - \boldsymbol{r})/|\boldsymbol{R} - \boldsymbol{r}|]$ is the scattering vector, and

$$K(\boldsymbol{\rho}, \boldsymbol{R}) = \langle |J(\boldsymbol{R}, \boldsymbol{r}_t)|^2 |J(\boldsymbol{R}, \boldsymbol{r})|^2 \rangle$$

is the enhancement factor that we have already considered. Now, the intensity $I_\mu^{(1)}$ may be represented as

$$\bar{I}_\mu^{(1)} = \int_V \frac{I_0(\boldsymbol{R})\, \sigma_\mu(\boldsymbol{q})\, K(\boldsymbol{\rho}, \boldsymbol{R})}{|\boldsymbol{r} - \boldsymbol{R}|^2}\, d^3R\,, \tag{2.22}$$

which is close to the traditional formula of Born. Here, $\sigma_\mu(\boldsymbol{q}) = \frac{1}{2}\pi k^4 \Phi_\mu(\boldsymbol{q})$ is the small-scale part of Born's scattering cross section per unit volume.

According to eq. (2.22), the effective scattering cross section $K\sigma_\mu$ differs from Born's quantity σ_μ by a factor K, which has a peak of enhancement toward the source (point $\boldsymbol{r}_t$) and is close to unity in all other directions.

It is an easy matter to demonstrate (VINOGRADOV and KRAVTSOV [1973]) that eq. (2.22) is invariant with respect to small variations of the boundary value $\varkappa^*$, if the small-scale component $\mu(\boldsymbol{r})$ does not cause a marked extinction over a distance L, i.e.,

$$2\alpha_\mu L = L\sigma_{\mu,\,\mathrm{tot}} = L\int \sigma_\mu(\boldsymbol{q})\, d\Omega \ll 1\,. \tag{2.23}$$

This inequality is much weaker than the usual condition of applicability of Born's approximation, i.e., $2\alpha_\varepsilon L = 2(\alpha_\nu + \alpha_\mu)L \ll 1$, because the extinction coefficient for the large-scale component α, exceeds considerably that of the small-scale component α_μ.

Thus the hybrid approach succeeds in not only revealing an enhanced backscattering, but also in considerably expanding the limits of applicability of Born's approximation. For this purpose it suffices to replace the total scattering cross section σ_ε with its small-scale part σ_μ. Moreover, the potentialities of this approach seem to be far from exhausted.

2.1.11. *Polarization effects*

Media with large-scale inhomogeneities ($l_\varepsilon \gg \lambda$) propagate electromagnetic waves almost without changing their polarization. This follows from the estimates obtained by TATARSKII [1967] for "diffraction" depolarization (described by Rytov's method or by the method of parabolic equation) and by KRAVTSOV [1970] for "geometric" depolarization caused by the rotation of field vectors due to torsion of rays. Both diffraction and geometric depolarization of a light wave are small, and therefore a consideration of light effects may be limited to a scalar approximation.

2.2. EXTENDED TRANSMITTERS, SCATTERERS, AND RECEIVERS

2.2.1. *Wave description within the parabolic equation framework*

A wave propagating through a medium with large-scale random inhomogeneities of permittivity suffers multiple scattering, which is predominantly directed forward in a narrow cone of angle $\theta \simeq \lambda/l_\varepsilon \ll 1$. As a result of the multiple scattering, the wave propagates practically in the emanant direction. It is convenient to describe this wave with the aid of the parabolic equation philosophy (see, e.g., the book of RYTOV, KRAVTSOV and TATARSKII [1989a,b]. This philosophy also may be applied to the description of the propagation of waves scattered from a body embedded in a turbulent medium.

Let a wave propagating along the x-axis have a complex amplitude $u_0(\boldsymbol{\rho})$ in the plane of the transmitter, $x = 0$ ($\boldsymbol{\rho}$ represents the transverse coordinates). Then the complex amplitude of the wave in a cross plane passing on x is given by

$$u(\boldsymbol{\rho}, x) = \int u_0(\boldsymbol{\rho}')\, g(\boldsymbol{\rho}', \boldsymbol{\rho}, x)\, \mathrm{d}^2\rho' \,. \tag{2.24}$$

The Green function $g(\boldsymbol{\rho}', \boldsymbol{\rho}, x)$ describing the field of a spherical wave emanated from point $\boldsymbol{\rho}'$, $x = 0$ satisfies the parabolic equation of quasi-optics

$$2ik \frac{\partial g}{\partial x} + \Delta_\perp g + k^2 \tilde{\varepsilon}(\boldsymbol{\rho}', x) g = 0 \,,$$

$$g(\boldsymbol{\rho}', \boldsymbol{\rho}, 0) = \delta(\boldsymbol{\rho} - \rho') \,,$$

where $\Delta_\perp$ is a two-dimensional Laplacian in a plane orthogonal to the x-axis.

Let a scatterer with a local reflection factor $f(\boldsymbol{\rho})$, recalculated for a plane $x = L$, be placed at point $x = L$. Using reversibility of light paths, the complex amplitude of the wave scattered backwards can be written (in the plane $x = 0$) as (GELFGAT [1976], SAICHEV [1978])

$$u_s(\boldsymbol{\rho}) = \int u(\boldsymbol{\rho}', L)\, f(\boldsymbol{\rho}')\, g(\boldsymbol{\rho}, \boldsymbol{\rho}', L)\, \mathrm{d}^2\rho'$$

$$= \int\int u_0(\boldsymbol{\rho}')\, f(\boldsymbol{\rho}'')\, g(\boldsymbol{\rho}, \boldsymbol{\rho}'', L)\, g(\boldsymbol{\rho}', \boldsymbol{\rho}'', L)\, \mathrm{d}^2\rho'\, \mathrm{d}^2\rho'' \,. \tag{2.25}$$

In the following description we need a theory of wave propagation without reflection in a random inhomogeneous medium. Valuable information about waves propagating in randomly inhomogeneous media may be obtained with the aid of moment functions. In the Markov approximation, these functions satisfy closed equations (see, e.g., ISHIMARU [1978], RYTOV, KRAVTSOV and TATARSKII [1989a,b], GURBATOV, MALAKHOV and SAICHEV [1991]). The equations for the average field $\langle u(\boldsymbol{\rho}, x)\rangle$ and for a coherence function have an exact solution. The average field of optical waves in a turbulent atmosphere is almost always zero. Therefore, we confine ourselves to the coherence function for the Green function $g(\boldsymbol{\rho}_0, \boldsymbol{\rho}, x)$,

$$\Gamma_g(\boldsymbol{R}_0, \boldsymbol{p}_0, \boldsymbol{R}, \boldsymbol{p}, x) = \langle g(\boldsymbol{R}_0 + \tfrac{1}{2}\boldsymbol{p}_0, \boldsymbol{R} + \tfrac{1}{2}\boldsymbol{p}, x)\, g^*(\boldsymbol{R}_0 - \tfrac{1}{2}\boldsymbol{p}_0, \boldsymbol{R} - \tfrac{1}{2}\boldsymbol{p}, x)\rangle$$

$$= \left(\frac{k}{2\pi x}\right)^2 \exp\left[\frac{\mathrm{i}k}{x}(\boldsymbol{R} - \boldsymbol{R}_0)(\boldsymbol{p} - \boldsymbol{p}_0) - \tfrac{1}{2}d(\boldsymbol{p}_0, \boldsymbol{p}, x)\right]. \tag{2.26}$$

The effect of random inhomogeneities of the medium is taken into account by the function

$$d(\boldsymbol{p}_0, \boldsymbol{p}, x) = \tfrac{1}{2}k^2 \int_0^x D\left[\boldsymbol{p}_0\left(1 - \frac{z}{x}\right) + \boldsymbol{p}\,\frac{z}{x}\right]\mathrm{d}z \,, \tag{2.27}$$

which is equal to the mean squared random phase difference calculated in the geometric optics approximation along two straight rays. The initial distance between these rays (in the $x = 0$ plane) is $\boldsymbol{p}_0$, and the final distance, at $z = x$, is $\boldsymbol{p}$. If p is in the inertial interval, $l_0 < p < L_0$, then (ISHIMARU [1978])

$$D(p) = 5.83 C_n^2 p^{5/3} \,, \tag{2.28}$$

where C_n^2 is the structural characteristic of fluctuations of the refractive index of the turbulent medium.

If the coherence function (2.26) is known, it is not hard to compute the coherence function of the wave field u,

$$\Gamma(\boldsymbol{R}, \boldsymbol{p}, x) = \langle u(\boldsymbol{R} + \tfrac{1}{2}\boldsymbol{p}, x)\, u^*(\boldsymbol{R} - \tfrac{1}{2}\boldsymbol{p}, x)\rangle$$
$$= \int\int u_0(\boldsymbol{R}' + \tfrac{1}{2}\boldsymbol{p}')\, u_0^*(\boldsymbol{R}' - \tfrac{1}{2}\boldsymbol{p}')\, \Gamma_g(\boldsymbol{R}', \boldsymbol{p}', \boldsymbol{R}, \boldsymbol{p}, x)\, \mathrm{d}^2R'\, \mathrm{d}^2p\,. \tag{2.29}$$

From this expression it follows that, in particular, for a spherical wave emanated from the origin ($\boldsymbol{\rho} = 0$, $x = 0$)

$$\Gamma_{\mathrm{sph}}(\boldsymbol{R}, \boldsymbol{p}, x) = \left(\frac{k}{2\pi x}\right)^2 \exp\left[\frac{\mathrm{i}k}{x}\,(\boldsymbol{R}\cdot\boldsymbol{p}) - \tfrac{1}{2}d(0, \boldsymbol{p}, x)\right].$$

Let us determine the coherence radius $\rho_c(x)$ of a spherical wave as the value of p at which the modulus of coherence function reduces by a factor of $1/e$ to give $d(0, \rho_c, x) = 2$. If $\rho_c(x)$ lies in the inertial interval, i.e., if (2.28) is valid, then

$$\rho_{c,\mathrm{sph}}(x) = 1.44(k^2C_n^2x)^{-3/5}\,, \tag{2.30}$$

and the coherence function of the spherical wave takes the form

$$\Gamma_{\mathrm{sph}}(\boldsymbol{R}, \boldsymbol{p}, x) = \left(\frac{k}{2\pi x}\right)^2 \exp\left\{\frac{\mathrm{i}k}{x}\,(\boldsymbol{R}\cdot\boldsymbol{p}) - [p/\rho_c(x)]^{5/3}\right\}. \tag{2.31}$$

The following coherence function corresponds to a plane wave $u_0(\boldsymbol{\rho}) = u_0 = \mathrm{const}$.

$$\Gamma_{\mathrm{pl}}(\boldsymbol{p}, x) = I_0 \exp[-\tfrac{1}{2}d(\boldsymbol{p}, \boldsymbol{p}, x)]\,, \quad I_0 = |u_0|^2\,. \tag{2.32}$$

Accordingly, the coherence radius of the plane wave is

$$\rho_{c,\mathrm{pl}}(x) = 0.8(k^2C_n^2x)^{-3/5}\,.$$

An important physical characteristic of a random wave field is the radiant intensity

$$\mathscr{I}(\boldsymbol{R}, \boldsymbol{\theta}, x) = \left(\frac{k}{2\pi}\right)^2 \int \Gamma(\boldsymbol{R}, p, x)\, \mathrm{e}^{-\mathrm{i}k(\boldsymbol{\theta}\cdot\boldsymbol{p})}\, \mathrm{d}^2p\,. \tag{2.33}$$

Substituting $\Gamma(\boldsymbol{R}, \boldsymbol{p}, x)$ from eq. (2.29), we obtain (VINOGRADOV, KOSTERIN, MEDOVIKOV and SAICHEV [1985])

$$\mathscr{I}(\boldsymbol{R}, \boldsymbol{\theta}, x) = \int\int \mathscr{I}_0(\boldsymbol{R}', \boldsymbol{\theta}', x)\, W(\boldsymbol{R} - \boldsymbol{R}', \boldsymbol{\theta} - \boldsymbol{\theta}', x)\, \mathrm{d}^2R'\, \mathrm{d}^2\theta'\,, \tag{2.34}$$

where $\mathscr{J}_0(\boldsymbol{R}, \boldsymbol{\theta}, x)$ is the radiant intensity of a wave propagating in vacuum ($\tilde{\varepsilon} = 0$), and the function

$$W(\boldsymbol{R}, \boldsymbol{\theta}, x) = \left(\frac{k}{2\pi}\right)^2 \left(\frac{k}{2\pi x}\right)^2 \times \int \exp\left[\frac{\mathrm{i}k}{x} \boldsymbol{R}(\boldsymbol{p} - \boldsymbol{p}') - \mathrm{i}k(\boldsymbol{\theta}\cdot\boldsymbol{p}) - \tfrac{1}{2} d(\boldsymbol{p}', \boldsymbol{p}, x)\right] \mathrm{d}^2p' \, \mathrm{d}^2p \tag{2.35}$$

may be given a simple geometrical interpretation; namely, it is the probability density of lateral shifts and angular deviations of rays propagating in a turbulent medium from the positions and directions of the respective rays in vacuum.

Averaging eq. (2.27) over the angles θ yields the average wave intensity

$$\langle I(\boldsymbol{\rho}, x)\rangle = \langle |u(\boldsymbol{\rho}, x)|^2 \rangle = \int I_0(\boldsymbol{\rho}', x)\, W_\rho(\boldsymbol{\rho} - \boldsymbol{\rho}', x)\, \mathrm{d}^2\rho' \,, \tag{2.36}$$

which is the intensity of the wave in vacuum, $I_0(\boldsymbol{\rho}, x)$, convoluted with the probability density of lateral shifts of rays in a turbulent medium

$$W_\rho(\boldsymbol{\rho}, x) = \left(\frac{k}{2\pi x}\right)^2 \int \exp\left[-\frac{\mathrm{i}k}{x}(\boldsymbol{\rho}\cdot\boldsymbol{p}) - \tfrac{1}{2} d(\boldsymbol{p}, 0, x)\right] \mathrm{d}^2p \,. \tag{2.37}$$

If $\rho_c(x)$ lies in the inertial interval, then

$$W_\rho(\boldsymbol{\rho}, x) = \frac{w(\rho/\sigma_\rho(x))}{4\pi\sigma_\rho^2(x)}, \tag{2.38}$$

where $\sigma_\rho(x)$ is the characteristic lateral shift of the rays of eq. (2.11) and

$$w(z) = \int_0^\infty J_0(z\sqrt{y}) \exp(-y^{5/6})\, \mathrm{d}y, \quad w(0) = 1.1 \,. \tag{2.39}$$

Let $a(x)$ be the radius of a wave bundle propagating in vacuum as measured in the cross section at x. Equation (2.36) suggests that if the lateral shift of rays σ_ρ is much less than the beam radius, then $\langle I(\boldsymbol{\rho}, x)\rangle = I_0(\boldsymbol{\rho}, x)$. Expressed differently, we can say that in this case random inhomogeneities do not affect the profile of the average beam intensity. Conversely, if $\sigma_\rho(x) \gg a(x)$, then $\langle I(\boldsymbol{\rho}, x)\rangle = P \cdot W_\rho(\boldsymbol{\rho}, x)$; i.e., the average intensity follows the profile of the

probability density of lateral shifts of rays. (Here, $P = \int I_0 \, d^2\rho$ is the total energy flux of the beam.)

Integrating eq. (2.34) with respect to $\boldsymbol{R}$, we obtain the angular distribution of the average energy flux of the wave passing through the cross section at x

$$P(\boldsymbol{\theta}, x) = \int P_0(\boldsymbol{\theta}', x)\, W_\theta(\boldsymbol{\theta} - \boldsymbol{\theta}', x)\, d\theta' \,. \tag{2.40}$$

This expression includes the probability density of fluctuations of oncoming angles for rays in a turbulent medium; for $l_0 < \rho_{c,pl}(x) < L_0$, it equals

$$W_\theta(\boldsymbol{\theta}, x) = \frac{w(\theta/\sigma_\theta(x))}{4\pi\sigma_\theta^2(x)} ,$$

where

$$\sigma_\theta(x) = 1/k\rho_{c,pl}(x) \tag{2.41}$$

is the characteristic angular deviation of rays from their directions in vacuum. Useful results on backscatter enhancement of laser radiation have been reported by AKSENOV and MIRONOV [1979] and AKSENOV, BANAKH and MIRONOV [1984].

2.2.2. *Statistical description of backscattered waves in the region of saturated fluctuations of intensity*

The effects of double passage of scattered waves through the same inhomogeneities of a medium are more clear cut in the case of saturated fluctuations of radiated intensity when the moment functions of random fields may be handled with the aid of Gaussian statistics. As an example, consider the coherence function of a backscattered wave in the plane of the transmitter. According to eq. (2.25), it is

$$\begin{aligned} \Gamma_s(\boldsymbol{R}, \boldsymbol{p}) &= \langle u_s(\boldsymbol{R} + \tfrac{1}{2}\boldsymbol{p})\, u_s^*(\boldsymbol{R} - \tfrac{1}{2}\boldsymbol{p}) \rangle \\ &= \int\int f(\boldsymbol{\rho}')\, f^*(\boldsymbol{\rho}'') \, \langle u(\boldsymbol{\rho}', L)\, g(\boldsymbol{R} + \tfrac{1}{2}\boldsymbol{p}, \boldsymbol{\rho}', L) \\ &\quad \times u^*(\boldsymbol{\rho}'', L)\, g^*(\boldsymbol{R} - \tfrac{1}{2}\boldsymbol{p}, \boldsymbol{\rho}'', L) \rangle \, d^2\rho' \, d^2\rho'' \,. \end{aligned}$$

A general solution of the equation for the fourth-order moment function entering this expression is yet to be found. However, given that the condition of saturated fluctuations of emanant intensity, eq. (2.10), is satisfied, the fields u and g can be deemed to be Gaussian with zero means and the last equality can be rewritten as

$$\Gamma_s(\boldsymbol{R}, \boldsymbol{p}) = \Gamma_1(\boldsymbol{R}, \boldsymbol{p}, L) + \Gamma_2(\boldsymbol{R}, \boldsymbol{p}, L) \,, \tag{2.42}$$

where

$$\begin{aligned}\Gamma_1(\boldsymbol{R}, \boldsymbol{p}, L) &= \int\int f(\boldsymbol{R}' + \tfrac{1}{2}\boldsymbol{q}')\, f^*(\boldsymbol{R}' - \tfrac{1}{2}\boldsymbol{q}') \\ &\quad \times \Gamma(\boldsymbol{R}, \boldsymbol{q}', L)\, \Gamma_g(\boldsymbol{R}, \boldsymbol{p}, \boldsymbol{R}', \boldsymbol{p})\, \mathrm{d}^2R'\, \mathrm{d}^2p' , \\ \Gamma_2(\boldsymbol{R}, \boldsymbol{p}, L) &= \int\int f(\boldsymbol{\rho}')\, f^*(\boldsymbol{\rho}'')\, \langle u(\boldsymbol{\rho}', L)\, g^*(\boldsymbol{R} - \tfrac{1}{2}\boldsymbol{p}, \boldsymbol{\rho}'', L)\rangle \\ &\quad \times \langle u^*(\boldsymbol{\rho}'', L)\, g(\boldsymbol{R} + \tfrac{1}{2}\boldsymbol{p}, \boldsymbol{\rho}', L)\rangle\, \mathrm{d}^2\rho'\, \mathrm{d}^2\rho'' .\end{aligned} \tag{2.43}$$

The first term on the right-hand side of eq. (2.42) describes the coherence function of a backscattered wave assuming that the random inhomogeneities encountered by the radiated and scattered waves are statistically independent, whereas Γ_2 takes into account the double passage of the wave through the same inhomogeneities.

The function $\Gamma_1(\boldsymbol{R}, \boldsymbol{p}, L)$ may be interpreted as the coherence of a wave that has passed, in a random inhomogeneous medium, a path of length $2L$, bisected by a semitransparent screen (at $x = L$) of transmittance $f_1(\boldsymbol{\rho})$. For an ideal mirror, when $f_1(\boldsymbol{\rho}) = 1$, $\Gamma_1(\boldsymbol{R}, \boldsymbol{p}, L) = \Gamma(\boldsymbol{R}, \boldsymbol{p}, 2L)$. In the case of a rough scatterer with small-scale inhomogeneities, we can assume

$$\langle f_1(\boldsymbol{R} + \tfrac{1}{2}\boldsymbol{p})\, f^*(\boldsymbol{R} - \tfrac{1}{2}\boldsymbol{p})\rangle = F_1(\boldsymbol{R})\, \delta(\boldsymbol{p}) . \tag{2.44}$$

Taking a additional averaging over the ensemble of realizations of the rough screen in eqs. (2.43) and (2.44), we obtain

$$\Gamma_1(\boldsymbol{R}, \boldsymbol{p}, L) = \int F_1(\boldsymbol{R}')\, \langle I(\boldsymbol{R}', L)\rangle\, \Gamma_{\mathrm{sph}}(\boldsymbol{R} - \boldsymbol{R}', \boldsymbol{p}, L)\, \mathrm{d}^2R' . \tag{2.45}$$

2.2.3. *Effect of extended size of a reflector*

To be clear, we shall consider a specular reflector with the Gaussian reflection factor

$$f(\boldsymbol{\rho}) = \exp(-\rho^2/a^2) . \tag{2.46}$$

In view of eq. (2.18), the average intensity of a reflected wave that has been emitted by a point source is

$$\begin{aligned}\langle I_s(\boldsymbol{\rho})\rangle &= \langle |u_s^2(\boldsymbol{\rho})| \rangle \\ &= \int f(\boldsymbol{R} + \tfrac{1}{2}\boldsymbol{p})\, f^*(\boldsymbol{R} - \tfrac{1}{2}\boldsymbol{p}) \\ &\quad \times \langle g(0, \boldsymbol{R} + \tfrac{1}{2}\boldsymbol{p}, L)\, g(\boldsymbol{\rho}, \boldsymbol{R} + \tfrac{1}{2}\boldsymbol{p}, L)\, g^*(0, \boldsymbol{R} - \tfrac{1}{2}\boldsymbol{p}, L) \\ &\quad \times g^*(\boldsymbol{\rho}, \boldsymbol{R} - \tfrac{1}{2}\boldsymbol{p}, L)\rangle\, \mathrm{d}^2R\, \mathrm{d}^2p .\end{aligned} \tag{2.47}$$

Making use of the small-angle approximation, we represent the random Green function in the form

$$g(\boldsymbol{\rho}_0, \boldsymbol{\rho}, x) = A(\boldsymbol{\rho}_0, \boldsymbol{\rho}, x)\, \frac{k}{2\pi \mathrm{i} x} \exp\left[\frac{\mathrm{i}k}{2x}\,(\boldsymbol{\rho} - \boldsymbol{\rho}_0)^2\right], \tag{2.48}$$

where $A(\boldsymbol{\rho}_0, \boldsymbol{\rho}, x)$ is a function statistically uniform in both $\boldsymbol{\rho}_0$ and $\boldsymbol{\rho}$ introduced to take into account the effect of the random inhomogeneities of the medium.

Substituting eqs. (2.48) and (2.46) into (2.47) yields

$$\begin{aligned}\langle I_s(\boldsymbol{\rho})\rangle = \left(\frac{k}{2\pi L}\right)^4 \int \exp\left[-\frac{2R^2}{a^2} - \frac{p^2}{2a^2} + \frac{2\mathrm{i}k}{L}\,(\boldsymbol{R}\cdot\boldsymbol{p}) - \frac{\mathrm{i}k}{L}\,(\boldsymbol{\rho}\cdot\boldsymbol{p})\right] \\ \times \langle A(0, \boldsymbol{R} + \tfrac{1}{2}\boldsymbol{p}, L)\, A(\boldsymbol{\rho}, \boldsymbol{R} + \tfrac{1}{2}\boldsymbol{p}, L) \\ \times A^*(0, \boldsymbol{R} - \tfrac{1}{2}\boldsymbol{p}, L)\, A^*(\boldsymbol{\rho}, \boldsymbol{R} - \tfrac{1}{2}\boldsymbol{p}, L)\rangle\, \mathrm{d}^2R\, \mathrm{d}^2p\,. \end{aligned} \tag{2.49}$$

Since $A(\boldsymbol{\rho}_0, \boldsymbol{\rho}, x)$ is statistically uniform, the preceding average depends only on $\boldsymbol{\rho}$ and $\boldsymbol{p}$, i.e., $\langle AAA^*A^*\rangle = B_A(\boldsymbol{\rho}, \boldsymbol{p}, L)$. In the circumstance, integration in (2.49) with respect to R gives

$$\langle I_s(\boldsymbol{\rho})\rangle = I_s^0(0)\, K(\boldsymbol{\rho}, L)\,,$$

where

$$I_s^0(0) = \left(\frac{k}{4\pi L}\right)^2 \frac{\Omega^2}{1 + \Omega^2}$$

is the intensity of a wave reflected in a vacuum, $\Omega = ka^2/L$, and

$$K(\boldsymbol{\rho}, L) = \int B_A(\boldsymbol{\rho}, \boldsymbol{p}, L)\, \mu(\boldsymbol{p}, L) \exp\left[-\frac{\mathrm{i}k}{L}\,(\boldsymbol{\rho}\cdot\boldsymbol{p})\right] \mathrm{d}^2p \tag{2.50}$$

is a coefficient describing backscatter enhancement and the redistribution of the average intensity of the reflected wave in the plane of the transmitter. The function

$$\mu(\boldsymbol{p}, L) = \frac{1}{2\pi a_{\mathrm{eff}}^2} \exp\left(-\frac{p^2}{2a_{\mathrm{eff}}^2}\right), \qquad \int_{-\infty}^{\infty} \mu\, \mathrm{d}^2p = 1\,,$$

indicates that the reflected wave is formed not by the whole mirror but, rather,

by an area with effective radius

$$a_{\text{eff}} = a[1 + (ka^2/L)^2]^{-1/2} . \tag{2.51}$$

Some properties of $B_A(\boldsymbol{\rho}, \boldsymbol{p}, L)$ are discussed below. It should be obvious that $B_A(\boldsymbol{\rho}, 0, L) = \langle J(\boldsymbol{\rho}, L) J(0, L)\rangle$ and the value of $B_A(0, 0, L)$ equals the mean square of relative intensity of a spherical wave $\langle J^2(0, L)\rangle$ at a distance L from the source. At higher p, the function $B_A(0, \boldsymbol{p}, L)$ tends to zero at a characteristic rate $\sim \rho_c(L)$. Specifically, if the mirror is in the range of saturated fluctuations of intensity of an emanating wave, the laws of Gaussian statistics may be applied to the averages (2.47) and (2.49) to give

$$B_A(0, \boldsymbol{p}, L) = 2 \exp\{-2[p/\rho_c(L)]^{5/3}\} .$$

In agreement with eq. (2.43), the backscatter enhancement factor is given by

$$R_{\text{bsc}} = K(0, L) = \int B_A(0, \boldsymbol{p}, L)\, \mu(\boldsymbol{p}, L)\, \mathrm{d}^2 p . \tag{2.52}$$

Clearly, the absolute effect of enhanced backscatter will be realized in the reflection from a mirror if $\mu(\boldsymbol{p}, L)$ singles out the value of $B_A(0, 0, L)$ corresponding to $\boldsymbol{p} = 0$. This is feasible if the size of the bright spot on the mirror is smaller than the coherence radius, i.e.,

$$a_{\text{eff}} \ll \rho_c(L) . \tag{2.53}$$

Then the absolute enhancement factor will be given by the familiar expression of eq. (2.5), namely $K_{\text{bsc}} = \langle J^2\rangle > 1$.

Condition (2.53) is not always valid. In the range of saturated fluctuations of intensity, the absolute effect of enhanced backscattering will be observed only for small ($a < \rho_c$) and substantially large ($a \gg \sigma_\rho$) mirrors. Moreover, in the interval $\rho_c < a < \sigma_\rho$ enhanced backscatter gives way to reduction of scattered intensity and $K < 1$. The situation is illustrated in fig. 2.12 by a_{eff}/ρ_c and K plotted as functions of $\log(a/\rho_c)$ for $\gamma = \sigma_\rho/\rho_c \cong 10$.

A reduction of the average backscattered intensity (compared with that in vacuum) in the interval $\rho_c < a < \sigma_\rho$ may be explained by analogy with eq. (2.36) as a reduction of the average intensity of the reflected wave due to random walk of the rays. Furthermore, it is easy to demonstrate that for any size of the mirror a relative effect of enhanced backscattering takes place, namely,

$$K_r(L) = \langle I_s(0)\rangle / I_1(0, L) > 1 . \tag{2.54}$$

Here, $I_1(\boldsymbol{\rho}, L) = \Gamma_1(\boldsymbol{\rho}, 0, L)$ is the average intensity of the reflected wave calculated under the assumption that random inhomogeneities of the medium encountered by the emanant and reflected waves are statistically independent.

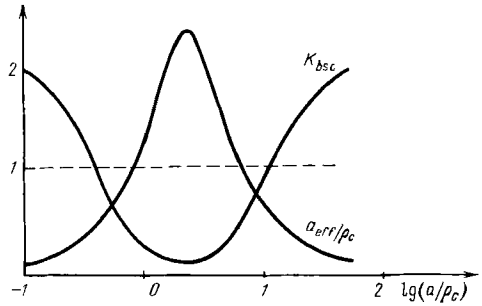

Fig. 2.12 Transition from enhancement ($K_{bsc} > 1$) to attenuation ($K_{bsc} < 1$) for greater ratios of mirror radius a to coherence radius ρ_c.

For a spherical wave GOCHELASHVILI and SHISHOV [1981] have noted the existence of enhanced backscattering whatever the size of the scattering body. Enhanced backscatter from extended bodies is also discussed in the monographs of MIRONOV [1981], BANAKH and MIRONOV [1987] and ZUEV, BANAKH and POKASOV [1988]. Recently, AGROVSKII, BOGATOV, GURVICH, KIREEV and MYAKININ [1991] and BOGATOV, GURVICH, KASHKAROV and MYAKININ [1991] have carried out a more accurate theoretical and experimental analysis and demonstrated that the backscatter coefficient K reduces when the size of the body is comparable with the coherence radius of the prime wave.

Finally, mention should be made about the spatial redistribution of the average intensity of a wave reflected from an unlimited mirror. In this case, $\mu(\boldsymbol{\rho}, L) = \delta(\boldsymbol{\rho})$ and from eq. (2.50) it follows that

$$K(\boldsymbol{\rho}, L) = B_A(\boldsymbol{\rho}, 0, L) = \langle J(\boldsymbol{\rho}, L) J(0, L) \rangle .$$

As in the case of the point scatterer defined by eq. (2.7), the quantity $K(\boldsymbol{\rho}, L)$ repeats the profile of the correlation function of the relative intensity of the spherical wave at a distance L from the source.

2.2.4. *Effect of long-distance correlations and partial reversal of the wavefront*

The effect of enhanced backscattering can be realized if the aperture b of the source does not exceed $\rho_c(L)$. When $b > \rho_c$, the enhancement effect gives way to the effect of long correlations (KRUPNIK and SAICHEV [1981], KRAVTSOV and SAICHEV [1982a,b]). With this effect, in addition to a narrow peak of radius $\sim \rho_c(L)$, the coherence function of the reflected wave acquires in the plane of the transmitter $x = 0$ a low but wide pedestal corresponding to long

correlations. It is displayed in full measure when the intensity fluctuations of an emitted wave are saturated. In what follows we confine ourselves to the analysis of this situation.

To be more specific we shall assume that the reflector is pointsize, i.e., $f(\boldsymbol{\rho}) = \delta(\boldsymbol{\rho})$, and that a collimated wave pencil of radius b is radiated in the plane $x = 0$. The coherence function of the reflected wave is given by eq. (2.42), where

$$\Gamma_1(\boldsymbol{R}, \boldsymbol{p}, L) = \langle I(0, L)\rangle \left(\frac{k}{2\pi L}\right)^2 \exp\left[-\left(\frac{p}{\rho_c(L)}\right)^{5/3} + \frac{ik}{L}(\boldsymbol{R}\cdot\boldsymbol{p})\right] \tag{2.55}$$

and the coherence-function component responsible for the effects of double passage is

$$\Gamma_2(\boldsymbol{R}, \boldsymbol{p}, L) = v^*(\boldsymbol{\rho}_1)\, v(\boldsymbol{\rho}_2)\,. \tag{2.56}$$

Here,

$$v(\boldsymbol{\rho}) = \left(\frac{k}{2\pi L}\right)^2 \int u_0(\boldsymbol{\rho} - \boldsymbol{p}) \exp\left[-\left(\frac{p}{\rho_c}\right)^{5/3} - \frac{ik}{L}(\boldsymbol{p}\cdot\boldsymbol{\rho})\right] \mathrm{d}^2 p\,, \tag{2.57}$$

and $\boldsymbol{\rho}_1 = \boldsymbol{R} + \frac{1}{2}\boldsymbol{p}$ and $\boldsymbol{\rho}_2 = \boldsymbol{R} - \frac{1}{2}\boldsymbol{p}$ are the coordinates of points in the plane $x = 0$, in which the mutual coherence of the field of the reflected wave is determined.

Suppose that the radius of the radiated beam is sufficiently large, $b \gg \rho_c$, then

$$v(\boldsymbol{\rho}) = u_0(\boldsymbol{\rho})\, W_\rho(\boldsymbol{\rho}, L)\,,$$

where $W_\rho(\boldsymbol{\rho}, L)$ is given by eqs. (2.38) and (2.39). Thus,

$$\Gamma_2 = u_0^*(\boldsymbol{\rho}_1)\, u_0(\boldsymbol{\rho}_2)\, W_\rho(\boldsymbol{\rho}_1, L)\, W_\rho(\boldsymbol{\rho}_2, L)\,. \tag{2.58}$$

Simple estimates obtained with the aid of eqs. (2.55), (2.58), and (2.36) indicate that for $b \gg \rho_c(L)$ we have $\Gamma_2(0, 0, L) \ll \Gamma_1(0, 0, L)$ and the backscatter enhancement effect is virtually indistinguishable. It is worth noting that the coherence function of the reflected wave considered as a function of distance between points of observation $p = |\boldsymbol{\rho}_1 - \boldsymbol{\rho}_2|$ consists of a narrow peak Γ_1, decreasing with p at a rate $\rho_c(L)$, and a wide pedestal Γ_2. A typical plot of Γ_s as a function of p for $\boldsymbol{R} = 0$ and $b \gg \rho_c(L)$ is shown in fig. 2.13.

We note that the component Γ_2 of the coherence function is proportional to the product of the primary fields,

$$\Gamma_2 \propto u_0^*(\boldsymbol{\rho}_1)\, u(\boldsymbol{\rho}_2)\,,$$

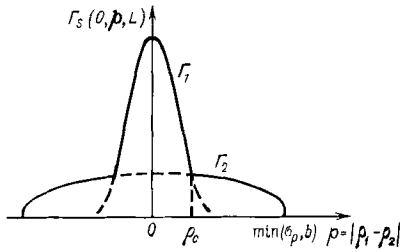

Fig. 2.13. Typical profile Γ_s of the coherence of backscattered field as a function of the distance between observation points $p = |\rho_1 - \rho_2|$.

which may be treated as the complex conjugate function of coherence of the emitted wave. As a result, the effect of long correlations may be thought of as coming from a partial reversal of the wavefront of the reflected wave with respect to the prime wave (KRAVTSOV and SAICHEV [1982a,b, 1985]).

We interpret the mechanism of partial reversal by way of a simple example of a wave produced by two mutually coherent point sources at points $\boldsymbol{r}_1$ and $\boldsymbol{r}_2$. Let such a wave be incident upon a scatterer at point $\boldsymbol{r}_s$ in a random inhomogeneous medium. If φ_1 and φ_2 are the phases of the emitted waves, the complex amplitude of the scattered wave at an arbitrary point $\boldsymbol{r}$ is

$$u_s(\boldsymbol{r}) = [e^{i\varphi_1} G(\boldsymbol{r}_1, \boldsymbol{r}_s) + e^{i\varphi_2} G(\boldsymbol{r}_2, \boldsymbol{r}_s)] G(\boldsymbol{r}_s, \boldsymbol{r}) .$$

If we assume that the point of observation coincides either with $\boldsymbol{r}_1$ or with $\boldsymbol{r}_2$, two opposite paths occur in the random inhomogeneous medium, $\boldsymbol{r}_1 \to \boldsymbol{r}_s \to \boldsymbol{r}_2$ and $\boldsymbol{r}_2 \to \boldsymbol{r}_s \to \boldsymbol{r}_1$. The mutually coherent components of the scattered wave are

$$u_{s,\mathrm{coh}}(\boldsymbol{r}_1) = e^{i\varphi_2} G_{21} ,$$

$$u_{s,\mathrm{coh}}(\boldsymbol{r}_2) = e^{i\varphi_1} G_{12} ,$$

$$G_{mn} = G(\boldsymbol{r}_m, \boldsymbol{r}_s) G(\boldsymbol{r}_s, \boldsymbol{r}_n) = |G_{mn}| e^{i\varphi_{mn}} .$$

By the reciprocity theorem we have $G_{12} = G_{21}$, $\varphi_{12} = \varphi_{21}$ and $|G_{12}| = |G_{21}|$, so that

$$u_{s,\mathrm{coh}}(\boldsymbol{r}_1) = |G_{12}| e^{i(\varphi_2 + \varphi_{12})} ,$$

$$u_{s,\mathrm{coh}}(\boldsymbol{r}_2) = |G_{12}| e^{i(\varphi_1 + \varphi_{12})} .$$

Denoting $\varphi = \varphi_1 + \varphi_2 + \varphi_{12}$ and rewriting $\varphi_1 + \varphi_{12} = -\varphi_2 + \varphi$ and $\varphi_2 + \varphi_{12} = -\varphi_1 + \varphi$, we note that the phases of the mutually coherent com-

ponents of the scattered wave are reversed with respect to the phases of the emitted waves accurate to within the additive phase φ,

$$u_{s,coh}(\boldsymbol{r}_1) = |G_{12}|\, e^{-i\varphi_1 + i\varphi},$$

$$u_{s,coh}(\boldsymbol{r}_2) = |G_{12}|\, e^{-i\varphi_2 + i\varphi}.$$

A similar semiquantitative explanation of the long correlation effect may be extended to the case of a collimated wide beam of radius $b \gg \rho_c(L)$. Imagine that the aperture of the source is divided into partial beams of radius $\sim \rho_c$. Let ρ_m and ρ_n be the centers of mth and nth partial beams separated by a large distance $[|\rho_m - \rho_n| \gg \rho_c(L)]$. Since the phases propagating in the opposite coherent paths $\rho_m \leftrightarrow r_s \leftrightarrow \rho_n$ are reversed, the coherence function of the scattered waves at points $\rho_1 = \rho_m$ and $\rho_2 = \rho_n$ is proportional to $u_0^*(\rho_1)\, u_0(\rho_2)$. A coherence path occurs, provided that the beams emanating from points ρ_m and ρ_n can arrive at the scatterer as the result of a random walk in the random inhomogeneous medium. Therefore, the coherence function defined by eq. (2.58) is proportional also to the product of the probability densities of lateral shifts of the beams. In the field of the scattered wave long correlations occur when $\sigma(L) \gg \rho_c(L)$; i.e., when conditions (2.10) and (2.11) of saturated fluctuations are satisfied, $\gamma = \sigma_\rho/\rho_c \gg 1$.

2.2.5. *Enhanced backscattering in the focal plane of a lens*

As has been pointed out for a wide beam with $b \gg \rho_c(L)$, no enhancement of backscattering is observed. However, a partial reversal of the wavefront in the field of the scattered wave gives rise to a highly coherent component that can be focused by a lens. This leads to another effect because of the partial reversal of the wavefront, namely, to an enhancement of the average intensity in the focal plane of the lens.

Let the scattered wave be incident upon a lens placed in the $x = 0$ plane. The lens aperture coincides with that of the source and is described by the function $u_0(\rho)$. The field in the focal plane of the lens is given by

$$u_F(\boldsymbol{\rho}) = \int u_0(\boldsymbol{\rho}')\, u_s(\boldsymbol{\rho}') \exp\left[-\frac{ik}{F}(\boldsymbol{\rho}\cdot\boldsymbol{\rho}')\right] d^2\rho'.$$

For a plane-emitted wave $[b \gg \sigma_\rho(L)]$, when the common enhancement effect is negligible, from eqs. (2.42), (2.55), and (2.58), it follows that the average

intensity of the field in the focal plane is proportional to

$$\langle J_F(\boldsymbol{\rho})\rangle = \langle |u_F(\boldsymbol{\rho})|^2\rangle$$

$$= J_{F1}(\boldsymbol{\rho}) + J_{F2}(\boldsymbol{\rho}),$$

where

$$J_{F1}(\boldsymbol{\rho}) = |u_0(0)|^2 \left| u_0\left(\frac{L}{F}\,\boldsymbol{\rho}\right)\right|^2,$$

$$J_{F2}(\boldsymbol{\rho}) = |u_0(0)|^4 \exp\left[-2\left(\frac{L\rho}{F\rho_c(L)}\right)^{5/3}\right].$$

In the middle of the focal plane ($\boldsymbol{\rho} = 0$) the average intensity of the scattered wave is twice the intensity in the homogeneous medium, $\langle J_F(0)\rangle = 2|u_0(0)|^4$. This implies the absolute effect of backscatter enhancement with $K_F = 2$.

The component $J_{F1}(\boldsymbol{\rho})$ corresponds to a wide pedestal with radius $\sim bF/L$, which is about the size of a spot produced by a spherical wave from a point scatterer in a homogeneous medium. The intensity $J_{F2}(\boldsymbol{\rho})$ forms a sharp peak corresponding to the quasi-plane (resulting from a reversal of the wavefront) component of the scattered wave with coherence radius $\sigma_\rho(L)$.

This enhancement effect in the focal plane may be treated as a common backscatter enhancement, if the primary field is assumed to be that of a point scatterer in the focal plane rather than the field of the plane-emitted wave. In turn, the ordinary backscatter enhancement, which was developed in the common scheme of a point source, namely, random inhomogeneous medium, point scatter, may be explained as the effect of focusing the reversed component of the scattered wave near the source (KRUPNIK [1985]).

The reversed component of the scattered wave is present in any plane between the source and scatterer. Near the scatterer it has a random character and a small coherence radius of about $\rho_c(L)$, similar to the wave incident upon the scatterer. Closer to the source the reversed component acquires a higher spatial coherence with simultaneous focusing on the source.

Despite the random character of this component, it can be detected as follows. Let $u(\boldsymbol{\rho}, x)$ be the complex amplitude of the prime wave at distance $x = \frac{1}{2}L$ from both source and scatterer, and let $u_s(\boldsymbol{\rho}, x)$ be the complex amplitude of the scattered wave in the plane with this coordinate. Recognizing that the reversed component of the scattered wave is proportional to $u^*(\boldsymbol{\rho}, x)$, one may verify (KRUPNIK [1985]) that in the presence of the reversed wave the

moment function

$$\langle u_s(\boldsymbol{\rho}_1, x)\, u(\boldsymbol{\rho}_1, x)\, u_s^*(\boldsymbol{\rho}_2, x)\, u^*(\boldsymbol{\rho}_2, x)\rangle$$
$$= \langle v(\boldsymbol{\rho}_1, x)\, u(\boldsymbol{\rho}_1, x)\, v^*(\boldsymbol{\rho}_2, x)\, u^*(\boldsymbol{\rho}_2, x)\rangle$$
$$\sim \langle I(\boldsymbol{\rho}_1, x)\rangle\, \langle (I(\boldsymbol{\rho}_2, x)\rangle$$

remains almost invariable when the points ρ_1 and ρ_2 are separated.

Thus, the enhancement of average backscattered intensity and the long correlation effect are two sides of the same coin, namely, the partial reversal of the wavefront of the scattered wave.

Using the concept of partial reversal as a point of departure provides an insight into the nature of enhanced backscattering in the conditions where the source in an extended antenna (YEH [1983], KRAVTSOV and SAICHEV [1985]). Suppose that $u_0(\boldsymbol{\rho})$ describes the distribution of current in an antenna in the transmitting mode. Then, in view of eq. (2.25) the scattered signal received by the antenna is proportional to

$$v_s = \int u_0(\boldsymbol{\rho})\, u_s(\boldsymbol{\rho})\, f(\boldsymbol{\rho})\, \mathrm{d}^2\rho$$
$$= \int f(\boldsymbol{\rho})\, u^2(\boldsymbol{\rho}, L)\, \mathrm{d}^2\rho\,, \tag{2.59}$$

and the average intensity of this signal is

$$\langle J_s\rangle = \langle |v_s|^2\rangle$$
$$= \int\int \langle f(\boldsymbol{\rho}')\, f^*(\boldsymbol{\rho}'')\rangle\, \langle u^2(\boldsymbol{\rho}, L)\, u^{*2}(\boldsymbol{\rho}, L)\rangle\, \mathrm{d}^2\rho'\, \mathrm{d}^2\rho''\,.$$

Specifically, for a rough scatterer, eq. (2.44), we obtain

$$\langle J_s\rangle = \int F(\boldsymbol{\rho})\, \langle I^2(\boldsymbol{\rho}, L)\rangle\, \mathrm{d}^2\rho\,. \tag{2.60}$$

Let us compare this quantity with the intensity of an oncoming signal

$$J_1 = \int F(\boldsymbol{\rho})\, \langle I(\boldsymbol{\rho}, L)\rangle^2\, \mathrm{d}^2\rho\,,$$

which has been calculated on the assumption that the random inhomogeneities in forward and reverse paths are statistically independent. In a random inhomogeneous medium $\langle I^2\rangle > \langle I\rangle^2$, therefore, the relative backscatter enhancement effect with $K_r = J_s/J_1 > 1$ can be observed independently of antenna size.

If the radiated wave is such that the average intensity $\langle I(\boldsymbol{\rho}, L)\rangle$ coincides with the intensity in the homogeneous medium $I_0(\boldsymbol{\rho}, L)$, then we obtain an absolute enhancement effect.

Assume that the antenna radiates a collimated beam of radius b. From eq. (2.36) it follows that $\langle I\rangle = I_0$ for sufficiently small radii ($b < \rho_c$) and sufficiently large ($b > \sigma_\rho$) radii. The first case corresponds to the ordinary backscatter enhancement for essentially a point source, and the second case corresponds to an absolute effect of enhanced backscattering in the middle of a focal plane of a large lens.

In scattering from solids embedded in a turbulent medium the partial reversal of the wavefront also may be considered as an echo effect observed in various physical systems.

2.2.6. *Enhancement of radiant intensity*

The partial reversal of a backscattered wave also produces the effect of enhancement of radiant intensity allied to the effect of backscatter enhancement in the middle of a focal plane of the lens. Representing the radiant intensity of a backscattered wave in the plane of radiation $x = 0$ in the form

$$\mathscr{I}_s(\boldsymbol{R}, \boldsymbol{\theta}) = \left(\frac{k}{2\pi}\right)^2 \int \Gamma_s(\boldsymbol{R}, \boldsymbol{p})\, \mathrm{e}^{-\mathrm{i}k(\boldsymbol{\theta}\cdot\boldsymbol{p})}\, \mathrm{d}^2 p\,. \tag{2.61}$$

As an example, let us discuss the case of a plane wave $u(\boldsymbol{\rho}, 0) = 1$ emitted in the plane $x = 0$, with the reflector being a phase screen, i.e., a statistically uniform rough surface which causes the phase of the reflected wave to be changed by a random quantity $\varphi(\boldsymbol{\rho})$, i.e., a surface with $f(\boldsymbol{\rho}) = \exp[\mathrm{i}\varphi(\boldsymbol{\rho})]$. Denoting the structural function of phase distortions $\langle[\varphi(\boldsymbol{r} + \boldsymbol{s}) - \varphi(\boldsymbol{\rho})]^2\rangle$, introduced by the reflecting surface, by $d_\varphi(\boldsymbol{s})$ we obtain

$$\langle f(\boldsymbol{\rho} + \boldsymbol{s}) f^*(\boldsymbol{\rho})\rangle = \exp[-\tfrac{1}{2} d_\varphi(\boldsymbol{s})]\,.$$

We assume that $d_\varphi(\boldsymbol{s})$ increases monotonically with $\boldsymbol{s}$, whereas $B_f(\boldsymbol{s})$ falls off to zero at a characteristic rate ρ_f.

After straightforward transformations exploiting the statistical homogeneity of the radiated wave $u(\boldsymbol{\rho}, L)$ with respect to $\boldsymbol{\rho}$, the coherence function of the scattered wave can be rewritten (SAICHEV [1980])

$$\Gamma_s(\boldsymbol{p}) = \int B_f(\boldsymbol{s})\, \Phi(\boldsymbol{p}, \boldsymbol{s}, L)\, \mathrm{d}^2 s\,, \tag{2.62}$$

where

$$\Phi(\boldsymbol{p}, \boldsymbol{s}, L) = \int \langle g(\boldsymbol{\rho} + \boldsymbol{p}, \boldsymbol{s}, L)\, g^*(\boldsymbol{\rho}, 0, L)\, u(\boldsymbol{s}, L)\, u^*(0, L)\rangle \, \mathrm{d}^2\rho \,.$$

From the orthogonality of the Green function in the parabolic equation formalism, i.e.,

$$\int g(\boldsymbol{\rho}, \boldsymbol{\rho}_1, x)\, g^*(\boldsymbol{\rho}, \boldsymbol{\rho}_2, x)\, \mathrm{d}^2\rho = \delta(\boldsymbol{\rho}_1 - \boldsymbol{\rho}_2) \,,$$

it follows that

$$\Phi(0, \boldsymbol{s}, L) = \langle I(0, L)\rangle\, \delta(\boldsymbol{s}) = \delta(\boldsymbol{s}) \,. \tag{2.63}$$

By virtue of eq. (2.62) the average reflected intensity

$$\Gamma_s(0) = \langle I_s(\boldsymbol{\rho})\rangle = B_f(0) = 1$$

coincides with the intensity of a plane wave reflected in a homogeneous medium from an ideal mirror of $f \equiv 1$. This implies that the ordinary enhancement effect is completely absent in the case under consideration.

The situation is completely different for the radiant intensity of the reflected wave. Substituting eq. (2.55) into eq. (2.54) yields

$$\mathscr{I}_s(\boldsymbol{\theta}) = \left(\frac{k}{2\pi}\right)^2 \int B_f(\boldsymbol{s})\, M(\boldsymbol{s}, \boldsymbol{\theta}, L)\, \mathrm{d}^2 s \,. \tag{2.64}$$

The quantity

$$\begin{aligned} M(\boldsymbol{s}, \boldsymbol{\theta}, L) &= \int \Phi(\boldsymbol{p}, \boldsymbol{s}, L) \exp[-\mathrm{i}k(\boldsymbol{\theta}\cdot\boldsymbol{p})]\, \mathrm{d}^2 p \\ &= \langle u(\boldsymbol{s}, L)\, u^*(0, L)\, u_\theta(\boldsymbol{s}, L)\, u_\theta^*(0, L)\rangle \end{aligned} \tag{2.65}$$

is the moment function of plane waves propagating at an angle θ to one another,

$$u_\theta(\boldsymbol{\rho}, 0) = \exp[-\mathrm{i}k(\boldsymbol{\theta}\cdot\boldsymbol{\rho})] \,, \qquad u_\theta(\boldsymbol{\rho}, x)|_{\theta=0} = u(\boldsymbol{\rho}, x) \,.$$

The radiant intensity of a wave reflected strictly backwards is

$$\mathscr{I}_s(0) = \left(\frac{k}{2\pi}\right)^2 \int B_f(\boldsymbol{s})\, B_u(\boldsymbol{s}, L)\, \mathrm{d}^2 s \,. \tag{2.66}$$

The quantity

$$B_u(\boldsymbol{s}, L) = \langle u^2(\boldsymbol{s}, L)\, u^{*2}(0, L)\rangle$$

is the coherence function of the squared wave function incident upon a reflecting surface. This function varies in s at a rate of $\rho_c(L)$. If the reflecting surface is constituted by small-scale inhomogeneities, then $\rho_f \ll \rho_c(L)$ and $B_f(s)$ singles out in eq. (2.66) the value

$$B_u(0, L) = \langle I^2(0, L)\rangle \equiv K > 1\,,$$

so that $\mathscr{J}_s(0)$ is K_{bsc} times the radiant intensity $J_s^0(0)$ of the wave backscattered in a vacuum.

For an arbitrary angle θ and a small-scale reflector with $\rho_f \ll \rho_c(L)$, from eq. (2.66) it follows that

$$\mathscr{J}_s(\theta) = K(\theta)\,\mathscr{J}_s^0(\theta)\,,$$

where

$$\mathscr{J}_s^0(\theta) = \left(\frac{k}{2\pi}\right)^2 \int B_f(s)\, e^{-ik(\theta\cdot s)}\, d^2s$$

is the radiant intensity of the wave reflected in a vacuum. Its characteristic angular spread is $\theta_0 \sim 1/k\rho_f$.

The coefficient $K(\theta) = \langle I(0, L)\, I_\theta(0, L)\rangle$ with $I_\theta(\rho, L) = |u_\theta^2(\rho, L)|$ describes the angular distribution of the radiant intensity resulting from the double passage of the wave through the same random inhomogeneities. From eq. (2.63) it follows that

$$\int \mathscr{J}(\theta)\, d^2\theta = \Gamma_s(0) = \int \mathscr{J}_s^{(0)}(\theta)\, d^2\theta\,,$$

in addition to the enhancement of the backscattered radiant intensity, the coefficient $K(\theta)$ describes some reduction in the intensity ($K < 1$) of the backscatter compared with $\mathscr{J}_s^0(\theta)$, as depicted in fig. 2.2c.

Finally, let us determine the radiant intensity of a reflected wave for the case of saturated fluctuations of the incident wave. Applying the laws of Gaussian statistics to the average in eq. (2.65) yields

$$\mathscr{J}_s(\theta) = \mathscr{J}_1(\theta, L) + \mathscr{J}_2(\theta, L)\,. \tag{2.67}$$

The quantity

$$\mathscr{J}_1(\theta, L) = \int \mathscr{J}_0(\theta')\, W_\theta(\theta - \theta', 2L)\, d^2\theta'$$

represents the radiant intensity of an initial plane wave that has passed in a

random inhomogeneous medium a distance $2L$ without reflections, subject to the condition that a phase screen is placed midway, thus introducing a phase distortion $\varphi(\boldsymbol{\rho})$. The expression for $\mathscr{J}_1$ also includes the probability density of oncoming angles $W_\theta(\boldsymbol{\theta}, 2L)$, whose characteristic scale in θ is $\sigma_\theta(2L)$, as outlined in eq. (2.41).

The second component of the radiant intensity,

$$\mathscr{J}_2(\boldsymbol{\theta}, L) = \left(\frac{k}{2\pi}\right)^2 \int B_f(\boldsymbol{s}) \times \exp[-\tfrac{1}{2}d(\boldsymbol{s}+\boldsymbol{\theta}L, \boldsymbol{s}, L) - \tfrac{1}{2}d(\boldsymbol{s}-\boldsymbol{\theta}L, \boldsymbol{s}, L) - \mathrm{i}k(\boldsymbol{\theta}\cdot\boldsymbol{s})]\,\mathrm{d}^2 s,$$

takes into account the double passage of the wave through the random inhomogeneous medium. This component is responsible for the backward enhancement of radiant intensity.

The radiant intensity of a wave reflected from an ideal mirror ($f \equiv 1$) in a random inhomogeneous medium is plotted in fig. 2.14. It consists of a narrow peak of $\mathscr{J}_2(\boldsymbol{\theta}, L)$ with semiangular width $\theta_c \sim \rho_c/L$ and a wide pedestal of $\mathscr{J}_1(\boldsymbol{\theta}, L) = W_\theta(\boldsymbol{\theta}, 2L)$ with characteristic angular scale $\sigma_\theta \sim 1/k\rho_c(L)$. There is no absolute enhancement of radiant intensity scattered strictly backwards in this case, but there is a relative enhancement with coefficient $K_r = \mathscr{J}_s(0)/\mathscr{J}_1(0) = 2$. This effect may be interpreted as being due to a partial reversal of the reflected wavefront in the random inhomogeneous medium.

Some applications of this formalism are worth noting. LUCHININ [1979] has established a radiant-intensity enhancement for the light reflected from the bottom which, thus, passed twice through the disturbed surface of the ocean. SAICHEV [1980] has described an enhancement of the radiant intensity backscattered from a system of discrete scatterers randomly dispersed in a random inhomogeneous medium. JAKEMAN [1988] has described in depth the effect of enhancement of the radiant intensity that has twice passed through a random phase screen, before and after reflection from a mirror.

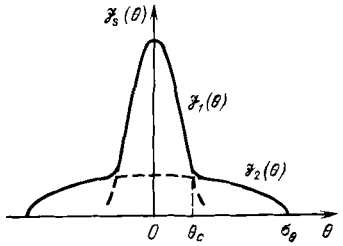

Fig. 2.14. Radiant intensity profile for a scatterer embedded in a turbulent medium.

2.2.7. *Giant backscatter enhancement in laser sounding of the ocean*

HOGE and SWIFT [1983a,b] have recorded strong fluctuations of echo pulses in laser sounding of scattering layers through the rippled surface of the ocean (fig. 2.15). They associated the strong fluctuations with a nonuniform distribution of scatterers in the horizontal. VLASOV [1985] has given a more plausible explanation by pointing out the important role of the double passage of the light through the wavy surface of the ocean, which has the same effect as a random phase screen. (Random focusing of light caused by a disturbed ocean surface also has been discussed by GEHLHEAR [1982].)

The theory of enhanced backscattering in the presence of a phase screen outlined in § 2.1.2 is not well suited to handle laser sounding of the ocean because at the air–water interface the width b of a laser beam is usually small compared with the characteristic scale of surface roughness, l_s. More extensive work has been done by BUNKIN, VLASOV and MIRKAMILOV [1987] and APRESYAN and VLASOV [1988], and, therefore, our discussion will be in line with these studies.

Suppose that the ocean surface is irradiated with a Gaussian beam $u = u_0 \exp(-\rho^2/b^2)$ of width b. Given $b \ll l_s$, the distortions of the eikonal $\psi(\boldsymbol{\rho})$ of the incident wave may be described by second-order polynomials

$$\psi(\boldsymbol{\rho}) = \psi_0 + \boldsymbol{\theta}\cdot\boldsymbol{\rho} + \tfrac{1}{2}(\alpha_1\rho_1^2 + \alpha_2\rho_2^2)\,.$$

Here, the directions of ρ_1 and ρ_2 are taken to coincide with those of the main lines of curvature of $\psi(\boldsymbol{\rho})$. The vector $\boldsymbol{\theta} = (\theta_1, \theta_2)$ describes the angular deviations of the beam from the vertical x-axis, whereas $\alpha_{1,2} = 1/R_{1,2}$, where $R_{1,2}$

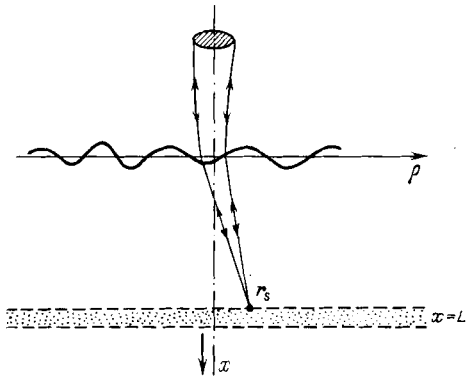

Fig. 2.15. Backscattering of a narrow laser beam from scatterers under a rough sea surface.

are the main curvature radii of the phase front immediately behind the phase screen.

In this approximation the beam remains Gaussian at any distance from the rough surface, its intensity in a plane at $x = L$ being

$$I(\boldsymbol{\rho}, L) = |u_0|^2 \gamma_1(\rho_1 - \theta_1 L)\, \gamma_2(\rho_2 - \theta_2 L)\,, \tag{2.68}$$

where the quantities

$$\gamma_{1,2}(y) = \exp[-y^2/b^2 \varkappa_{1,2}^2(L)]/\varkappa_{1,2}(L)$$

and

$$\varkappa_{1,2}^2(L) = \sqrt{(1 - \alpha_{1,2} L)^2 + \beta^2}\,, \quad \beta = 2L/kb^2\,,$$

characterize the compression or expansion of the beam in ρ_1 and ρ_2.

Let $F(\boldsymbol{\rho}, L)$ be proportional to the cross section of backscattering by a unit volume of water at depth x. Then the intensity $I_s(L)$ of the echo signal from a depth of L in monostatic measurement is given by

$$I_s(L) = \int F(\boldsymbol{\rho}, L)\, I^2(\boldsymbol{\rho}, L)\, \mathrm{d}^2\rho\,. \tag{2.69}$$

Unlike eq. (2.60), this expression has not been averaged over all of the random inhomogeneities of the surface (over random values of slope $\theta_{1,2}$ and curvature $\alpha_{1,2}$ in the case of a narrow beam) because we wish to know not only the averages I_s but also the deviations from these values (fluctuations).

Substituting eq. (2.68) into eq. (2.69) and assuming that the scattering layer is statistically uniform, $F = \text{const.}$, we obtain for

$$K(L) = I_s(L)/I_s^0(L)\,,$$

where $I_s^0(L)$ is the intensity for the case of a plane interface ($\alpha_{1,2} = 0$),

$$K(L) = \frac{\varkappa_0^2(L)}{\varkappa_1(L)\, \varkappa_2(L)}$$

$$= \frac{1 + \beta^2}{\sqrt{[(1 - \alpha_1 L)^2 + \beta^2]\,[(1 - \alpha_2 L)^2 + \beta^2]}}\,, \tag{2.70}$$

where $b\varkappa_0(L) = b\sqrt{1 + \beta^2}$ is the radius of the diffraction-broadened, undisturbed, Gaussian beam in the plane of scatterers at $x = L$.

From eq. (2.70) it follows that if the rough surface focuses the beam in the plane of scatterers ($\alpha_1 = \alpha_2 = 1/L$), the intensity of the received signal

experiences a giant enhancement, namely, it becomes $K_{max} = (1 + \beta^2)/\beta^2$ times that for the plane interface (APRESYAN and VLASOV [1988]). In a typical sounding situation of an upper layer of the ocean with $k = 10^7\,\mathrm{m}^{-1}$, $b = 0.01$ m, and $L = 10$ m, we have $K_{max} = 2.5 \times 10^3$. Of course, practical intensity peaks are smaller because the focusing in one coordinate is often accompanied by an expansion of the beam in the other coordinate. In particular, when the random eikonal $\psi(\boldsymbol{\rho})$ is a statistically isotropic Gaussian field with correlation function

$$B_\psi(s) = \langle \psi(\boldsymbol{\rho})\, \psi(\boldsymbol{\rho} + \boldsymbol{s}) \rangle$$
$$= \langle \psi^2 \rangle - \tfrac{1}{2}\sigma_\theta^2 s^2 + \tfrac{1}{32}\sigma_\alpha^2 s^4 - \dots ,$$

the joint probability density of curvatures α_1 and α_2 (assuming $\alpha_2 > \alpha_1$) is

$$w_\alpha(\alpha_1, \alpha_2) = \frac{2(\alpha_2 - \alpha_1)}{\sqrt{\pi}\,\sigma_\alpha^3} \exp\left[-\frac{1}{\sigma_\alpha^2} (3\alpha_1^2 + 3\alpha_2^2 - 2\alpha_1\alpha_2) \right].$$

It is obvious that w_α vanishes for identical curvature radii of the wavefront, so that the compression of the beam is essentially different in various coordinates.

In a case more typical of the ocean surface, when the eikonal depends only upon one coordinate ρ_1, the enhancement factor of the received intensity

$$K(L) = \sqrt{\frac{1 + \beta^2}{(1 - \alpha L)^2 + \beta^2}}$$

is caused by the one-dimensional focusing of the sounding beam.

Complete information for the frequency of unusually large values of K may be obtained from the probability density $w_K(K)$. Let $\psi(\rho_1)$ be a random Gaussian function for which the probability density of curvature α of the wavefront is

$$w_\alpha(\alpha) = \frac{1}{\sqrt{2\pi}\,\sigma_\alpha} \exp\left(-\frac{\alpha^2}{2\sigma_\alpha^2} \right).$$

In this case, the probability density of K is given by

$$w_K(K) = g_K\left(\frac{K}{K_*}\right) \Big/ K_* , \tag{2.71}$$

where

$$g_K(K) = \frac{2\beta_* \exp(-1/2z^2)}{n^2\sqrt{2\pi(1-n^2)}} \times \exp\left[-\frac{\beta_*^2(1-n^2)}{2n^2}\right] \cosh\left(\frac{\beta_*\sqrt{1-n^2}}{zn}\right), \quad \text{for } 0 < n < 1,$$

$$= 0 \quad \text{for } n > 1.$$

Also, $K_* = \sqrt{(1+\beta_*^2 z^2)/\beta_*^2 z^2}$ is the maximum feasible value of K corresponding to the focusing of the beam in the plane of scatterers, $z = \sigma_\alpha L = L/R_*$ is the dimensionless thickness of the scattering slab, $R_* = 1/\sigma_\alpha$ is the typical depth of focusing, and $\beta_* = 2R_*/kb^2$ is the wave parameter of the beam at depth $L = R_*$.

Exceedingly large values of K can be observed for $K_* \gg 1$ or, equivalently, at $\beta_* z \ll 1$. For moderate values of K that are far from $K_* \sim 1/\beta_* z$ the probability density (2.64) is described by a relatively simple expression, corresponding to the geometrical optics approximation ($\beta_* \to 0$),

$$w_K(K) = \frac{2}{K^2 z\sqrt{2\pi}} \exp\left[-\frac{1}{2z^2}(1 + K^{-2})\right] \cosh(1/Kz^2). \qquad (2.72)$$

The plots of $w_K(K)$ for $z = 0.5$, 1, and 2 are given in fig. 2.16. The maximum has shifted toward values of K that do not exceed unity. This implies that detection of a reduction, rather than an enhancement, of the signal, compared with that due to the plane interface, is more probable. For example, at $z = 1$ the probability of obtaining $K = 1$ is 0.523. At the same time, from eq. (2.72) it is clear that for $1 \ll K \ll K_*$ the probability density falls at a comparatively

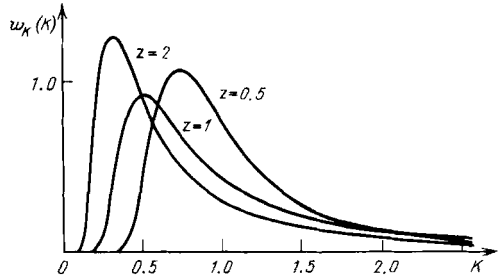

Fig. 2.16. Probability density of the backscatter enhancement factor for a surface with Gaussian statistics of the curvature.

slow rate, approximately as K^{-2}. This means that fadings of the signal, which correspond to $K < 1$, alternate with giant surges of $K \gg 1$. These rare but strong intensity surges can raise the average enhancement factor

$$\langle K \rangle = \sqrt{\frac{1 + \beta_*^2 z^2}{2\pi}} \int \frac{\exp(-\frac{1}{2}y^2)\,dy}{\sqrt{(1 - yz)^2 + \beta_*^2 z^2}}$$

significantly above unity. The plots of $\langle K(L) \rangle$ versus dimensionless depth $z = L/R_*$ for $\beta_* = 0.01$ and 0.05 are given in fig. 2.17.

A sizeable rise of $\langle K \rangle$ above unity at $z \sim 1$ and $\beta_* \ll 1$ will result in an equal measure of reduction for $z \gg 1$ (APRESYAN and VLASOV [1988]). Indeed, at a great distance where $z \gg 1$, the rough surface always causes a defocusing of the beam, even where there is a focusing action, as in the initial segment $0 < L < R_*$. The beam width increases in proportion to $\theta_f L$, with $\theta_f = 2/\sigma_\alpha b = 2R_*/b$ being a typical angle of divergence of the beam. On the other hand, the unperturbed beam expands at large depths as $\theta_0 L$, where $\theta_0 = 1/kb$ is the angle of beam divergence due to diffraction.

At large depths of the scattering layer the competing defocusing and diffraction divergence of the beam leads to

$$K \sim \theta_0/\sqrt{\theta_0^2 + \theta_f^2} = \beta_*/\sqrt{1 + \beta_*^2},$$

which becomes small for $\beta_* \ll 1$. In the case of Gaussian curvature of the rough surface α, more accurate developments yield the ultimate value as

$$\langle K(\infty) \rangle = \frac{\beta_*}{\sqrt{2\pi}} \int \frac{\exp(-\frac{1}{2}y^2)}{\sqrt{y^2 + \beta_*^2}}\,dy.$$

Specifically, at $\beta_* = 0.01$, $\langle K(\infty) \rangle = 0.22$.

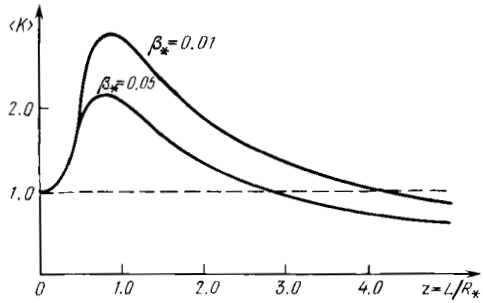

Fig. 2.17. Enhancement factor $\langle K \rangle$ as a function of the dimensionless depth $z = L/R_*$.

2.2.8. *Backscattering of pulse signals*

A backscattered echo pulse is expanded in time because of multiple paths of backscattering; moreover, its arrival time becomes a random variable. For very short pulses the echo signals corresponding to various coherent channels diverge in time and no backscatter enhancement will be observed. This leads us to the following condition for observation of enhanced backscattering of pulse signals. The pulse duration T should greatly exceed the mean square time of random lag, i.e.,

$$T \gg \sigma_\tau , \tag{2.73}$$

The quantity σ_τ^2 consists of two terms. The first, $\sigma_{\tau 0}^2$, is the variance of time it takes to propagate along a straightened ray

$$\tilde{\tau} = \frac{1}{2c} \int_0^L \tilde{\varepsilon}(\boldsymbol{\rho}, x)\, \mathrm{d}x .$$

This quantity is related to the variance of the eikonal σ_ψ^2 as $\sigma_{\tau 0}^2 = \sigma_\psi^2/c^2$.

The second part, $\sigma_{\tau 1}^2$, is due to the elongation of the ray caused by the random inhomogeneous medium. It may be estimated by

$$\begin{aligned} \sigma_{\tau 1} &= [\sqrt{L^2 + \sigma_\rho^2(L)} - L]/c \\ &\approx \sigma_\rho^2(L)/2cL , \end{aligned}$$

where σ_ρ^2 is the mean square of lateral deviation of a ray defined by eq. (2.11).

Condition (2.73) for enhanced backscattering also allows a spectral treatment. The bandwidth $\Omega = 2\pi/T$ of the signal should not exceed the band of coherence $\Omega_c = 2\pi/\sigma_\tau$. Since the variance of phase increases twice on the way from source to scatterer and back when compared with the variance of phase on the rectilinear path of length $2L$ (see § 6.3), one might expect doubling of the variance of the arrival time. As far as our information goes, this effect has not yet been subjected to experimental verification in laser sounding applications.

2.2.9. *Moving random inhomogeneities of the medium*

The reciprocity theorem, eq. (2.1), holds true only in media whose inhomogeneities are time invariant. Time-dependent fluctuations of permittivity

can lead to a reduction and even disappearance of the enhancement effect because the wave has to pass through different inhomogeneities on its forward and backward paths.

To illustrate the effects feasible, let us calculate the average intensity of a wave emitted by a point source $u_0(\boldsymbol{\rho}) = \delta(\boldsymbol{\rho})$ and backscattered by a point scatterer of $f(\boldsymbol{\rho}) = \delta(\boldsymbol{\rho})$. Given saturated fluctuations and uniform "frozen" motion of inhomogeneities in the atmosphere with wind velocity V, then

$$\langle I_s(\boldsymbol{\rho})\rangle = I_s^0\{1 + \exp[-d(0, \boldsymbol{\rho} - \boldsymbol{\theta}_v L, L)]\}, \tag{2.74}$$

where $\boldsymbol{\theta}_v = \boldsymbol{V}_\perp/c$, $\boldsymbol{V}_\perp$ is transverse to the ray, and $d(\boldsymbol{p}_0, \boldsymbol{p}, x)$ is the mean square of the phase difference over a distance x when the points of radiation are spaced by $\boldsymbol{p}_0$ and the points of observation by $\boldsymbol{p}$. [This quantity is defined by eq. (2.27).]

From eq. (2.74) it follows that a uniform drift of the inhomogeneities at a velocity V shifts the enhancement effect of $K = 2$ from the point of emittance a distance $\boldsymbol{\rho}_v = 2\boldsymbol{\theta}_v L$ by an amount equal to the transverse travel of the inhomogeneities in time $\Delta t = 2L/c$. This effect of the shift of the enhancement region has been noted by AKHUNOV, BUNKIN, VLASOV and KRAVTSOV [1984] and KRAVTSOV and SAICHEV [1985]. It should be obvious that when the magnitude and direction of the drift change markedly along the path, the enhancement effect weakens until it vanishes altogether. The effect also disappears when the condition that the inhomogeneities travel as a "frozen" cluster is no longer velid, i.e., when the inequality $\Delta t = 2L/c \ll \tau_\varepsilon$ is violated, where τ_ε is the lifetime of an inhomogeneity in the system where it is at rest. This effect of vanishing enhancement, i.e., the transition from $\langle I_s\rangle = 2I_s^0$ to $\langle I_s\rangle = I_s^0$, may be employed for monitoring the atmosphere.

2.3. REFLECTION FROM WAVEFRONT-REVERSING MIRRORS EMBEDDED IN A RANDOM INHOMOGENEOUS MEDIUM

2.3.1. *Compensation of the effect of random inhomogeneities upon the reflected wave*

The effect of double passage of a wave through the same random inhomogeneities of the medium is essential in evaluating the efficiency of adaptive systems and phase-conjugation systems, i.e., mirrors reversing the wavefront (WFR mirrors). Such systems are being designed to compensate the effect of

random inhomogeneities in the medium and to attain the diffraction limit in focusing the reflected intensity into the neighborhood of the source.

In considering the properties of a wave reflected in a random inhomogeneous medium, we shall assume an ideal reversal of the wavefront within the aperture of the WFR mirror and suppose also that in a time $\Delta t = 2L/c$, while the wave travels from source to mirror and back, the inhomogeneities will remain almost unchanged.

If a monochromatic wave with complex amplitude $u_0(\boldsymbol{\rho})$ emitted in the plane $x = 0$ toward a WFR mirror with reflection factor $f(\boldsymbol{\rho})$ placed at $x = L$, then the complex amplitude of the reflected wave measured in the source plane $x = 0$ is

$$u_s(\boldsymbol{\rho}) = \int f(\boldsymbol{\rho}')\, u^*(\boldsymbol{\rho}', L)\, g(\boldsymbol{\rho}, \boldsymbol{\rho}', L)\, \mathrm{d}^2\rho'$$

$$= \int u_0^*(\boldsymbol{\rho}')\, f(\boldsymbol{\rho}'')\, g^*(\boldsymbol{\rho}', \boldsymbol{\rho}'', L)\, g(\boldsymbol{\rho}', \boldsymbol{\rho}'', L)\, \mathrm{d}^2\rho'\, \mathrm{d}^2\rho'' \,. \tag{2.75}$$

We look for a condition which would ensure that the WFR mirror makes up for the effect of random inhomogeneities of the medium on the field of the reflected wave. For this purpose it suffices to consider the expression derived by POLOVINKIN and SAICHEV [1981] for the average field.

From eqs. (2.75) and (2.26) it follows that

$$\langle u_s(\boldsymbol{\rho}) \rangle = \frac{1}{L^2} \int u_0^*(\boldsymbol{\rho} - \boldsymbol{p})\, F(\boldsymbol{p}/L)$$

$$\times \exp\left[- \left(\frac{p}{\rho_c}\right)^{5/3} + \frac{\mathrm{i}k}{L} (\boldsymbol{\rho}\cdot\boldsymbol{p}) - \frac{\mathrm{i}k}{2L} p^2 \right] \mathrm{d}^2 p \,, \tag{2.76}$$

where

$$F(\boldsymbol{\theta}) = \left(\frac{k}{2\pi}\right)^2 \int f(\boldsymbol{\rho}) \exp[-\mathrm{i}k(\boldsymbol{\rho}\cdot\boldsymbol{\theta})]\, \mathrm{d}^2\rho \tag{2.77}$$

is the scattering diagram of the mirror with an angular width of $\Delta\theta = 1/ka$, where a is the mirror radius.

If

$$p \sim \Delta\theta L \ll \rho_c(L) \,, \tag{2.78}$$

from eq. (2.76) it is obvious that the average field of a wave reflected by a WFR mirror in a turbulent medium coincides with that reflected in vacuum. There-

fore, under this condition a WFR mirror compensates completely for the effect of random inhomogeneities on the field of the reflected wave in the plane $x = 0$.

Condition (2.78) allows for a dual interpretation. On the one hand, in order to achieve compensation it is required that the random phase increment along any backscattered ray should almost coincide with that along the respective incident ray. Backscattered rays lie in a cone with an included angle $\Delta\theta \sim 1/ka$. Clearly, the phase increments acquired along the incident and reflected rays will differ little from one another when the characteristic distance between them, $L\,\Delta\theta$, in the plane of the source is smaller than $\rho_c(L)$, which leads to eq. (2.78). On the other hand, compensation in a turbulent medium requires that the rays incident on the WFR mirror should be almost the same as in vacuum. This requirement will be met if the characteristic lateral shift σ_ρ of the rays due to the random walk in the turbulent medium is within the mirror aperture, i.e., $\sigma_\rho(L) \lesssim a$. Clearly, this inequality is also equivalent to condition (2.78) (SAICHEV [1982]).

2.3.2. *Average intensity of a wave reflected from a WFR mirror: Effect of superfocusing*

In applications the major interest is focused on the distribution of the average power flux of the reflected wave in the vicinity of the source. The total flux is given by

$$P = \int \langle I_s(\boldsymbol{\rho})\rangle \, \mathrm{d}^2\rho = \int |f(\boldsymbol{\rho})|^2 \, \langle I(\boldsymbol{\rho}, L)\rangle \, \mathrm{d}^2\rho \,. \tag{2.79}$$

We limit our analysis to a typical situation where the prime field u_0 is due to a point source. Then,

$$P = I_0(L) \int |f(\boldsymbol{\rho})|^2 \, \mathrm{d}^2\rho \,, \tag{2.80}$$

$I_0(L) \sim 1/L^2$ being the intensity of a spherical wave incident on the mirror in vacuum.

We represent the average intensity of a wave reflected from the WFR mirror as a sum of the coherent and noncoherent components

$$\langle I_s(\boldsymbol{\rho})\rangle = I_c(\boldsymbol{\rho}) + I_n(\boldsymbol{\rho}) \,, \tag{2.81}$$

with

$$I_c(\boldsymbol{\rho}) = |\langle u_s(\boldsymbol{\rho})\rangle|^2$$

and

$$I_n(\boldsymbol{\rho}) = \langle |u_s(\boldsymbol{\rho}) - \langle u_s(\boldsymbol{\rho})\rangle|^2\rangle .$$

The coherent component $I_c(\boldsymbol{\rho})$ is the lower bound of the average intensity of the reflected wave, since always $I_c(\rho) \leqslant \langle I_s(\boldsymbol{\rho})\rangle$. For a point source,

$$I_c(\boldsymbol{\rho}) = I_s^0(\boldsymbol{\rho}) \exp[-2(\rho/\rho_c)^{5/3}] , \tag{2.82}$$

where

$$I_s^0(\boldsymbol{\rho}) = I_0(L)\,|F(\boldsymbol{\rho}/L)|^2/L^2$$

is the intensity of the wave reflected by the WFR mirror in vacuum. It is remarkable that $I_c(0) = I_s^0(0)$, which implies that the average intensity of the reflected wave, as measured near the source, cannot be lower than the intensity $I_s^0(0)$ of the wave reflected in vacuum. In other words, a turbulent medium cannot reduce the wave intensity at the light spot (AKHUNOV, BUNKIN, VLASOV and KRAVTSOV [1984]).

Once condition (2.78) is satisfied, then $I_c(\boldsymbol{\rho}) = I_s^0(\boldsymbol{\rho})$, so that the radius of the focal spot in the plane of the source is L/ka as it is in vacuum. However, when condition (2.78) is violated, the focal spot of the reflected wave defined by eq. (2.82) contracts to about a size of $\rho_c \sim L/ka$. We shall refer to such focusing of a coherent field improved over that in vacuum as superfocusing. The effect of superfocusing is explained by a contraction of the effective radiation pattern of the WFR mirror, which forms the coherent component,

$$F_{\text{eff}}(\boldsymbol{\theta}) = F(\boldsymbol{\theta}) \exp[-(\theta/\theta_c)^{5/3}] . \tag{2.83}$$

In agreement with this formula only those rays which are reflected within the coherence cone $\theta \leqslant \theta_c(L) \simeq \rho_c(L)/L$ contribute to the coherent component of the reflected field.

The superfocusing of the coherent component may also be treated as an effective increase of WFR mirror size in a turbulent medium. We determine the effective reflection coefficient for the coherent component as

$$f_{\text{eff}}(\boldsymbol{\rho}) = \int F_{\text{eff}}(\boldsymbol{\theta}) \exp(ik\boldsymbol{\rho}\cdot\boldsymbol{\theta})\, d^2\theta$$

$$= \int f(\boldsymbol{\rho} + \boldsymbol{\rho}')\, W_\rho(\boldsymbol{\rho}', L)\, d^2\rho' ,$$

where $W_\rho(\boldsymbol{\rho}, L)$ is, as before, the probability density of the lateral shifts of rays determined by eq. (2.37).

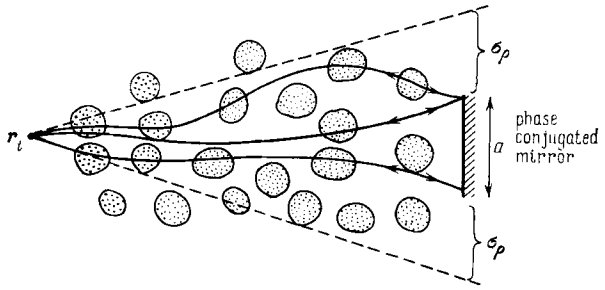

Fig. 2.18. Effective rise of WFR mirror size in a turbulent medium due to random walk of rays (effect of superfocusing).

The effective enlargement of the WFR mirror may be readily explained by a random walk of rays in the turbulent medium. Indeed, random walks can carry to the mirror even those rays which missed the mirror in vacuum (fig. 2.18). Accordingly, for a coherent field the size of the mirror increases to $a + \sigma_\rho(L)$.

Physically, the reasons for obtaining a narrow region of focusing for $I_c(\boldsymbol{\rho})$ are different for $\rho_c > \sigma_\rho$ and $\rho_c < \sigma_\rho$. The first inequality, $\rho_c > \sigma_\rho$, holds true in the range of weak fluctuations of intensity incident on a wavefront-reversing mirror. Excluding amplitude fluctuations, which are insignificant in this case, the field of a reflected wave in the plane of the source may be represented as

$$u_s(\boldsymbol{\rho}) = u_s^0(\boldsymbol{\rho}) \exp[i\varphi(\boldsymbol{\rho}, L)],$$

where $u_s^0(\boldsymbol{\rho})$ is the complex amplitude of the reflected wave in vacuum, and $\varphi(\boldsymbol{\rho}, L)$ is the random phase increment (with account for phase inversion) acquired along the paths of the incident and reflected waves. The mean square of $\varphi(\boldsymbol{\rho}, L)$ is comparable to unity only at $\rho \sim \rho_c(L)$. Consequently, if $\rho_c(L) > \sigma_\rho(L)$, then $\langle I_s(\boldsymbol{\rho})\rangle \simeq I_s^0(\boldsymbol{\rho})$, irrespective of the WFR mirror size, and for $a < \sigma_\rho$ the superfocusing is caused by purely phase effects, i.e., by an incomplete compensation achieved with the WFR mirror of the random phase increments en route from the source (i.e., WFR mirror) point of observation.

Now we turn to long paths along which $\sigma_\rho(L) > \rho_c(L)$. If we separate the correlations with the rules appropriate for a Gaussian field, under saturated fluctuations we obtain for the average intensity

$$\langle I_s(\boldsymbol{\rho})\rangle = I_c(\boldsymbol{\rho}) + I_{ind}(\boldsymbol{\rho}), \tag{2.84}$$

where

$$I_{\mathrm{ind}}(\rho) = \int I_{\mathrm{s}}^{0}(\boldsymbol{\rho} + \boldsymbol{\rho}_1)\, W_{\rho}(\boldsymbol{\rho}_1, L)\, \mathrm{d}^2\rho_1 \tag{2.85}$$

is the intensity of the reflected wave calculated on the assumption that the fluctuations are statistically *independent* in the forward and backward paths, $W_{\rho}(\boldsymbol{\rho})$ is defined by eq. (2.37), and for the turbulent medium $d(\rho) = 4(\rho/\rho_{\mathrm{c}})^{5/3}$.

From eq. (2.84) it follows that $I_{\mathrm{ind}}(\boldsymbol{\rho}) \simeq I_{\mathrm{s}}^{0}(\rho)$ for sufficiently small mirrors only ($a < \rho_{\mathrm{c}}$), when the diffraction divergence of the rays reflected from the mirror is about L/ka, which exceeds the lateral shift σ_{ρ}, i.e., when the WFR mirror is nowhere better than an ordinary reflector of the same size $a < \rho_{\mathrm{c}}$.

The simple approximation (2.84) does not always lead to physically correct conclusions. For example, the full power flux of the reflected wave is $P + P_{\mathrm{c}}$ rather than P, i.e., exceeds the true average flux (2.80) by

$$P_{\mathrm{c}} = \int I_{\mathrm{c}}(\boldsymbol{\rho})\, \mathrm{d}^2\rho\,.$$

Specifically, when condition (2.79) of compensation of the effect of inhomogeneities is satisfied, then $P_{\mathrm{c}} = P$ so that the average flux computed with eq. (2.84) is twice the true value. Nevertheless, the easy-tractable ray considerations allow to modify the expression for the noncoherent component $I_{\mathrm{n}}(\boldsymbol{\rho})$ so as to keep the advantages of eq. (2.84) but to eliminate the energy paradoxes peculiar to this expression.

As already mentioned, the coherent part of the field of the reflected wave is formed by rays whose angle of reflection differs from the angles of incidence by a value smaller than the angle of coherence, $\theta \lesssim \theta_{\mathrm{c}}(L)$. The other rays do not contribute to the coherent part of the reflected field and form an incoherent component. If we suppress the coherent part responsible for scattering within the cone $\theta \lesssim \theta_{\mathrm{c}}$ in the scattering pattern of the mirror (2.77), we obtain an effective pattern for the noncoherent component of the reflected field, e.g., in the form

$$F_{\mathrm{n}}(\boldsymbol{\theta}) = F(\boldsymbol{\theta})\{1 - \exp[-2(\theta L/\rho_{\mathrm{c}})^{5/3}]\}^{1/2}\,,$$

which secures the energy balance

$$|F_{\mathrm{c}}(\boldsymbol{\theta})|^2 = |F(\boldsymbol{\theta})|^2\,.$$

If we calculate I_{n} with this F_{n} directional pattern, assuming statistical independence of random inhomogeneities of the medium in the forward and back-

ward paths, we obtain

$$I_n(\boldsymbol{\rho}) = I_{ind} - \int I_c(\boldsymbol{\rho} + \boldsymbol{\rho}_1)\, W_\rho(\boldsymbol{\rho}_1, L)\, d^2\rho_1 . \tag{2.86}$$

Now, eq. (2.81) takes the form

$$\langle I_s \rangle = I_c + I_{ind} - \int I_c(\boldsymbol{\rho} + \boldsymbol{\rho}_1)\, W_\rho(\boldsymbol{\rho}_1, L)\, d^2\rho \tag{2.87}$$

and yields correct results in all the preceding situations that have been considered.

In particular, in the saturated fluctuation regime ($\rho_c \ll \sigma_\rho$) eq. (2.87) yields the expression

$$\langle I_s(\boldsymbol{\rho}) \rangle = I_c(\boldsymbol{\rho}) + I_{ind}(\boldsymbol{\rho}) - P_c\, W_\rho(\rho, L) ,$$

which at $a \ll \sigma_\rho$ almost coincides with eq. (2.84) in view of the smallness of the last term on the right-hand side. For strong fluctuations, $\rho_c \lesssim \sigma_\rho$, this formula suggests that the envelope of the average intensity of the reflected wave will have a different structure, depending on the WFR mirror size.

When $a > \sigma_\rho$, the mirror completely compensates the effect of turbulence on the reflected field, so that $\langle I_s(\boldsymbol{\rho}) \rangle = I_s^0(\boldsymbol{\rho})$ as in the case of weak intensity fluctuations. For $\sigma_\rho > a > \rho_c$ the average intensity consists of a high, sharp peak of $I_c(\boldsymbol{\rho})$ of radius $\sim \rho_c$, rising up to $I_c^0(0)$ over a wide and low pedestal $\sim I_{ind}(\boldsymbol{\rho})$, which, however, carries a considerable proportion of the energy flux.

When $a < \rho_c$, the average intensity of the reflected wave does not differ from the average intensity of the wave reflected from a common reflector of the same size.

Certain aspects of the spatial flux distribution of a wave reflected from a WFR mirror have been described by AKHUNOV and KRAVTSOV [1983a], SAICHEV [1983], KRAVTSOV and SAICHEV [1985], and MALAKHOV, POLOVINKIN and SAICHEV [1983, 1987].

2.3.3. *Effect of a drift of random inhomogeneities on the efficiency of WFR mirrors*

A time variability of the random inhomogeneities of the medium and even a transverse drift of inhomogeneities can result in a degraded focusing of the wave reflected from a WFR mirror in the neighborhood of the source (MALAKHOV and SAICHEV [1981], AKHUNOV, BUNKIN, VLASOV and KRAVTSOV [1982, 1984], and POLOVINKIN and SAICHEV [1984]). In this

section we limit consideration to a case of turbulent inhomogeneities that drift across the path with a constant velocity V.

Using reasoning similar to that employed earlier leads us to conclude that the average intensity of the reflected wave is given by eq. (2.87) in the vicinity of the point source, $I_{\text{ind}}(\boldsymbol{\rho})$ is defined by eq. (2.85), and the coherent component of the reflected field is given by

$$I_c(\boldsymbol{\rho}) = I_s^0(\boldsymbol{\rho}) \exp\left\{-2\left[\frac{|\boldsymbol{\rho} - 2\boldsymbol{\theta}_v L|}{\rho_c(L)}\right]^{5/3}\right\}, \tag{2.88}$$

where $\boldsymbol{\theta}_v = V_\perp/c$. It is obvious that the motion of inhomogeneities alters the distribution of the average reflected intensity if the angle of the drift $2\theta_v$ exceeds the angle of coherence $\theta_c \sim \rho_c/L$; i.e., $2\theta_v > \theta_c$.

However paradoxical it may seem at first glance, in a turbulent medium the efficiency of a WFR mirror is least for large mirrors, $a > \max\{\rho_c, \sigma_\rho\}$. In this case, from eqs. (2.85)–(2.88) we have

$$\langle I_s(\boldsymbol{\rho})\rangle = I_s^0(\boldsymbol{\rho})\, v + P(1 - v)\, W_\rho(\boldsymbol{\rho}, L),$$

where

$$v = \exp[-2(\theta_v/\theta_c)^{5/3}]$$

is introduced to reflect a reduction of the coherent component of the reflected wave.

The low efficiency of focusing by a large WFR mirror in a drifting turbulent medium is attributed to a narrow directional pattern of the large mirror ($\Delta\theta = 1/ka < \theta_c$). Therefore, rays reflected from the mirror pass through random inhomogeneities and emerge shifted in the transverse direction by a distance $2\theta_v L$ from the locations of the inhomogeneities through which the incident rays have passed.

In contrast to the situation in vacuum, the reduction of the WFR mirror size in a turbulent medium may result in a relative improvement of the focusing (POLOVINKIN and SAICHEV [1984]) because in the cone of reflected rays with the included angle $\Delta\theta > 2\theta_v$, there always exist rays passing through the same inhomogeneities through which the respective incident rays have passed. As a result, the superfocusing spot of the coherent component shifts, with respect to the source, a distance $2\theta_v L$ rather than disappears as is the case for a large mirror.

2.3.4. *Magic-cap effect: Compensation of backscattering from small-scale inhomogeneities by a WFR mirror*

With an ideal, boundless WFR mirror of reflectivity $|f| \equiv 1$, one more very interesting effect may be observed that will be referred to as the effect of the magic cap. This effect occurs because the ideal WFR mirror compensates not only the phase fluctuations of the field caused by large-scale inhomogeneities but also the backscattering from small-scale inhomogeneities (SAICHEV [1981, 1982]). A closely related effect of compensation of phase distortions in wavefront inversion in random acoustic waveguides has been pointed out by GELFGAT [1981].

We illustrate the magic-cap effect by the example of a scalar monochromatic wave satisfying the Helmholtz equation

$$\Delta u + k^2[1 + \tilde{\varepsilon}(\boldsymbol{\rho}, x)]u = 0 .$$

Assume that inhomogeneities are present only in a final layer $0 < x < L$ bounded at $x = L$ by a wavefront-reversing mirror of reflectivity f. Following MALAKHOV and SAICHEV [1979], we represent the field as $u(\boldsymbol{\rho}, x) = T(\boldsymbol{\rho}, x) + R(\boldsymbol{\rho}, x)$, where $T(\boldsymbol{\rho}, x)$ is the field of the forward wave propagating along the x-axis, and $R(\boldsymbol{\rho}, x)$ is a wave in the backward direction. These waves satisfy the following equations,

$$\begin{aligned} \frac{\partial T}{\partial x} &= \hat{M}T - \tfrac{1}{2}k^2\hat{N}\tilde{\varepsilon}\,T - \tfrac{1}{2}k^2\hat{N}\tilde{\varepsilon}\,R , \\ -\frac{\partial R}{\partial x} &= \hat{M}R - \tfrac{1}{2}k^2\hat{N}\tilde{\varepsilon}\,R - \tfrac{1}{2}k^2\hat{N}\tilde{\varepsilon}\,T . \end{aligned} \tag{2.89}$$

Here, the operator $\hat{M} = \mathrm{i}\sqrt{k^2 + \Delta_\perp}$ and $\hat{N} = 1/\hat{M}$.

Let a wave equal to $u_0(\boldsymbol{\rho})$ at $x = 0$ be incident on the inhomogeneous layer from the side of negative x-values. Then eqs. (2.89) should be solved with the boundary conditions

$$\begin{aligned} T(\boldsymbol{\rho}, 0) &= u_0(\boldsymbol{\rho}) , \\ R(\boldsymbol{\rho}, L) &= fT^*(\boldsymbol{\rho}, L) . \end{aligned} \tag{2.90}$$

If we suppose that $\hat{M}$ and $\hat{N}$ are purely imaginary, which corresponds to neglecting the total internal reflection, then with (2.89) and (2.90) we can verify

that the difference $Q = R(\rho, x) - fT^*(\rho, x)$ satisfies the equation

$$\frac{\partial Q}{\partial x} + \hat{M}Q = \tfrac{1}{2}k^2\hat{N}\tilde{\varepsilon}\,(Q - fQ^*) + (1 - |f|^2)\tfrac{1}{2}k^2\hat{N}\tilde{\varepsilon}\,T \tag{2.91}$$

with the boundary condition $Q(\rho, L) = 0$.

If $|f| = 1$, i.e., ideal reflection, then the last term of eq. (2.91) equals zero, the equation becomes closed for Q, and its solution is identically zero, $Q(\rho, x) \equiv 0$. Hence, for $|f| = 1$, the relation

$$R(\rho, x) = fT^*(\rho, x)$$

holds true at any distance from the mirror. In particular, at $x = 0$ we have $R(\rho, 0) = fu_0^*(\rho)$, which implies that even under backscattering from inhomogeneities of the medium the ideal WFR mirror provides a complete compensation of the distortions introduced by these inhomogeneities in the reflected wave. Actually, the WFR mirror sets up such phase relations between the fields of T and R that they extinguish the backscattering from small-scale disseminations, making them invisible for the observer outside the inhomogeneous layer, i.e., at $x < 0$.

Let us also examine the behavior of the field inside a random inhomogeneous layer confined by an ideal WFR mirror. Assume for simplicity that both the wave incident on the inhomogeneous layer and the inhomogeneities of the layer proper change smoothly along the transverse coordinates in the scale of the wavelength. It is convenient to represent the field inside the layer in the form

$$u(\rho, x) = \mathrm{e}^{\mathrm{i}kx}\,U(\rho, x) + \mathrm{e}^{\mathrm{i}k(L-x)}\,V(\rho, x)\,,$$

where the complex amplitudes U and V of the forward and reflected waves satisfy the system of parabolic equations following from eq. (2.89) upon substituting $\mathrm{i}k(1 + \frac{1}{2}\Delta_\perp)$ for $\hat{M}$ and $-\mathrm{i}k$ for $\hat{N}$, viz.,

$$\begin{aligned}
&2\mathrm{i}k\,\frac{\partial U}{\partial x} + \Delta_\perp U + k^2\tilde{\varepsilon}\,U + k^2\tilde{\mu}\,V = 0\,,\\
&-2\mathrm{i}k\,\frac{\partial V}{\partial x} + \Delta_\perp V + k^2\tilde{\varepsilon}\,V + k^2\tilde{\mu}^*U = 0\,,\\
&U(\rho, 0) = u_0(\rho)\,,\\
&V(\rho, L) = fU^*(\rho, L)\,,\\
&\tilde{\mu}\,(\rho, x) = \tilde{\varepsilon}\,(\rho, x)\exp(-2\mathrm{i}kz + \mathrm{i}kL)\,.
\end{aligned} \tag{2.92}$$

If we represent the complex amplitude of the reflected wave as the sum

$$V(\boldsymbol{\rho}, x) = fU^*(\boldsymbol{\rho}, x) + W(\boldsymbol{\rho}, x), \tag{2.93}$$

the equations for $U(\boldsymbol{\rho}, x)$ and $W(\boldsymbol{\rho}, x)$ follow from eq. (2.92) in the form

$$\begin{aligned}
&2ik\frac{\partial U}{\partial x} + \Delta_\perp U + k^2\tilde{\varepsilon}U + k^2\tilde{\mu}fU^* + k^2\tilde{\mu}W = 0,\\
&-2ik\frac{\partial W}{\partial x} + \Delta_\perp W + k^2\tilde{\varepsilon}W - k^2\tilde{\mu}^*fW^* + k^2(1-|f|^2)\mu^*U = 0,\\
&U(\boldsymbol{\rho}, 0) = u_0(\boldsymbol{\rho}),\\
&W(\boldsymbol{\rho}, L) = 0.
\end{aligned} \tag{2.94}$$

If the backscattered intensity is rather weak in a random inhomogeneous medium, in the equation in W we may neglect the two last terms responsible for backscattering (in formal terms this corresponds to $\tilde{\mu} = 0$). In this case $W \equiv 0$ for any f, and eq. (2.93) describes the familiar effect of compensation of the effect of large-scale inhomogeneities on the wave reflected from a WFR mirror of a sufficiently large size.

If the backscattering from small-scale inhomogeneities of the medium is significant, then, as noted for the more general case, for $x < 0$ the inhomogeneities do not influence the profile of the reflected wave only if $|f| \equiv 1$.

An interesting effect of localization (accumulation) of the energy of a wave in the small-scale random inhomogeneous layer positioned in front of the WFR mirror occurs where a compensation of backscattering takes place. To demonstrate this effect, we assume that the random inhomogeneities in the layer $0 < x < L$ are such that the diffusion approximation (see, e.g., the monograph by KLYATSKIN [1980]) is justified. This approximation is equivalent to replacing small-scale fluctuations $\tilde{\varepsilon}(\boldsymbol{\rho}, x)$ and $\tilde{\mu}(\boldsymbol{\rho}, x)$ with Gaussian δ-correlated random fields with correlation functions

$$\begin{aligned}
&\langle \tilde{\varepsilon}(\boldsymbol{\rho}, x)\,\tilde{\varepsilon}(\boldsymbol{\rho}+\boldsymbol{s}, x+\xi)\rangle = A(\boldsymbol{s})\,\delta(\xi),\\
&\langle \tilde{\mu}(\boldsymbol{\rho}, x)\,\tilde{\mu}^*(\boldsymbol{\rho}+\boldsymbol{s}, x+\xi)\rangle = a(\boldsymbol{s})\,\delta(\xi),\\
&\langle \tilde{\varepsilon}\,\tilde{\mu}\rangle = 0,
\end{aligned}$$

in which for clarity we assume that $A(\boldsymbol{s}) \geqslant 0$ and $a(\boldsymbol{s}) \geqslant 0$.

For $|f| \equiv 1$ the field $U(\boldsymbol{\rho}, x)$ satisfies the equation

$$2ik \frac{\partial U}{\partial x} + \Delta_\perp U + k^2 \tilde{\varepsilon} U + k^2 \tilde{\mu} f U^* = 0 ,$$

$$U(\boldsymbol{\rho}, 0) = u_0(\boldsymbol{\rho}) ,$$

which follows from eq. (2.94). Using standard closing procedures for closing averages (see, e.g., KLYATSKIN [1980]), it is not hard to transform this equation to the one for the coherence function of field $U(\boldsymbol{\rho}, x)$, namely

$$\frac{\partial \Gamma}{\partial x} - \frac{\mathrm{i}}{k} (\nabla_p \nabla_R) \Gamma + \tfrac{1}{2} k^2 [D(\boldsymbol{p}) - a] \Gamma = \tfrac{1}{4} k^2 a(s) \Gamma ,$$

$$D(\boldsymbol{p}) = A - A(\boldsymbol{p}) , \qquad A = A(0) , \quad a = a(0) . \tag{2.95}$$

Although a general solution of this equation is yet to be found, it is not hard to determine the flux

$$P(\boldsymbol{p}, x) = \int \Gamma(\boldsymbol{R}, \boldsymbol{p}, x) \, \mathrm{d}^2 R .$$

Assuming for simplicity that $P(\boldsymbol{p}, 0)$ is a real function of $\boldsymbol{p}$, which is valid, e.g., for the normal incidence of a collimated beam on a nonhomogeneous medium, we obtain from eq. (2.95)

$$P(\boldsymbol{p}, x) = P(\boldsymbol{p}, 0) \exp[-\tfrac{1}{4} k^2 D(\boldsymbol{p}) x + \tfrac{1}{4} k^2 (a + a(\boldsymbol{p})) x] .$$

It should be obvious that in the presence of small-scale inhomogeneities of the medium ($a > 0$), the average flux of the incident (as well as the reflected) wave increases exponentially as it approaches the WFR mirror,

$$P(x) = \int \langle I(\boldsymbol{\rho}, x) \rangle \, \mathrm{d}^2 \rho = P(0) \exp(\tfrac{1}{4} k^2 a x) .$$

Thus the small-scale, random inhomogeneous layer in front of the $|f| = 1$ mirror accumulates, on average, the energy of the incident wave. Inversion of the phase of a wave reflected from the WFR mirror actually converts the inhomogeneous layer into a resonator. This seems to prove indirectly that the effects of partial reversal of backscattered wavefronts caused by multiple coherence paths may be one of the mechanisms of wave localization in multi-dimensional, small-scale, random inhomogeneous media.

§ 3. Enhanced Backscattering by a Random Medium

3.1. OVERVIEW

In the preceding section we have considered backscatter enhancement in light scattered from a body embedded in a random medium. A similar phenomenon occurs in multiple scattering of light, or other types of waves, in a randomly inhomogeneous medium where there are no clear-cut scatterers that stand out against a background. In this case, the intensity of the backscattered radiation is found to be almost twice as large as that predicted by transport theory. This effect, called coherent backscattering, has been extensively discussed in the literature. It seems to have been first noted by RUFFINE and DE WOLF [1965] and WATSON [1969] in a theoretical analysis of radio waves backscattered by the turbulent ionospheric plasma (see also DE WOLF [1971]). BARABANENKOV [1973, 1975] had discussed the effect in connection with a microscopic basis for the phenomenological theory of radiative transport that ignores the previously mentioned interference processes.

The salient features of the effect have been demonstrated experimentally by KUGA and ISHIMARU [1984] and KUGA, TSANG and ISHIMARU [1985], who observed an enhanced backscattering from a medium composed of a suspension of latex particles. The earlier enhancement was less significant that that in later experiments. TSANG and ISHIMARU [1984, 1985] have interpreted the results by considering first double and then multiple scattering.

A recent upsurge of interest in the effect is attributed primarily to the recognition that the processes underlying coherent backscattering are intimately related to the similar processes that occur when electrons interact with impurities in disordered metals (JOHN and STEPHEN [1983], AKKERMANS and MAYNARD [1985]).

Effects of the type of coherent backscattering, commonly referred to as weak localization (ABRAHAMS, ANDERSON, LICCARDELLO and RAMAKRISHNAN [1979], GORKOV, LARKIN and KHMELNITSKII [1979], BERGMANN [1984]), lead to a decreased conductivity at low temperatures when compared with that predicted by the classical kinetic theory. Simultaneously with the interference effects the behavior of conductivity is considerably influenced by the Coulomb interaction of electrons (ALTSHULER, ARONOV, KHMELNITSKII and LARKIN [1982]).

Optical experiments make it possible to observe directly how the pure effects of weak localization enhance backscattering of light from dense water suspensions of submicron particles of latex or polystyrene (WOLF and MARET

[1985], VAN ALBADA and LAGENDIJK [1985], LAGENDIJK, VAN ALBADA and VAN DER MARK [1986], VAN DER MARK, VAN ALBADA and LAGENDIJK [1988], WOLF, MARET, AKKERMANS and MAYNARD [1988], ETEMAD [1988], DAINTY, QU and XU [1988], QU and DAINTY [1988]). Similar experiments with solid disordered media have been reported by ETEMAD, THOMPSON and ANDREJCO [1986] and KAVEH, ROSENBLUH, EDREI and FREUND [1986]. These studies have demonstrated that the angular distribution of scattered intensity is an almost triangular peak pointed backwards, the relative enhancement being close to two. The form of the peak as a function of depth of scattering layer, extinction, size of scatterers, and polarization of incident and detected radiation has been also investigated.

A theoretical treatment of the effect has been carried out by AKKERMANS, WOLF and MAYNARD [1986] with the scalar theory formalism. They calculated the contribution to the beam intensity of cyclical (or maximally crossed) diagrams and their sum for the case of point scatterers. The sum was computed with the aid of the diffusion approximation of radiation transport theory, which has been devised for this purpose by BARABANENKOV [1973]. This approximation has been explored by STEPHEN and CWILICH [1986] and CWILICH and STEPHEN [1987] to investigate polarization effects in coherent backscattering, and by BARABANENKOV and OZRIN [1988] and ISHIMARU and TSANG [1988] to study the effect of the size of the scatterers on the angular distribution of intensity. The characteristic features of the angular distribution have been elucidated by SCHMELTZER and KAVEH [1987] on the basis of field-theoretical methods.

Extensive research efforts have been devoted to various factors leading to a smoothing of the coherent backscattering peak. These are primarily the finite extension of the scattering medium and its extension (ISHIMARU and TSANG [1988], ETEMAD, THOMPSON, ANDREJCO, JOHN and MACKINTOSH [1987], EDREI and KAVEH [1987], AKKERMANS, WOLF, MAYNARD and MARET [1988]), the motion of scatterers (GOLUBENTSEV [1984a]), and the presence of a magnetic field in the case of a gyrotropic medium (GOLUBENTSEV [1984b] and MACKINTOSH and JOHN [1988]). The two last factors result in a breakdown of the symmetry relative to the inversion of time and violate the reciprocity condition.

This brief overview indicates that various aspects of coherent backscattering and weak localization of light have been well documented recently. In electron transfer theory the weak localization is thought to foretell the strong or Anderson localization. In the optical range the possibility of strong localization has also been considered (see, e.g., the review papers of KAVEH [1987] and JOHN [1988]), but so far no observation has been reported for this regime.

3.2. GENERAL THEORY OF MULTIPLE SCATTERING: LADDER AND MAXIMALLY CROSSED DIAGRAMS

A simple case of a scalar wave field $u(\boldsymbol{r})$ satisfying the Helmholtz equation will be considered initially. Note in passing that the solution of the scalar problem is applicable when the illumination and detection beams are co-polarized. Let a plane monochromatic wave $u_0(\boldsymbol{s}_0, \boldsymbol{r}) = \exp(\mathrm{i}k_0\boldsymbol{s}_0 \cdot \boldsymbol{r})$, $k_0 = 2\pi/\lambda$, propagating along the direction of the unit vector $\boldsymbol{s}_0$ be incident on a confined random inhomogeneous medium. Then the field obeys the equation

$$\begin{aligned} &[\Delta + k_0^2(1 + \tilde{\varepsilon}(\boldsymbol{r}))]\, u(\boldsymbol{s}_0, \boldsymbol{r}) = 0\,, \\ &u(\boldsymbol{s}_0, \boldsymbol{r})|_{\boldsymbol{s}_0 \cdot \boldsymbol{r} \to -\infty} = u_0(\boldsymbol{s}_0, \boldsymbol{r})\,, \end{aligned} \tag{3.1}$$

where $\tilde{\varepsilon}(\boldsymbol{r})$ is the random part of dielectric permittivity responsible for multiple scattering. For a source at infinity the solution of Helmholtz equation (3.1) is represented with the aid of the scattering operator $T(\boldsymbol{r}, \boldsymbol{r}')$ as (LAX [1951], FRISCH [1965] and GOLDBERGER and WATSON [1964])

$$u(\mathrm{r}) = u_0(\boldsymbol{r}) + \int \mathrm{d}^3 r_1\, \mathrm{d}^3 r_1'\; G_0(\boldsymbol{r} - \boldsymbol{r}_1)\, T(\boldsymbol{r}_1, \boldsymbol{r}_1') u_0(\boldsymbol{r}_1'). \tag{3.2}$$

Here and below it is assumed that the integration is taken over the entire volume occupied by the scattering medium, and $G_0(\boldsymbol{r}) = (-4\pi r)^{-1} \exp(\mathrm{i}k_0 r)$ is the Green function for free space where $\tilde{\varepsilon} = 0$.

According to eq. (3.2), in the Fraunhofer zone, the wavefield $u(\boldsymbol{r})$ is the sum of the incident wave and a spherical scattered wave whose amplitude is the Fourier transform of the scattering operator accurate to a constant multiplier.

We assume, for clarity, that the scattering medium is constituted by discrete scatterers. The preceding enhanced backscattering experiments used dense discrete media in which the average interscatter distance was comparable with the size of the scatterer. In such media, mutual correlations of scatterers may play a significant role.

Let us expand the scattering operator T into the orders of multiple scattering from individual scatterers, and substitute the result into eq. (3.2). Averaging the respective expansions of $u(\boldsymbol{r})$ and $u(\boldsymbol{r}_1)\, u^*(\boldsymbol{r}_2)$ over the ensemble of realizations of the scatterers yields the Dyson and Bethe–Salpeter equations for average field and coherence functions (FRISCH [1965] and FINKELBERG [1967]

$$\langle u(\boldsymbol{r}) \rangle = u_0(\boldsymbol{r}) + \int \mathrm{d}^3 r_1\, \mathrm{d}^3 r_1'\; G_0(\boldsymbol{r} - \boldsymbol{r}_1)\, M(\boldsymbol{r}_1, \boldsymbol{r}_1')\, \langle u(\boldsymbol{r}_1') \rangle\,, \tag{3.3}$$

$$\langle u(\boldsymbol{r}_1)\, u^*(\boldsymbol{r}_2)\rangle = \langle u(\boldsymbol{r}_1)\rangle \langle u^*(\boldsymbol{r}_2)\rangle + \int \mathrm{d}^3 r_1' \,\mathrm{d}^3 r_1'' \,\mathrm{d}^3 r_2' \,\mathrm{d}^3 r_2'' \,\langle G(\boldsymbol{r}_1, \boldsymbol{r}_1')\rangle \langle G^*(\boldsymbol{r}_2, \boldsymbol{r}_2')\rangle \times K(\boldsymbol{r}_1', \boldsymbol{r}_2'; \boldsymbol{r}_1'', \boldsymbol{r}_2'') \langle u(\boldsymbol{r}_1'')\, u(\boldsymbol{r}_2'')\rangle , \tag{3.4}$$

where $G(\boldsymbol{r}_1, \boldsymbol{r}_1')$ is the Green function of Helmholtz equation (3.1) having the average $\langle G(\boldsymbol{r}_1, \boldsymbol{r}_1')\rangle$, which satisfies the Dyson equation, which differs from eq. (3.3) by having $G_0(\boldsymbol{r} - \boldsymbol{r}')$ and $\langle G(\boldsymbol{r}, \boldsymbol{r}')\rangle$ in place of $u_0(\boldsymbol{r})$ and $\langle u(\boldsymbol{r})\rangle$, respectively.

The mass operator $M(\boldsymbol{r}, \boldsymbol{r}')$ and the intensity operator $K(\boldsymbol{r}_1, \boldsymbol{r}_2; \boldsymbol{r}_1', \boldsymbol{r}_2')$ of the Dyson and Bethe–Salpeter equations characterize the optical properties of the effective inhomogeneities for coherent and incoherent (or partially coherent) fields. These operators are evaluated by the diagram technique for the respective discrete medium. Examples of diagrams for both M and K are given in fig. 3.1.

The solution of the Bethe–Salpeter equation may be represented with the aid of the correlation function of the scattering operator (LAX [1951], BARABANENKOV [1975])

$$U(\boldsymbol{r}_1, \boldsymbol{r}_2; \boldsymbol{r}_1', \boldsymbol{r}_2') = \langle T(\boldsymbol{r}_1, \boldsymbol{r}_1')\, T^*(\boldsymbol{r}_2, \boldsymbol{r}_2')\rangle - \langle T(\boldsymbol{r}_1, \boldsymbol{r}_1')\rangle \langle T^*(\boldsymbol{r}_2, \boldsymbol{r}_2')\rangle ,$$

as follows,

$$\langle u(\boldsymbol{R}_1)\, u^*(\boldsymbol{R}_2)\rangle = \langle u(\boldsymbol{R}_1)\rangle \langle u^*(\boldsymbol{R}_2)\rangle + \int \mathrm{d}^3 r_1 \,\mathrm{d}^3 r_2 \,\mathrm{d}^3 r_1' \,\mathrm{d}^3 r_2' \, G_0(\boldsymbol{R}_1, \boldsymbol{r}_1)\, G^*(\boldsymbol{R}_2, \boldsymbol{r}_2) \times U(\boldsymbol{r}_1, \boldsymbol{r}_2; \boldsymbol{r}_1', \boldsymbol{r}_2')\, u_0(\boldsymbol{r}_1')\, u^*(\boldsymbol{r}_2') . \tag{3.5}$$

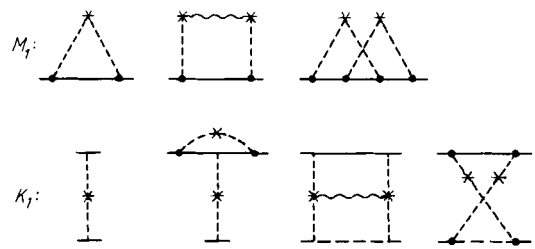

Fig. 3.1. Diagrams for the mass operator M_1 and intensity operator K_1 in the single-group approximation. Solid lines correspond to the Green function G_0, horizontal dashed lines to G_0^*, and wavy lines to the correlation function of scatterers. Nonhorizontal dashed lines correspond to the interaction operator or the scattering operator for an isolated scatterer, but in the last case the first diagram for M_1 is absent.

This representation indicates that the correlation function of the field is expressed directly through the correlation function of the scattering operator. Denote by $\Pi_{\text{incoh}}(\boldsymbol{r})$ the average energy flux of the wavefield less the energy flux of the average field. Incorporating the concept of albedo (see, e.g., AKKERMANS, WOLF and MAYNARD [1986]), $a(\boldsymbol{s}, \boldsymbol{s}_0)$, which characterizes the intensity of the fluctuation component of the scattered field propagating along the direction of the unit vector $\boldsymbol{s}$, into the representation of eq. (3.5), we obtain for the Fraunhofer zone of the medium

$$a(\boldsymbol{s}, \boldsymbol{s}_0) = \left. \frac{R^2 \boldsymbol{s}\, \Pi_{\text{incoh}}(\boldsymbol{R})}{k_0 \Sigma} \right|_{R \to \infty}$$

$$= \frac{1}{(4\pi)^2 \Sigma} \tilde{U}(k_0 \boldsymbol{s}, k_0 \boldsymbol{s}; k_0 \boldsymbol{s}_0, k_0 \boldsymbol{s}_0) , \tag{3.6}$$

where $\boldsymbol{s} = \boldsymbol{R}/R$, Σ is the cross section of the medium, and

$$\tilde{U}(\boldsymbol{p}, \boldsymbol{q}; \boldsymbol{p}', \boldsymbol{q}') = \int \mathrm{d}^3 r_1 \, \mathrm{d}^3 r_2 \, \mathrm{d}^3 r_1' \, \mathrm{d}^3 r_2' \, U(\boldsymbol{r}_1, \boldsymbol{r}_2; \boldsymbol{r}_1', \boldsymbol{r}_2')$$
$$\times \exp(-\mathrm{i}\boldsymbol{p} \cdot \boldsymbol{r}_1 + \mathrm{i}\boldsymbol{q} \cdot \boldsymbol{r}_2 + \mathrm{i}\boldsymbol{p}' \cdot \boldsymbol{r}_1' - \mathrm{i}\boldsymbol{q}' \cdot \boldsymbol{r}_2')$$

is the Fourier transform of the correlation function of the scattering operator.

In addition to eq. (3.5) actual fluctuations of the scattering operator are calculated with another representation of the Bethe–Salpeter equation

$$\langle u(\boldsymbol{r}_1)\, u^*(\boldsymbol{r}_2) \rangle = \langle u(\boldsymbol{r}_1) \rangle \, \langle u^*(\boldsymbol{r}_2) \rangle$$
$$+ \int \mathrm{d}^3 r_1' \, \mathrm{d}^3 r_2' \, \mathrm{d}^3 r_1'' \, \mathrm{d}^3 r_2'' \, \langle G(\boldsymbol{r}_1, \boldsymbol{r}_1') \rangle \, \langle G^*(\boldsymbol{r}_2, \boldsymbol{r}_2') \rangle$$
$$\times \Gamma(\boldsymbol{r}_1', \boldsymbol{r}_2'; \boldsymbol{r}_1'', \boldsymbol{r}_2'') \, \langle u(\boldsymbol{r}_1'') \rangle \, \langle u^*(\boldsymbol{r}_2'') \rangle . \tag{3.7}$$

The vertex function $\Gamma(\boldsymbol{r}_1, \boldsymbol{r}_2; \boldsymbol{r}_1', \boldsymbol{r}_2')$ satisfies an equation obtained by substituting eq. (3.7) into the Bethe–Salpeter equation (3.4), which, written symbolically, has the form

$$\Gamma = K + K \langle G \rangle \, \langle G^* \rangle \, \Gamma , \tag{3.8}$$

where for brevity we have dropped the arguments of functions and integrations like (3.4).

Comparison of the two representations (3.5) and (3.7) of the solution to the Bethe–Salpeter equation yields a relation between the correlation function of

the scattering operator and the vertex function,

$$G_0 G_0^* U G_0 G_0^* = \langle G \rangle \langle G \rangle \Gamma \langle G \rangle \langle G^* \rangle ,$$

which is resolved for the correlation function of the scattering operator

$$U = XX^* \Gamma YY^*$$

with the aid of two auxiliary operators

$$X = 1 + \langle T \rangle G_0 \quad \text{and} \quad Y = 1 + G_0 \langle T \rangle ,$$

whose origin may be easily traced by representing the field (3.2) in terms of the scattering operator of the medium. In view of the reciprocity of the scattering operator (FRISCH [1965])

$$T(\boldsymbol{r}, \boldsymbol{r}') = T(\boldsymbol{r}', \boldsymbol{r}) , \tag{3.9}$$

the operators $X(\boldsymbol{r}, \boldsymbol{r}')$ and $Y(\boldsymbol{r}, \boldsymbol{r}')$ are related by

$$X(\boldsymbol{r}, \boldsymbol{r}') = Y(\boldsymbol{r}', \boldsymbol{r}) ,$$

Finally, from the definition of Y and eq. (3.2) it follows that

$$\int \mathrm{d}^3 r' \; Y(\boldsymbol{r}, \boldsymbol{r}') u_0(\boldsymbol{r}') = \langle u(\boldsymbol{r}) \rangle .$$

Now, we have arrived at the fundamental formula for the albedo

$$a(\boldsymbol{s}, \boldsymbol{s}_0) = \frac{1}{(4\pi)^2 \Sigma} \int \mathrm{d}^3 r_1 \, \mathrm{d}^3 r_2 \, \mathrm{d}^3 r_1' \, \mathrm{d}^3 r_2' \times \langle u(-\boldsymbol{s}, \boldsymbol{r}_1) \rangle \langle u^*(-\boldsymbol{s}, \boldsymbol{r}_2) \rangle \Gamma(\boldsymbol{r}_1, \boldsymbol{r}_2; \boldsymbol{r}_1', \boldsymbol{r}_2') \times \langle u(\boldsymbol{s}_0, \boldsymbol{r}_1') \rangle \langle u^*(\boldsymbol{s}_0, \boldsymbol{r}_2') \rangle , \tag{3.10}$$

where $\langle u(\boldsymbol{s}, \boldsymbol{r}) \rangle$ represents the solution to eq. (3.3) with the boundary condition involving $u_0(\boldsymbol{s}, \boldsymbol{r})$.

Formula (3.10) is exact and rather general. It is commonly used under some simplifying assumptions made with respect to the medium and the wavefield. The model of a medium constituted by independent (uncorrelated) scatterers of characteristic size r_0 (FOLDY [1945], LAX [1951], DOLGINOV, GNEDIN and SILANTYEV [1979]) is appropriate at a low density n of scatterers distributed in space so that $nr_0^3 \ll 1$.

For dense scattering media where nr_0^3 is not small any longer, a model should take into account the correlations of scatterers. The single-group approximation (FINKELBERG [1967], BARABANENKOV and FINKELBERG [1967],

BARABANENKOV [1975]) takes into account the correlation functions of scatterers of all orders. In this approximation the mass operator M and intensity operator K equal the sums M_1 and K_1 of all possible diagrams linear in the correlation functions of scatterers. Some of these diagrams are depicted in fig. 3.1. The kernels M_1 and K_1 are put in correspondence to inhomogeneities of the medium of a spatial scale r_0 that is of the same order as the maximum of either the size of scatterers or their correlation radius.

The representation of localized inhomogeneities forms the basis of a physically appealing approach to coherent and incoherent scattering of waves. This approach is based on the assumption that the main contribution to wave scattering is due to the far configurations of inhomogeneities when these are in the Fraunhofer zone with respect to one another (BARABANENKOV and FINKELBERG [1967]). For coherent scattering the Fraunhofer approximation is equivalent to neglecting the spatial dispersion, and for incoherent scattering it is equivalent to a description in terms of radiative transfer theory.

Neglecting the spatial dispersion reduces the Dyson equation for the average Green function in an unbounded scattering medium to the Helmholtz equation with an effective compiex wavenumber k_1 related to the Fourier transform of the mass operator $M_1(p)$ by the relation

$$k_1^2 \approx k_0^2 - M_1(k_0) .$$

The expression for the average function G_1 satisfying the Dyson equation with M_1 is then

$$G_1(\boldsymbol{r}, \boldsymbol{r}') \approx -(4\pi R)^{-1} \exp(\mathrm{i}kR - R/2l_{\mathrm{eff}}) , \tag{3.11}$$

where $R = |\boldsymbol{r} - \boldsymbol{r}'|$, and l_{eff}^{-1} involves the contributions due to elastic scattering, $1/l$, and due to true absorption, $1/l_{\mathrm{ab}}$, namely,

$$l_{\mathrm{eff}}^{-1} = -\operatorname{Im}\{M_1(k_0)\}/k_0 = 1/l + 1/l_{\mathrm{ab}} . \tag{3.12}$$

In eq. (3.11) it is assumed that k_1/k_0 is close to unity,

$$\lambda \ll l_{\mathrm{eff}} . \tag{3.13}$$

For a bounded scattering medium the question of whether or not it is possible to neglect dispersion near the boundary requires a separate consideration. Digressing from this problem for a moment, the average field in the medium on neglecting the reflection and refraction of waves at the interface can be written as

$$\langle u(\boldsymbol{s}, \boldsymbol{r}) \rangle \approx \exp(\mathrm{i}k_0 \boldsymbol{s} \cdot \boldsymbol{r} - r/2l_{\mathrm{eff}}) , \tag{3.14}$$

where the origin is also placed inside the medium.

Denote

$$\Phi_0(\boldsymbol{r}_1, \boldsymbol{r}_2; \boldsymbol{r}_1', \boldsymbol{r}_2') = \langle G(\boldsymbol{r}_1, \boldsymbol{r}_1') \rangle \langle G^*(\boldsymbol{r}_2, \boldsymbol{r}_2') \rangle \tag{3.15}$$

and consider the solution $\Phi^{(L)}$ to the approximate Bethe–Salpeter equation for an unbounded medium, which is derived from eq. (3.4) by substituting eqs. (3.15) and (3.11) for the inhomogeneous term and K_1 for the intensity operator. In this "ladder" approximation, in agreement with eq. (3.8), the vertex function Γ becomes

$$\Gamma \approx K_1 + \Gamma^{(L)}, \qquad \Gamma^{(L)} = K_1 \Phi^{(L)} K_1 . \tag{3.16}$$

Expanding $\Phi^{(L)}$ in scattering orders, i.e., in powers of K_1, yields a representation of $\Phi^{(L)}$ in the form of a series whose terms can be represented by ladder diagrams, one of which is shown in fig. 3.2, along with the respective patterns of disturbance travel.

The condition

$$r_0 \ll l_{\text{eff}}, \quad k_0 r_0^3 \ll l_{\text{eff}}^2 \tag{3.17}$$

assumes that inhomogeneities of the medium are in the Fraunhofer zone with respect to one another (BARABANENKOV [1975]). The intensity operator K_1 then can be represented as

$$K_1(\boldsymbol{R} + \tfrac{1}{2}\boldsymbol{r}, \boldsymbol{R} - \tfrac{1}{2}\boldsymbol{r}; \boldsymbol{R}' + \tfrac{1}{2}\boldsymbol{r}', \boldsymbol{R}' - \tfrac{1}{2}\boldsymbol{r}')$$
$$\approx (4\pi)^2 \delta(\boldsymbol{R} - \boldsymbol{R}') \int \frac{\mathrm{d}^3k\, \mathrm{d}^3k'}{(2\pi)^6} \exp(\mathrm{i}\boldsymbol{k}\cdot\boldsymbol{r} - \mathrm{i}\boldsymbol{k}'\cdot\boldsymbol{r}')\, W(\boldsymbol{k}, \boldsymbol{k}'), \tag{3.18}$$

and the following relations holds for both $\Phi^{(L)}$ and Φ_0 (BARABANENKOV [1969]), the latter being defined as $f(\boldsymbol{R} + \frac{1}{2}\boldsymbol{r}, \boldsymbol{R} - \frac{1}{2}\boldsymbol{r}; \boldsymbol{R}' + \frac{1}{2}\boldsymbol{r}', \boldsymbol{R}' - \frac{1}{2}\boldsymbol{r}')$

$$\int \mathrm{d}^3r\, \mathrm{d}^3r' \exp(-\mathrm{i}\boldsymbol{k}\cdot\boldsymbol{r} + \mathrm{i}\boldsymbol{k}\cdot\boldsymbol{r}')\, (\Phi^{(L)}; \Phi_0)$$
$$\approx (2\pi)^6 k_0^{-4} \delta(k - k_0)\, \delta(k' - k_0)\, (\mathscr{F}; \mathscr{F}_0), \tag{3.19}$$

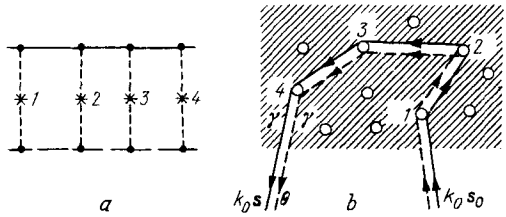

Fig. 3.2. (a) Typical ladder diagram: the solid line corresponds to $G_1 = G_0 + G_0 M_1 G_1$, horizontal dashed line to G_1^*, and vertical dashed lines to K_1. (b) The path γ corresponding to the ladder diagram in real space.

where $s = k/k$, $s' = k'/k$,

$$\mathscr{F}_0(R, s; R', s') = \delta(s - s')\,\delta(s - s_{RR'}) \times (4\pi|R - R'|)^{-2} \exp(-|R - R'|/l_{\text{eff}}), \tag{3.20}$$

$s_{RR'} = (R - R')/|R - R'|$, and the quantity $\mathscr{F}$ is the Green function of the transport equation (CASE and ZWEIFEL [1967]), which follows from the Bethe–Salpeter equation for $\Phi^{(L)}$, namely,

$$\mathscr{F}(r, s; r', s') = \mathscr{F}_0(r, s; r', s') + (4\pi)^2 \int d^3r_1\, d^2s_1\, d^2s_1'\, \mathscr{F}_0(r, s; r_1, s_1) \times n\sigma(s_1, s_1')\, \mathscr{F}(r_1, s_1'; r', s'). \tag{3.21}$$

Here and below d^2s is an elementary solid angle.

The coefficient of elastic scattering of a unit volume of the medium is defined as

$$n\sigma(s, s') = W(k_0 s, k_0 s'). \tag{3.22}$$

For uncorrelated scatterers, $\sigma(s, s')$ is the cross section of scattering of an individual particle. The mean free path l in elastic scattering can be obtained by

$$l^{-1} = n \int ds\, \sigma(s, s'). \tag{3.23}$$

Now we return to eq. (3.10) for the albedo of the medium. We assume the scattering medium under consideration is a plane parallel slab perpendicular to the z-axis as shown in fig. 3.3. The transverse size of the slab is supposed

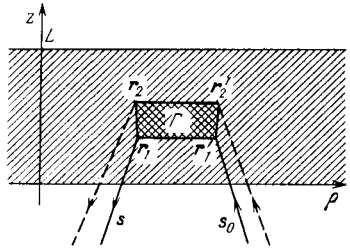

Fig. 3.3. Geometry of the problem for albedo calculation [eqs. (3.10) and (3.24)]. The arrowed lines represent the average fields $\langle u \rangle$ and $\langle u^* \rangle$. The quadrilateral represents a vertex function Γ.

to be rather wide so that we may safely neglect edge effects and make use of the translation invariance of the vertex function Γ with respect to shifts along the slab. The final expression for the albedo, with taking into account eq. (3.14), becomes

$$a(\boldsymbol{s}, \boldsymbol{s}_0) = (4\pi L_\perp)^{-2} \int \mathrm{d}^3 r_1 \, \mathrm{d}^3 r_2 \, \mathrm{d}^3 r_1' \, \mathrm{d}^3 r_2' \, \Gamma(\boldsymbol{r}_1, \boldsymbol{r}_2; \boldsymbol{r}_1', \boldsymbol{r}_2')$$

$$\times \exp\left[-\mathrm{i}k_0 \boldsymbol{s}(\boldsymbol{r}_1 - \boldsymbol{r}_2) + \mathrm{i}k_0 \boldsymbol{s}_0(\boldsymbol{r}_1' - \boldsymbol{r}_2') - \frac{z_1 + z_2}{2 l_{\mathrm{eff}} |s_z|} - \frac{z_1' + z_2'}{2 l_{\mathrm{eff}} s_{0z}} \right] \quad (3.24)$$

where $\boldsymbol{r}_j = (\boldsymbol{\rho}_j, z_j)$, the integration is over the entire slab $0 < z < L$, $|\rho_j| < L_\perp \to \infty$, and for backscattering $s_z < 0$ for $s_{0z} > 0$.

Substitution of eqs. (3.16), (3.18), and (3.19) into eq. (3.24) yields the albedo in the form of a sum, $a \approx a^{(1)} + a^{(\mathrm{L})}$, where $a^{(1)}$ stands for the first term on the right-hand side of eq. (3.16), i.e., corresponds to single scattering, and the computation of the ladder part $a^{(\mathrm{L})}$ of the albedo is a matter of solving the transfer equation, eq. (3.21).

The ladder approximation and transfer theory are known to provide a satisfactory description of incoherent scattering for almost all directions $\boldsymbol{s}$ (see, e.g., BARABANENKOV [1975], ISHIMARU [1978]) except for the narrow cone around the retroreflection direction with an included angle of $\Delta\theta \lesssim 1/k_0 l$, where θ is the angle between $\boldsymbol{s}$ and $-\boldsymbol{s}_0$, i.e. $\cos\theta = -\boldsymbol{s} \cdot \boldsymbol{s}_0$. At these angles the contribution of the interference processes that fail to be explained by the ladder approximation is insignificant. A qualitative insight into the matter may be provided by referring to the reasoning of AKKERMANS, WOLF and MAYNARD [1986] (see also MACKINTOSH and JOHN [1988]).

Consider a half-space filled by randomly spaced scatterers. Denote by u_γ the contribution to the scattered field due to the passage of the wave along a path γ including, in that order, the points $\boldsymbol{R}_1, \ldots, \boldsymbol{R}_N$, locating the position of scatterers, which are assumed for simplicity to be point-like and uncorrelated. A typical path γ is shown in figs. 3.2 and 3.4 by a continuous line. The overall field u is the sum of u_j over all possible paths γ_j, and this is readily recognized to be an expansion of u in a series of multiple scattering devised by GOLDBERGER and WATSON [1964].

The analysis can additionally be simplified by considering, at each section, $\boldsymbol{R}_{j+1} - \boldsymbol{R}_j$ instead of a diverging wave represented by the function $G_0(\boldsymbol{R}_{j+1} - \boldsymbol{R}_j)$, one of its plane components $\exp[\mathrm{i}\boldsymbol{k}_j(\boldsymbol{R}_{j+1} - \boldsymbol{R}_j)]$, and by assuming that u_γ is defined not only by the positions of the scatterers $\boldsymbol{R}_1, \ldots, \boldsymbol{R}_N$ but also by a fixed set of wave vectors $\boldsymbol{k}_0 = k_0 \boldsymbol{s}_0, \ldots, \boldsymbol{k}_1, \boldsymbol{k}_{N-1}$, $\boldsymbol{k}_N = k_0 \boldsymbol{s}$. The intensity $|u|^2$ will, of course, contain cross terms $u_\gamma u_\gamma^*$, due to

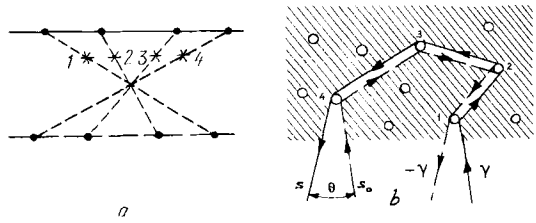

Fig. 3.4. (a) Typical maximally crossed (cyclical) diagram; (b) corresponding paths γ and $-\gamma$, which interfere coherently at small θ.

the interference of different paths, but the ladder approximation disregards these cross terms, retaining only the terms like $|u_\gamma|^2$.

It is worth noting that the scalar waves passing through $\boldsymbol{R}_1, \ldots, \boldsymbol{R}_N$, and the amplitudes of scattering at these points are the same for the path γ and the time-reserved path $-\gamma$ (dashed line in fig. 3.4), in which these points are traversed in reverse order. In the plane-wave representation the set of wave vectors $\boldsymbol{k}_0, \boldsymbol{k}_1, \ldots,$ and $\boldsymbol{k}_N$ is replaced by the set $\boldsymbol{k}_0, -\boldsymbol{k}_{N-1}, \ldots, -\boldsymbol{k}_1, \boldsymbol{k}_N$. Consequently, u_γ and $u_{-\gamma}$ can only differ due to the sections from the medium boundary to the first and to the last scatterer. If we neglect extinction in this section, the difference will consist of the phase multiplier, i.e., $u_\gamma u^*_{-\gamma} = |u_\gamma|^2 \exp[i\boldsymbol{k}_0(\boldsymbol{s} + \boldsymbol{s}_0)\cdot(\boldsymbol{R}_1 - \boldsymbol{R}_N)]$.

Thus, the contribution of the sum of these two paths to the intensity takes the form

$$|u_\gamma + u_{-\gamma}|^2 = 2|u_\gamma|^2 + 2|u_\gamma|^2 \cos[\boldsymbol{k}_0(\boldsymbol{s} + \boldsymbol{s}_0)\cdot(\boldsymbol{R}_1 - \boldsymbol{R}_N)],$$

where the first term on the right-hand side corresponds to the contribution of ladder diagrams (see fig. 3.2), and the second oscillating term, due to the interference of γ and $-\gamma$ paths, can be pictured as a cyclical, or maximally crossed, diagram such as the one shown in fig. 3.4. Clearly, for backscattering at zero angle, when $\boldsymbol{s} = -\boldsymbol{s}_0$, these quantities coincide for any path γ. In this case, their contributions to the albedo are equal; i.e.,

$$a^{(L)}(-\boldsymbol{s}_0, \boldsymbol{s}_0) = a^{(C)}(-\boldsymbol{s}_0, \boldsymbol{s}_0) \tag{3.25}$$

and the sum is twice the classical value of $a^{(L)}$.

We can estimate the angular width of the backscatter peak by assuming that the vector $\boldsymbol{R}_1 - \boldsymbol{R}_N$ is parallel to the medium boundary and that the incident light is normal to this boundary so that $s_{0z} = 1$. Then, the interference (cyclical) term will give a sizeable contribution in the intensity provided that the phase

increment is small; i.e., $k_0(s + s_0)\cdot(\boldsymbol{R}_1 - \boldsymbol{R}_N) \approx k_0\theta\cdot|\boldsymbol{R}_1 - \boldsymbol{R}_N| \ll 1$. The average value of the distance $|\boldsymbol{R}_1 - \boldsymbol{R}_N|$ for the minimum number of scattering events ($N = 2$) is the mean free path of the travelling light, i.e., the extinction length l. Therefore, an enhancement will be observed in a cone with included angle $\Delta\theta \lesssim 1/k_0 l$. From this result one may conclude, by the way, that the wings of the coherent backscatter peak ($\theta > 1/k_0 l$) are mainly due to the contribution from double scattering (BARABANENKOV [1973], ISHIMARU and TSANG [1988], GORODNICHEV, DUDAREV and ROGOZKIN [1989]).

When N grows large, we may assume that the path γ consists of random segments and make good use of the diffusion approximation, which yields $|\boldsymbol{R}_1 - \boldsymbol{R}_N|^2 \approx D(t_N - t_1) = lS_N/3$, where the path length $S_N = c(t_N - t_1)$ is estimated as lN. This implies that a path of length S_N contributes to the interference part of the intensity only within the cone $\theta < \theta_N \approx 1/k_0(lS_N)^{1/2}$; consequently, the top part of the backscattering peak is mainly formed by high multiplicity scattering. If path lengths are limited by a value of $S_{\max}$, say, due to a finite thickness (or transverse dimension) of the slab, when $S_{\max} \sim L$ (or $S_{\max} \sim L_\perp$), or due to absorption when $S_{\max} \sim l_{ab}$, then we can expect that the peak will be rounded off at angles $\theta < \theta_{\max} \lesssim 1/k_0(lS_{\max})^{1/2}$. A similar rounding off, associated with the suppression of the contribution of high multiplicity scattering, must be observed in the presence of factors breaking down the time-reversal invariance (MACKINTOSH and JOHN [1988]).

Proceeding along the lines of this qualitative reasoning, one can verify that the interference terms $u_\gamma u_{\gamma'}^*$ corresponding to different paths $\gamma' \neq \pm\gamma$, will contain, even at $s = -s_0$, uncompensated factors of the type $\exp[ik_0 s_n\cdot(\boldsymbol{R}_i - \boldsymbol{R}_j)]$, which depend not only on the random locations $\boldsymbol{R}_i$, $\boldsymbol{R}_j$, but also on the random direction s_n. The averaging of such quantities will introduce (for $1/k_0 l \ll 1$) only insignificant corrections to the intensity. Therefore, in describing coherent backscattering, we may safely limit ourselves to consider only the ladder and maximally crossed (cyclical) diagrams.

Now we turn to a more rigorous substantiation of the preceding results, specifically, equality (3.25) (BARABANENKOV [1973, 1975]). The key point here is the property of reciprocity of the scattering operator (Green function) formulated by eq. (3.9) and the respective property of the intensity operator in the single-group approximation

$$K_1(\boldsymbol{r}_1, \boldsymbol{r}_2; \boldsymbol{r}_1', \boldsymbol{r}_2') = K_1(\boldsymbol{r}_1, \boldsymbol{r}_2'; \boldsymbol{r}_1', \boldsymbol{r}_2) = K_1(\boldsymbol{r}_1', \boldsymbol{r}_2; \boldsymbol{r}_1, \boldsymbol{r}_2')\,. \tag{3.26}$$

Based on the symmetry of the intensity operator K_1 and the reciprocity

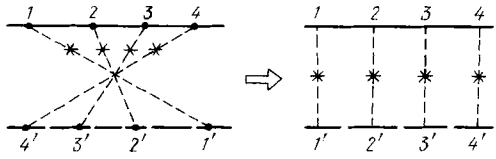

Fig. 3.5. Equivalence of ladder diagrams and maximally crossed diagrams. Inversion of points on the upper (lower) row in a maximally crossed diagram transforms the diagram into the corresponding ladder diagram.

condition for the average Green function G_1, eq. (3.11), satisfying the Dyson equation with mass operator M_1, we can establish a type of equivalency of maximally crossed diagrams and ladder diagrams under inversion of the points on the upper or lower row in a diagram (fig. 3.5). This brings us to a fundamental conclusion for backscatter enhancement theory. Let $K^{(C)}(\boldsymbol{r}_1, \boldsymbol{r}_2; \boldsymbol{r}_1', \boldsymbol{r}_2')$ represent the sum of all maximally crossed diagrams, then

$$K^{(C)}(\boldsymbol{r}_1, \boldsymbol{r}_2, \boldsymbol{r}_1', \boldsymbol{r}_2') = \Gamma^{(L)}(\boldsymbol{r}_1, \boldsymbol{r}_2'; \boldsymbol{r}_1', \boldsymbol{r}_2) = \Gamma^{(L)}(\boldsymbol{r}_1', \boldsymbol{r}_2; \boldsymbol{r}_1, \boldsymbol{r}_2'). \tag{3.27}$$

This relation represents the contribution of the sum of all maximally crossed diagrams in the intensity operator in terms of the vertex function in the ladder approximation, eq. (3.16). The quantity $K^{(C)}$ is also the contribution of the sum of maximally crossed diagrams in the vertex function,

$$\Gamma^{(C)}(\boldsymbol{r}_1, \boldsymbol{r}_2; \boldsymbol{r}_1', \boldsymbol{r}_2') = K^{(C)}(\boldsymbol{r}_1, \boldsymbol{r}_2; \boldsymbol{r}_1', \boldsymbol{r}_2'), \tag{3.28}$$

and is an approximate solution to eq. (3.8) with $K \approx K_1 + K^{(C)}$.

Substituting $\Gamma^{(L)}$ or $\Gamma^{(C)}$ for the vertex function Γ in the general formula for the albedo [eq. (3.10)] yields, respectively, the expressions for the ladder part, $a^{(L)}(\boldsymbol{s}, \boldsymbol{s}_0)$, or the maximally crossed (cyclical) part, $a^{(C)}(\boldsymbol{s}, \boldsymbol{s}_0)$, of the total albedo. If in these integrals we let $\boldsymbol{s} = -\boldsymbol{s}_0$ and make use of eqs. (3.27) and (3.28), we obtain equality (3.25).

3.3. TRANSFER EQUATION AND ENHANCED BACKSCATTERING

The qualitative consideration in the preceding section indicated that enhanced backscattering can be explained by choosing the vertex function in the form

$$\Gamma \approx K_1 + \Gamma^{(L)} + \Gamma^{(C)}. \tag{3.29}$$

We recall that the random inhomogeneous media under consideration are those with parameters satisfying conditions (3.13) and (3.17). This means that both the ladder $\Gamma^{(L)}$ and the associated maximally crossed $\Gamma^{(C)}$ vertex function can be expressed through the solution of the transfer equation. Thus, the formulas (3.16)–(3.22) and (3.28) form a computational basis for the albedo.

Substituting eqs. (3.29) to (3.24), we obtain after some algebra

$$a = a^{(1)} + a' , \tag{3.30}$$

where $a^{(1)}$ is the contribution of single scattering,

$$a^{(1)}(\boldsymbol{s}, \boldsymbol{s}_0) = n l_{\text{eff}} \sigma(\boldsymbol{s}, \boldsymbol{s}_0) \times \frac{s_{0z}|s_z|}{s_{0z} + |s_z|} \left[1 - \exp\left(- L \frac{s_{0z} + |s_z|}{l_{\text{eff}} s_{0z} |s_z|} \right) \right] . \tag{3.31}$$

The second term in eq. (3.30) is

$$a' = a^{(L)} + a^{(C)} , \tag{3.32}$$

where

$$a^{(L)}(\boldsymbol{s}, \boldsymbol{s}_0) = (\omega/4\pi) F(0; \mathrm{i}/|s_z|, \mathrm{i}/s_{0z}) ,$$

$$a^{(C)}(\boldsymbol{s}, \boldsymbol{s}_0) = (\omega/4\pi) F(\boldsymbol{q}; p, -p^*) ,$$

$$\boldsymbol{q} = k_0 l_{\text{eff}} (\boldsymbol{s}_\perp + \boldsymbol{s}_{0\perp}) ,$$

$$p = k_0 l_{\text{eff}} (s_z + s_{0z}) + \mathrm{i}(s_{0z} + |s_z|)/2|s_z| s_{0z} .$$

Thus the sum a' depends on the parameters $\boldsymbol{q}$ and p and the albedo due to scattering from an isolated inhomogeneity $\omega = l_{\text{eff}}/l$.

The function $F(\boldsymbol{q}, p, p')$ may be written as the integral transform

$$F(\boldsymbol{q}, p, p') = \int_0^{L/l_{\text{eff}}} \mathrm{d}z \, \mathrm{d}z' \, \mathrm{e}^{\mathrm{i}pz + \mathrm{i}p'z} \tilde{F}(\boldsymbol{q}; z, z') \tag{3.33}$$

of the function $\tilde{F}(\boldsymbol{q}; z, z')$, which is expressed through the Green function of the transfer equation

$$\mathscr{F}(\boldsymbol{r}, \boldsymbol{s}; \boldsymbol{r}', \boldsymbol{s}') = \mathscr{F}(\boldsymbol{\rho} - \boldsymbol{\rho}', z, \boldsymbol{s}; z', \boldsymbol{s}') ,$$

namely,

$$\tilde{F}(\boldsymbol{q}, z, z') = 4\pi\omega(4\pi n l l_{\text{eff}})^2 \int \mathrm{d}^2\rho \exp(\mathrm{i}\boldsymbol{q} \cdot \boldsymbol{\rho}) \times \int \mathrm{d}\boldsymbol{s}_1 \, \mathrm{d}\boldsymbol{s}_2 \, \sigma(-\boldsymbol{s}_0, \boldsymbol{s}_1) \, \sigma(\boldsymbol{s}_2, \boldsymbol{s}_0) \times \mathscr{F}(l_{\text{eff}}\boldsymbol{\rho}; l_{\text{eff}} z, \boldsymbol{s}_1; l_{\text{eff}} z', \boldsymbol{s}_2) . \tag{3.34}$$

The first term on the right-hand side of eq. (3.32) is the contribution of the ladder diagrams, i.e., the result of classical transport theory, and the second term is the contribution of maximally crossed diagrams that take into account the interference effects.

In deriving (3.32)–(3.34), we assumed that the angle θ between $\boldsymbol{s}$ and $-\boldsymbol{s}_0$ is small; indeed, in coherent backscattering experiments this angle never exceeded 100 mrad. If we proceeded without this assumption, in the expression for $a^{(L)}$ instead of the cross section $\sigma(-\boldsymbol{s}_0, \boldsymbol{s}_1)$ we would put $\sigma(\boldsymbol{s}, \boldsymbol{s}_1)$, and in the expression for $a^{(C)}$ instead of $\sigma(\pm\boldsymbol{s}_0, \boldsymbol{s}')$ we would use the function $W(\pm\boldsymbol{k}_0', k_0\boldsymbol{s}')$ with $\boldsymbol{k}_0' = \frac{1}{2}k_0(\boldsymbol{s}_0 - \boldsymbol{s})$ and $|\boldsymbol{k}_0'| = k_0\cos(\frac{1}{2}\theta)$, which is defined in eqs. (3.18) and (3.22), and at $k_0' \approx k_0$ can be approximated by the cross section $\sigma(\pm\boldsymbol{s}_0', \boldsymbol{s}')$ with $\boldsymbol{s}_0' = (\boldsymbol{s}_0 - \boldsymbol{s})/|\boldsymbol{s}_0 - \boldsymbol{s}|$ (BARABANENKOV and OZRIN [1988]).

The assumptions made in (3.32) and (3.34) are justified for $\theta \ll 1$ when the sharp maximum of the differential cross section $\sigma(\boldsymbol{s}, \boldsymbol{s}')$, if any, points forward, and $\boldsymbol{s}\cdot\boldsymbol{s}' = 1$, as is usually the case. A similar approximation has been employed by ISHIMARU and TSANG [1988] in considering the bistatic scattering coefficient $\gamma = 4\pi a/|s_z|$.

The condition $\theta \ll 1$ makes it possible to neglect in the exponent of eq. (3.33) some insignificant differences to the result obtained by AKKERMANS, WOLF, MAYNARD and MARET [1988] in the framework of a heuristic approach. It should be emphasized that for random inhomogeneous media for which $1/k_0 l_{\text{eff}} \ll 1$, the condition $\theta \ll 1$, in fact, has no effect on the experimental line shapes of coherent backscattering confined within a cone such that $k_0 l_{\text{eff}} \Delta\theta \lesssim 1$.

Thus, the calculation of the angular dependence of the albedo has been reduced to the evaluation of the Green function of the transfer equation for the slab. First, let us consider the simplified situation of a medium consisting of point-like uncorrelated scatterers with isotropic scattering cross section

$$\sigma(\boldsymbol{s}, \boldsymbol{s}') = 1/(4\pi nl)\,. \tag{3.35}$$

In this case, transfer equation (3.21) simplifies appreciably, and for the function $\tilde{F}(\boldsymbol{q}; z, z')$ defined in eq. (3.34) it takes the form

$$\tilde{F}(q; z, z') = \tilde{F}_0(q; z - z') + \int_0^{L/l_{\text{eff}}} \mathrm{d}z''\, \tilde{F}_0(q; z - z'')\, \tilde{F}(q; z'', z')\,, \tag{3.36}$$

where

$$\tilde{F}_0(q, z) = \omega \int \mathrm{d}^2\rho\, \frac{\exp(\mathrm{i}\boldsymbol{q}\cdot\boldsymbol{\rho} - r)}{4\pi r^2} \tag{3.37}$$

with $r = \sqrt{\rho^2 + z^2}$.

RYBICKI [1971] has investigated eq. (3.36) in depth, both for finite optical depths L/l_{eff} and for the half-space with $L/l_{\text{eff}} \to \infty$. The last case is of particular interest because for L tending to infinity, eq. (3.36) can be solved explicitly. This solution may be used as the point of departure for subsequent studies of the angular profile of the albedo under more complicated, and realistic, conditions.

Indeed, as $L \to \infty$ from eq. (3.36), it follows (SOBOLEV [1963])

$$\left(\frac{\partial}{\partial z} + \frac{\partial}{\partial z'}\right) \tilde{F}(q; z, z') = \tilde{F}(q; z, 0)\, \tilde{F}(q; 0, z')\,. \tag{3.38}$$

After the transformation (3.33) (at $L = \infty$ this is the Laplace transform), this expression becomes

$$F(q; p, p') = \frac{\mathrm{i}}{p + p'} \left[F(q, p)\, F(q, p') + F(q, p) + F(q, p')\right], \tag{3.39}$$

where the condition of symmetry $\tilde{F}(q, z, z') = \tilde{F}(q; z', z)$ following from eq. (3.36) has been used, and $F(q, p)$ stands for the Laplace transform of $\tilde{F}(q; z, 0)$.

For this function eq. (3.36) is an integral equation of the type of convolution on a half-axis with the kernel $\tilde{F}_0(q, z)$ that exponentially decays as $|z| \to \infty$. Therefore, this equation can be solved by the standard Wiener–Hopf approach, which operates with the Laplace transform $F(q, p)$ analytical on the half-plane $\mathrm{Im}\{p\} > 0$ and vanishing as $|p| \to \infty$.

The Wiener–Hopf method produces an auxiliary function $\Lambda(q, p)$ related to the kernel of the integral equation by

$$\begin{aligned} \Lambda(q, p) &= 1 - \int_{-\infty}^{\infty} \mathrm{d}z\, \mathrm{e}^{\mathrm{i}pz}\, \tilde{F}_0(q, z) \\ &= 1 - \frac{\omega}{2\mathrm{i}k} \ln\left(\frac{1 + \mathrm{i}k}{1 - rk}\right), \end{aligned} \tag{3.40}$$

with $k = \sqrt{p^2 + q^2}$. This function is analytic on the complex plane cut along the imaginary axis $\mathrm{Re}\{p\} = 0$, $|\mathrm{Im}\{p\}| > \sqrt{1 + q^2}$, and has two simple zeros at $p = \pm \mathrm{i}p_0(q)$, $p_0(q) < \sqrt{1 + q^2}$ where for $q \ll 1$ and $0 < 1 - \omega \ll 1$, $p_0(q) \approx \sqrt{q^2 + 3(1 - \omega)}$.

The analytic strip commonly considered in the Wiener–Hopf method lies along the real axis $|\mathrm{Im}\{p\}| < p_0(q)$. In this strip, the function $\Lambda(q, p)$ can be easily factorized, and the solution becomes

$$F(q, p) = H(q, \mathrm{i}/p) - 1\,, \tag{3.41}$$

where $H(q, w)$ is the generalized Chandrasekhar function introduced by RYBICKI [1971]

$$H(q, w) = \exp\left\{-\frac{w}{\pi}\int_0^\infty \frac{d\xi}{1 + w^2\xi^2} \ln\left(1 - \omega \frac{\arctan\sqrt{q^2 + \xi^2}}{\sqrt{q^2 + \xi^2}}\right)\right\}, \tag{3.42}$$

where $\mathrm{Re}\{w\} > 0$. This function satisfies the nonlinear integral equation

$$H^{-1}(q, w) = 1 - \tfrac{1}{2}\omega w \int_0^{\xi^*} \frac{H(q, \xi)\, d\xi}{(w + \xi)\sqrt{1 - q^2\xi^2}},$$

where $\xi^* = (1 + q^2)^{-1/2}$. At $q = 0$, this function coincides with the ordinary function from CHANDRASEKHAR [1960].

Formulas (3.41) and (3.39) yield a solution to the albedo problem (3.32) for point-like scatterers occupying a half-space. Summing up the preceding results, we obtain (GORODNICHEV, DUDAREV and ROGOZKIN [1989])

$$a(s, s_0) = \frac{\omega}{4\pi} \frac{s_{0z}|s_z|}{s_{0z} + |s_z|} \left\{H(0, |s_z|)\, H(0, s_{0z}) + \left[\left|H\left(q, \frac{i}{p}\right)\right|^2 - 1\right]\right\}, \tag{3.43}$$

with the parameters p and q given in eq. (3.32).

3.4. ANGULAR DISTRIBUTION OF BACKSCATTERED INTENSITY

Let us analyze the angular behavior of the albedo for the rather frequently encountered experimental situation of almost normal incidence of light upon an interface, i.e., $s_{0z} \approx 1$, with a small angle of backscattering $\theta \ll 1$, so that $s_z = \cos\theta \approx -1$ and $p \approx i$ in eq. (3.43), whereas $q = k_0 l_{\mathrm{eff}} \sin\theta \approx k_0 l_{\mathrm{eff}}\theta$ being not necessarily small by virtue of $k_0 l_{\mathrm{eff}} \gg 1$.

The first term in braces in eq. (3.43) represents the contribution of ladder diagrams and single scattering in the albedo; i.e., it corresponds to the result of the classical transfer theory. This quantity, denoted by a_{cl}, remains almost constant for angle θ varying in the range $\Delta\theta \sim 1/k_0 l_{\mathrm{eff}}$. On the other hand, the second, interference (cyclic) term almost coincides with the first at $\theta = 0$ or $q = 0$ and decays for $q \gg 1$ as q^{-1}.

We introduce the backscatter enhancement factor $K(\theta)$ as the ratio of the albedo $a(s, s_0) = a(\theta)$ to its value on the plateau, i.e. for $q > 1$, where it

coincides with the classical value a_{cl},

$$K(\theta) = a(\theta)/a_{cl} . \tag{3.44}$$

On substitution of $a(s, s_0)$ from eq. (3.43), we obtain

$$K(\theta) = 2 + [H^2(q, 1) - H^2(0, 1) - 1]/H^2(0, 1) . \tag{3.45}$$

According to eq. (3.42), at weak absorption, i.e., $1 - \omega \ll 1$, and a small value of q, the function $H(q, w)$ behaves like

$$H(q, 1) \approx [H(0, 1)]_{\omega = 1} [1 - \sqrt{q^2 + 3(1 - \omega)}] . \tag{3.46}$$

It decreases monotonously in the region of high q's and for $q \gg 1$ becomes

$$H(q, 1) \approx 1 + \pi\omega/4q . \tag{3.47}$$

Thus, for elastic scatterers, $K(\theta)$ of the angular distribution of coherent backscattering has a triangular line shape peaked about the backward direction with

$$K(\theta) - K(0) \approx -2q , \qquad q = k_0 l\theta \ll 1 , \qquad \omega = 1 . \tag{3.48}$$

The halfwidth of this peak calculated at the level $K(\theta_{1/2}) = 1.44$ amounts to $q_{1/2} = 0.36$; or $\theta_{1/2} = 0.36\, k_0 l$. The maximum value of the enhancement factor $K(0) = 2 - H^{-2}(0, 1) \approx 1.88$ is somewhat less than two as a result of the contribution of single scattering; indeed, from eqs. (3.25) and (3.30), $a^{(L)}(0) = a^{(C)}(0)$ and

$$K(0) = (a^{(1)} + 2a^{(L)})/(a^{(1)} + a^{(L)}) = 2 - a^{(1)}/a_{cl} .$$

For large q,

$$K(\theta) \approx 1 + \frac{\omega\pi}{2H^2(0, 1)}\, q^{-1} , \qquad q > 1 . \tag{3.49}$$

This result can be obtained by direct computation by including the contribution of only one maximally crossed diagram of second order in the interference term $a^{(C)}$. (In eq. (3.36) this corresponds to neglecting the integral term.) Consequently, the background of the coherent backscattering line shape is determined mainly by double scattering events, as predicted by BARABANENKOV [1973].

As can be seen from eq. (3.46), weak absorption, $1 - \omega \ll 1$, leads to a reduced albedo $a(0)$ and to a reduced peak of $K(\theta)$ in the range $q \lesssim \sqrt{3(1 - \omega)}$, which confirms the estimates derived earlier. A similar alteration of the $K(\theta)$ line shape is observed for slabs of finite optical depth $\tau = L/l_{eff}$. This conclusion has been drawn by TSANG and ISHIMARU [1985] and VAN DER MARK, VAN

Albada and LAGENDIJK [1988] on the basis of numerical solutions of eq. (3.36) for various τ and ω. These solutions indicate in particular that at $\tau = 32$ ($\omega = 1$), $a(\theta)$ amounts to 95% of the albedo at $\tau = \infty$. We note in passing that for $q \ll 1$ a transition from the linear dependence of $a(\theta)$ for a semi-infinite medium with $\tau = \infty$ to a quadratic dependence for $\tau < \infty$ can be demonstrated with an equation for the derivative of $\tilde{F}(q; z, z')$ with respect to q, which follows from eq. (3.36) and at $q = 0$ and $\tau < \infty$ has only a trivial solution.

An analysis of eq. (3.36), performed by GORODNICHEV, DUDAREV and ROGOZKIN [1990b], indicates that for $1 \ll \tau < \infty$, equality (3.48) for $K(\theta) - K(0)$ holds true if $\tau^{-1/2} \ll q \ll 1$, and in the region of $q^2\tau \ll 1$ its right-hand side must be replaced with $-2q^2\tau/3$.

One more circumstance is worth noting. In formulating a theory describing coherent backscattering, we have considered a situation when a plane wave or a beam of width L_0 far exceeding the lateral size of an illuminated region, $L_\perp$, is incident on the region occupied by a scattering medium. On the other hand, in a standard experiment generally the diameter of a spot illuminated by the laser beam is such that $L_0 \gg L_\perp$. Thus, we may assume for simplicity that the wave incident along the normal to the surface of the slab under consideration has the form

$$u_0(r) \approx \exp(ik_0 z - \rho^2/2L_0^2) .$$

Then in eq. (3.10) the incident average fields

$$\langle u(s_0, r)\rangle \approx \exp\left(ik_0 z - \frac{z}{2l_{\text{eff}}} - \frac{\rho^2}{2L_0^2}\right), \tag{3.50}$$

and the outcoming average fields $\langle u(-s, r)\rangle$ obey eq. (3.14). Incorporating the respective modifications in eq. (3.24) and observing (3.28) and (3.29) yield for the classical part of the albedo, $a_{\text{cl}} = a^{(1)} + a^{(L)}$, the following simple expression

$$a_{\text{cl}}(\theta, L_0) = (L_0/L_\perp)^2 \pi a_{\text{cl}}(\theta) , \tag{3.51}$$

where $a_{\text{cl}}(\theta)$ corresponds to $L_0 = \infty$.

Now, the interference part of the albedo has the form of a convolution and the enhancement factor is given by

$$K(\theta, L_0) = \frac{L_0^2}{\pi l_{\text{eff}}^2} \int d^2q_1 \, K\left(\frac{q - q_1}{k_0 l_{\text{eff}}}\right) \exp\left(-\frac{L_0^2 q_1^2}{l_{\text{eff}}^2}\right). \tag{3.52}$$

Given $l_{\text{eff}} \ll L_0$, the enhancement factor decreases by a factor of l/L_0 because

of the finite size of the beam, and the line shape peak rounds off in the range of angles $k_0 l\theta < \sqrt{l/L_0}$.

3.5. DIFFUSION APPROXIMATION

The scalar version of the theory developed for point-like scatterers described the salient features of coherent backscattering well. However, to attain a quantitative agreement with experiment, this simple version should incorporate several additional factors. The first factor is, beyond doubt, the finite dimensions of scatterers, which are frequently of the order of the wavelength, and also the anisotropy of the scattering properties when the extinction length l is a fraction of the transport length $l_{\rm tr} = l/(1 - \mu)$, where μ is the average cosine of the angle of scattering.

Unfortunately, no explicit solution of the transport equation for an arbitrary cross section of scattering $\sigma(\boldsymbol{s}, \boldsymbol{s}')$ is known. Nevertheless, there exists a simple method of approximate calculation of the albedo $a(\theta)$ for small angles, which also allows a useful physical interpretation. From eqs. (3.32)–(3.34), it follows that the deviation of the interference part of the albedo $a(\theta) = a(\boldsymbol{s}, \boldsymbol{s}_0)$, $s_{0z} = 1$ from the value at $\theta = 0$, has the structure

$$a(\theta) - a(0) = \int \mathrm{d}^2\rho \, [\mathrm{e}^{\mathrm{i}\boldsymbol{q}\cdot\boldsymbol{\rho}} - 1] \, f(\rho) , \tag{3.53}$$

where $f(\rho)$ is expressed through an integral with the Green function of the transfer equation for the slab. An asymptotic expansion of the integral in eq. (3.53) for $q = k_0 l\theta \to 0$ is governed by the behavior of $f(\rho)$ as $\rho \to \infty$; the expansion begins with a term linear in q only if $f(\rho) \sim \rho^{-3}$. This is the asymptotic diffusion expansion of the solution of the transfer equation for a half-space.

Thus, to evaluate the difference $a(\theta) - a(0)$ for small angles, we may represent the Green function of the transfer equation in the form

$$\mathscr{F}(\rho - \rho'; z, \boldsymbol{s}; z', \boldsymbol{s}') = [1 - 3D(\boldsymbol{s}\cdot\nabla - \boldsymbol{s}'\cdot\nabla')] \, \mathscr{F}(\boldsymbol{\rho} - \boldsymbol{\rho}'; z, z') , \tag{3.54}$$

where $\mathscr{F}(\boldsymbol{\rho}; z, z')$ obeys the stationary diffusion equation

$$D\nabla^2 \mathscr{F}(\rho - \rho', z, z') = -\delta(\boldsymbol{r} - \boldsymbol{r}')/(4\pi)^2 , \tag{3.55}$$

with the diffusion coefficient

$$D = \tfrac{1}{3} l_{\mathrm{tr}} , \tag{3.56}$$

where $l_{\mathrm{tr}} = l/(1 - \mu)$, and

$$\mu = nl \int \boldsymbol{s} \cdot \boldsymbol{s}' \, \sigma(\boldsymbol{s}, \boldsymbol{s}') \, \mathrm{d}^2 s .$$

The diffusion approximation is faced with a major difficulty due to the approximate condition for $\mathscr{F}(\boldsymbol{\rho}; z, z')$ at the boundary of the scattering medium. This approximation must be used in place of the exact conditions on the Green function of the transfer equation $\mathscr{F}(\boldsymbol{\rho}; z, \boldsymbol{s}; z', \boldsymbol{s}') = 0$, $s_z > 0$, $z = 0$ or $s_z < 0$, $z = L$. One version of the boundary conditions used by ISHIMARU and TSANG [1988] and BARABANENKOV and OZRIN [1988] corresponds to the integral flux from a source inside the layer vanishing at the boundary $z = 0$ or $z = L$. Then,

$$\left[2D\gamma \frac{\partial}{\partial z} F(\boldsymbol{\rho}; z, z') - F(\boldsymbol{\rho}; z, z') \right]_{z=0} = 0 , \tag{3.57a}$$

and on the other boundary, $z = L$, the respective equality differs from this by the sign of the derivative. The parameter γ is usually unity; it has been incorporated to compare the results with another popular version of the boundary condition, that of the "absorbing plane" type, when

$$\begin{aligned} &\mathscr{F}(\boldsymbol{\rho}; z = -z_0^*, z') = 0 , \\ &\mathscr{F}(\boldsymbol{\rho}; z, z' = L + z_0^*) = 0 , \end{aligned} \tag{3.57b}$$

where $z_0^* \approx 0.71 l_{\mathrm{tr}}$, and at $\mu = 0$ this is the extrapolated length in Milne's problem (CASE and ZWEIFEL [1967]). It is not hard to verify that the asymptotic expansions of the solutions of eq. (3.55) with the boundary condition (3.57a) obtained for $\gamma = z_0^*/2D$ and with the boundary condition (3.57b) for $\rho \to \infty$ coincide.

The boundary conditions (3.57a) were first used by BARABANENKOV [1973] to estimate the contribution of maximally crossed diagrams in the backscattering intensity. Based on this approximation, AKKERMANS, WOLF and MAYNARD [1986] investigated the angular profile of the intensity in coherent backscattering for both isotropic and anisotropic situations. A number of workers have used this approximation to estimate how various factors affect the peak line shape (EDREI and KAVEH [1987], FREUND, ROSENBLUH,

BERKOVITS and KAVEH [1988], VAN DER MARK, VAN ALBADA and LAGENDIJK [1988], AKKERMANS, WOLF, MAYNARD and MARET [1988]).

It should be emphasized that none of the afore-mentioned boundary conditions is perfectly appropriate for albedo calculations. Their derivation is based on a study of how the solution to the transfer equation behaves for $z' \gg l$ or $z, z' \gg l$, whereas the main contribution to integrals (3.33) and (3.34) is due to the region $0 \leqslant z, z' \lesssim l$ near the boundary. This disadvantage is, of course, irrelevant for the exact solution for isotropic scatterers occupying the half-space, which has been outlined in the preceding section.

The asymptotic expansion of the exact solution coincides with the solution to the diffusion problem subject to eq. (3.57a) obtained at $\gamma = z_1/2D$ or subject to eq. (3.57b) after the substitution of z_1 for z_0^*, where $z_1/l = -1 + H(0, 1)/\sqrt{3} \approx 0.68$. Since no exact solution is known for the general case of anisotropic scatterers, we can only assume that $\gamma = z_1^*/2D$ with $z_1^* \approx 0.68\, l_{\mathrm{tr}}$ is a suitable choice in this case.

In fact, the different listed boundary conditions lead to almost identical results for the albedo in the range of small angles θ. It is worth noting that there exist different ways of expressing the diffusion formula eq. (3.54) for the Green function of the transport equation. Sometimes, the gradient terms are dropped, being treated as small corrections (ISHIMARU and TSANG [1988]). These terms are small for an infinite medium, or for $z, z' \gg l_{\mathrm{tr}}$ in the case of a half-space. However, in the situation under consideration the key role is played by the region $0 \leqslant z, z' \lesssim l$, where from eq. (3.56) it follows that $|l\nabla \mathscr{F}| \sim \mathscr{F}$ so that all terms on the right-hand side of eq. (3.54) have the same order of magnitude.

After substitution in eq. (3.54) and then in eqs. (3.32)–(3.34) the solution of the problem (3.55) subject to eq. (3.57) is an explicit expression for the albedo (BARABANENKOV and OZRIN [1988]). We give a simplified formula for the enhancement factor by omitting the contribution due to single scattering. For normal incidence of a wave on the interface of a medium occupying a half-space, we have for small angles θ,

$$K(\theta) = 1 + (1 + q)^{-2}\left[1 - \frac{2(\mu + \frac{1}{3}\gamma)}{1 + 3(1 + \mu)/4\gamma}\,\frac{q}{1 - \mu + \frac{2}{3}\gamma q}\right], \tag{3.58}$$

where $q = k_0 l\theta$. In the limit of small q, this expression yields

$$K(\theta) \approx 2(1 - q/4q_{1/2}), \quad q \ll 1 - \mu.$$
$$4q_{1/2} = \frac{(1 - \mu)(1 + \mu + \frac{4}{3}\gamma)}{(1 + \frac{2}{3}\gamma)^2 - \mu^2}, \tag{3.59}$$

At $\theta = 0$, $K(\theta)$ has a triangular line shape of halfwidth $q_{1/2}$ dependent on μ. In the case of isotropic scatterers, $\mu \ll 1$, eq. (3.59) coincides with the result obtained by AKKERMANS, WOLF and MAYNARD [1986], accurate to within the substitution $\gamma = 3z_0/l$. For large-scale inhomogeneities, $1 - \mu \ll 1$,

$$4q_{1/2} \sim 3(1 - \mu)(1 + \tfrac{2}{3}\gamma)[2\gamma(1 + \tfrac{1}{3}\gamma)]^{-1}.$$

In general, the line shape of $K(\theta)$ depends appreciably on the average cosine of μ. For $\mu < \mu_{cr} = \frac{1}{3}$, $K(\theta)$ monotonously decreases as q increases. For $\mu > \mu_{cr}$, the contribution of maximally crossed diagrams becomes negative at sufficiently large angles of scattering and $K(\theta)$ crosses the axis $K = 1$ at $q = q_0$, peaks at $q = q_m$, and asymptotically approaches $K = 1$ as q^{-2}. The value q_0 and a rough estimate of q_m may be obtained from

$$q_0 \approx 2(1 - \mu)[1 + 3(1 + \mu)/4\gamma/(3\mu - 1)],$$

$$q_m \approx [(3 + \gamma)(1 - \mu)/2\gamma]^{1/2},$$

where $1 - \mu \ll 1$. The behavior of $K(\theta)$ as a function of q for different μ is illustrated in fig. 3.6.

A noticeable feature of $K(\theta)$ behavior is the presence of a minimum in the case of large-scale scatterers. This result is usually consistent with the general representations of the interference pattern and with the results quoted in the previous section. However, in deriving eq. (3.58), we have used the boundary condition (3.57a), which is, of course, an approximation. Moreover, if we solve the problem subject to the boundary condition (3.57b), the enhancement factor

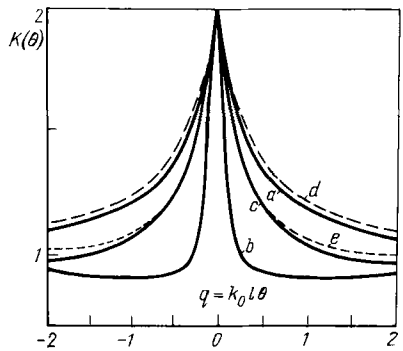

Fig. 3.6. Enhancement factor $K(\theta)$ calculated for coherent backscattering: (a), (b), and (c) show the diffusion approximation (3.58) with $\gamma = 1$ computed for $\mu = 0$, 0.93 and 0.67, respectively; (d) exact solution for isotropic scatterers ($\mu = 0$) represented for $K(\theta)/0.94$; (e) diffusion approximation with boundary condition (3.57b) of the absorbing-plane type calculated for $\mu = 0.67$.

becomes

$$K(\theta) = 1 + (1+q)^{-2}\left\{1 - \frac{2\alpha_0 q - (1-\mu-2\mu q)\,[1-\exp(-2\alpha_0 q/(1-\mu))]}{q(1+\mu+2\alpha_0)}\right\}, \tag{3.60}$$

where $\alpha_0 \approx 0.71$. This $K(\theta)$ is seen to be a monotonous function of q. Its difference from the results of AKKERMANS, WOLF, MAYNARD and MARET [1988] and VAN DER MARK, VAN ALBADA and LAGENDIJK [1988] may be attributed to the fact that in considering the diffusion approximation with the boundary condition (3.57b), these authors failed to account for the gradient terms in eq. (3.54) and also substituted l_{tr} for l in the exponents of (3.32) and (3.33).

It is noteworthy that the position of the minimum belongs to the range of angles and parameter q in which, strictly speaking, the diffusion approximation (accurate for $q \to 0$) is inapplicable. Therefore, the question of whether or not the minimum exists can be answered only with the aid of an exact solution of the transfer equation for a half-space with nonisotropic scatterers.

Another fact worthy of note is that the diffusion approximation gives a lowered value of the albedo in the maximum $\theta = 0$ and a distorted pattern of $K(\theta)$ at large q. Actually, as in the isotropic case, $K(\theta) \sim q^{-1}$, $q \gg 1$. This aspect has been treated in detail by ISHIMARU and TSANG [1988]. However, in the range of small q, $q \lesssim 1$, where the diffusion approximation is operable, results (3.58) and (3.60) agree well with the experimental evidence (fig. 3.7).

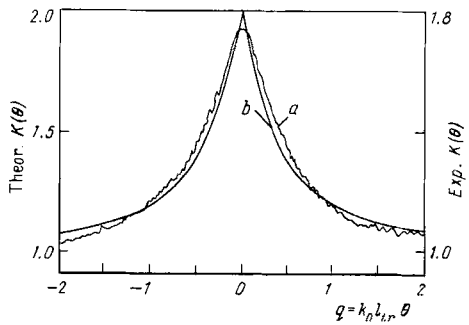

Fig. 3.7. (a) Experimental enhanced backscattering from a 10% water suspension of 0.46 μm diameter polystyrene spheres, where $l_{tr} = 20$ μm, the incident and detected wave vectors are co-polarized so that $|e \cdot e_0| = 1$, and the plane of scanning is perpendicular to e_0 (WOLF, MARET, AKKERMANS and MAYNARD [1988]); (b) diffusion approximation curve obtained with a boundary condition of the absorbing-plane type.

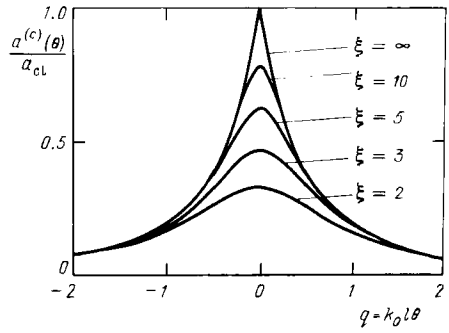

Fig. 3.8. Relative intensity of coherent backscattering calculated for scalar waves in the diffusion approximation with $\xi = \sqrt{l_{ab}/3l}$ (MACKINTOSH and JOHN [1988]). Similar $K(\theta)$ profiles have been obtained for: (1) a layer of finite thickness ($\xi = L/l$) in the scalar problem or the co-polarized configuration, or identical helicities of circularly polarized waves, and (2) Faraday rotation for identical circular polarizations ($\xi = 1/gk_0l$).

The diffusion approximation is well suited for an account of the effects of absorption. For this purpose in the diffusion equation, eq. (3.55), one should replace the operator $D\nabla^2$ with $[D\nabla^2 - l_{ab}^{-1}]$, with $l_{ab} = \omega l/(1-\omega)$. Then in the final formulas (3.58) or (3.60) the parameter q is replaced by $\sqrt{q^2 + 3(1-\omega)}$, and the backscattering peak finds itself rounded off as for isotropic scatterers (fig. 3.8). For a slab of finite thickness, like in the presence of absorption, the asymptotic behavior to the diffusion equation changes as $\rho \to \infty$, and it decays exponentially rather than by a power law (ρ^{-3}). For example, for boundary condition (3.57b), $L \gg z_0$, and $\rho \to \infty$, we have

$$\mathscr{F}(\rho; z, z') = \frac{\pi z z'}{(4\pi L)^2 D\sqrt{2L\rho}} \exp(-\pi\rho/L).$$

Therefore, near the maximum the enhancement factor becomes

$$K(\theta) \approx 2 - \frac{2l}{3L}(k_0 L\theta)^2 (1 + \tfrac{2}{3}\gamma)(1 + \tfrac{4}{3}\gamma)^{-1}, \qquad (3.61)$$

$$\mu = 0, \qquad k_0 L\theta \ll 1,$$

and at larger angles θ, $K(\theta)$ again becomes a linear function. Similar estimates have been obtained by EDREI and KAVEH [1987].

3.6. POLARIZATION EFFECTS

The vectorial nature of the electromagnetic field is another factor that appreciably affects the coherent backscattering. Polarization effects have been studied in the experiments of WOLF and MARET [1985], VAN ALBADA and LAGENDIJK [1985], ETEMAD, THOMPSON and ANDREJCO [1986], ROSENBLUH, EDREI, KAVEH and FREUND [1987], ETEMAD [1988], and WOLF, MARET, AKKERMANS and MAYNARD [1988]. They have demonstrated that the backscattering pattern is strongly dependent on the angle between the polarizations of the incident and detected radiation.

Before we begin discussing polarization effects, we wish to introduce necessary corrections to the statement of the problem formulated in § 3.2. The medium under consideration is nonmagnetic, is isotropic on the average, and exhibits a fluctuating permittivity or refractive index. Let a linearly polarized plane monochromatic wave

$$E^{(0)}(s_0, r) = e_0 \exp(ik_0 s_0 r),$$

with $e_0 \cdot s_0 = 0$ and $|e_0| = 1$ be incident on the space occupied by the medium in the direction of s_0. The field in the space obeys the Maxwell equations, which may be written in the form

$$\begin{aligned} &\{[\nabla^2 + k_0^2(1 + \tilde{\varepsilon})]\,\delta_{\alpha\beta} - \nabla_\alpha \nabla_\beta\}\, E_\beta(e_0, s_0, r) = 0, \\ &E_\alpha(e_0, s_0, r)|_{s_0 \cdot r \to -\infty} = e_{0\alpha} \exp(ik_0 s_0 r), \end{aligned} \tag{3.62}$$

where α and β label the Cartesian projections of the vectors, and summation is assumed over the repeating indices. For the average field $\langle E_\alpha(r)\rangle$ and the mutual coherence function $\langle E_\alpha(r) E_\beta^*(r)\rangle$, tensor analogs of eqs. (3.3) and (3.7) are formulated, which involve a tensor mass operator $M_{\alpha\beta}(r, r')$, average Green function $\langle G_{\alpha\beta}(r, r')\rangle$ of eq. (3.62), and vertex function $\Gamma_{\alpha\beta;\,\alpha'\beta'}(r_1, r_2; r_1', r_2')$.

For free space and $r \to \infty$, the Green function becomes

$$G_{\alpha\beta}^{(0)}(r) \approx -(4\pi r)^{-1} P_{\alpha\beta}(s) \exp(ik_0 r),$$

where $s = r/r$, and the polarization matrix

$$P_{\alpha\beta}(s) = \delta_{\alpha\beta} - s_\alpha s_\beta \tag{3.63}$$

secures the transversality condition. Similarly to eq. (3.6), we introduce the albedo

$$a(s, s_0; e, e_0) = \left.\frac{R^2 I(R, e)}{\Sigma}\right|_{R \to \infty}, \tag{3.64}$$

where $s = R/R$, and $I(R, e) = \langle |e \cdot E(R)|^2 \rangle$ is the intensity corresponding to the component of scattered field polarized along unit vector e; i.e., $e \cdot s = 0$.

Making use of the Dyson equation and the reciprocity condition, which is now written as

$$G_{\alpha\beta}(r, r') = G_{\beta\alpha}(r', r), \tag{3.65}$$

we may generalize (3.10)–(3.14) and (3.24) for the case of the vector field.

If we take for the average field in the medium the effective wavenumber approximation

$$\langle E_\alpha(e, s, r) \rangle \approx e_\alpha \exp(ik_0 s \cdot r - r/2l_{\text{eff}}),$$

then the expression for the albedo is

$$\begin{aligned} a(s, s_0; e, e_0) &= (4\pi L_\perp)^{-2} \int dr_1\, dr_2\, dr_1'\, dr_2'\, e_\alpha e_\beta e_{0\alpha'} e_{0\beta'}\, \Gamma_{\alpha\beta;\,\alpha'\beta'}(r_1, r_2; r_1', r_2') \\ &\quad \times \exp\left[-\frac{z_1 + z_2}{2l_{\text{eff}} s_z} - \frac{z_1' + z_2'}{2l_{\text{eff}} s_{0z}} - ik_0 s \cdot (r_1 - r_2) + ik_0 s_0 \cdot (r_1' - r_2') \right]. \end{aligned} \tag{3.66}$$

This expression "automatically" takes into account the transversality of the incident and scattered waves.

We will again consider the contribution to the vertex function from single-scattering events and ladder and maximally crossed diagrams. As in the case of a scalar field, the qualitative reasoning underlying this constraint is based on the analysis of the phase relationships (see § 3.2). For the vector field, however, these relationships are not enough to ensure that the contributions of the ladder and maximally crossed diagrams coincide. The rotation that the polarization vector undergoes in the processes of scattering should also be taken into account.

Following AKKERMANS, WOLF and MAYNARD [1986] (see also for a more detailed discussion and estimates, AKKERMANS, WOLF, MAYNARD and MARET [1988]), we consider a simple case of Rayleigh scattering by an isolated scatterer, in which the polarization vector e_1 of the scattered field has the form $e_1 = P(s_1)\, e_0$, where $P(s_1)$ is the polarization matrix (3.63).

Along a trajectory γ defined by fixed positions of scatterers, $R_1, \ldots, R_N$, and a sequence of wave vectors $k_0 = s_0 k_0$, $k_1, \ldots, k_{N-1}$, $k_N = sk_0$, the polarization vector of the outcoming wave is $e_\gamma = M_\gamma e_0$, where $M_\gamma = P(s_N)\, P(s_{N-1}) \ldots P(s_1)\, P(s_0)$, and $s_j = k_j/k_j$. For the time-reversed path

$-\gamma$ with the sequence of wave vectors $\boldsymbol{k}_0, -\boldsymbol{k}_{N-1}, \ldots, -\boldsymbol{k}_1, \boldsymbol{k}_N$, the polarization vector of the outcoming wave is $\boldsymbol{e}_{-\gamma} = M_{-\gamma}\boldsymbol{e}_0$. The matrices $P(s_j)$ are symmetrical and independent of the sign of $\boldsymbol{k}_j$. Therefore, for backscattering at zero angles when $\boldsymbol{k}_N = -\boldsymbol{k}_0$, we have $M_{-\gamma} = (M_\gamma)^{\mathrm{T}}$. It is conceivable that in this case the projections of $\boldsymbol{e}_\gamma$ and $\boldsymbol{e}_{-\gamma}$ on the direction of $\boldsymbol{e} = \pm\boldsymbol{e}_0$ coincide [the case of the parallel (co-polarized) polarization of incident and detected radiation]. The coherence is conserved, and an enhancement of backscattering may be expected which is similar to that of the scalar case with $K(0) \approx 2$.

For orthogonal polarization, $\boldsymbol{e} \perp \boldsymbol{e}_0$, the projections $\boldsymbol{e}\cdot\boldsymbol{e}_\gamma$ and $\boldsymbol{e}\cdot\boldsymbol{e}_{-\gamma}$ differ for all N except $N = 2$. This leads to the suppression of the interference part of the intensity, which peaks to about one half of its classical value.

To obtain a more detailed description of the polarization effects, we consider a simple model of a medium constituted by a point-like, nonabsorbing, isotropically polarized species. The reciprocity condition, eq. (3.65), leads to a relation combining the contributions of the ladder and maximally crossed diagrams into the vertex function

$$\begin{aligned}\Gamma^{(\mathrm{C})}_{\alpha\beta;\,\alpha'\beta'}(\boldsymbol{r}_1, \boldsymbol{r}_2; \boldsymbol{r}_1', \boldsymbol{r}_2') &= \Gamma^{(\mathrm{L})}_{\alpha\beta';\,\alpha'\beta}(\boldsymbol{r}_1, \boldsymbol{r}_2'; \boldsymbol{r}_1', \boldsymbol{r}_2) \\ &= \Gamma^{(\mathrm{L})}_{\alpha'\beta;\,\alpha\beta'}(\boldsymbol{r}_1', \boldsymbol{r}_2; \boldsymbol{r}_1, \boldsymbol{r}_2') \qquad (3.67)\end{aligned}$$

which differs from (3.27) and (3.28) by an additional transposition of the polarization indices. To calculate $\Gamma^{(\mathrm{L})}$ and $\Gamma^{(\mathrm{C})}$, we may resort to the scheme of transfer theory, outlined in § 3.2 and § 3.3, as generalized for an electromagnetic field.

The intensity operator of a pointline scatterer will be written as

$$\begin{aligned}K_{\alpha\beta;\,\alpha'\beta'}(\boldsymbol{r}_1, \boldsymbol{r}_2; \boldsymbol{r}_1', \boldsymbol{r}_2') &= (6\pi/l)\,\delta_{\alpha\alpha'}\,\delta_{\beta\beta'}\,\delta(\boldsymbol{r}_1 - \boldsymbol{r}_2) \\ &\quad \times \delta(\boldsymbol{r}_1' - \boldsymbol{r}_2')\,\delta(\boldsymbol{r}_1 - \boldsymbol{r}_1')\,. \qquad (3.68)\end{aligned}$$

Then for the medium occupying the space, we obtain

$$a(\boldsymbol{s}, \boldsymbol{s}_0; \boldsymbol{e}, \boldsymbol{e}_0) = a^{(1)} + a^{(\mathrm{L})} + a^{(\mathrm{C})},$$

where the contribution due to single scattering is

$$a^{(1)} = \frac{3\mathrm{i}}{8\pi}\,\frac{(\boldsymbol{e}\cdot\boldsymbol{e}_0)^2}{p - p^*}, \qquad (3.69)$$

and the contribution due to the ladder and maximally crossed (cyclical)

diagrams are

$$a^{(L)} = \frac{3}{8\pi}\, e_\alpha e_\beta e_{0\alpha'} e_{0\beta'}\, F_{\alpha\beta;\,\alpha'\beta'}\left(0;\, \frac{i}{|s_z|},\, \frac{i}{s_{0z}}\right), \tag{3.70}$$

$$a^{(C)} = \frac{3}{8\pi}\, e_\alpha e_\beta e_{0\alpha'} e_{0\beta'}\, F_{\alpha\beta';\,\alpha'\beta}(\boldsymbol{q}; p, -p^*), \tag{3.71}$$

with the parameters

$$\boldsymbol{q} = k_0 l(\boldsymbol{s}_\perp + \boldsymbol{s}_{0\perp}),$$

$$p = k_0 l(s_z + s_{0z}) + i(s_{0z} + |s_z|)/2s_{0z}|s_z|\,.$$

Here,

$$F_{\alpha\beta;\,\alpha'\beta'}(\boldsymbol{q}; p, p') = \int\int_0^\infty dz\, dz'\, e^{ipz + ip'z'}\, \tilde{F}_{\alpha\beta;\,\alpha'\beta'}(\boldsymbol{q}; z, z') \tag{3.72}$$

is related to the Fourier transform $\tilde{F}$ in the difference of transverse coordinates $\boldsymbol{\rho} - \boldsymbol{\rho}'$ of the Green function $\mathcal{F}_{\alpha\beta;\,\alpha'\beta'}(\boldsymbol{\rho} - \boldsymbol{\rho}'; z, z')$ of the transfer equation for an electromagnetic field in the medium occupying a half-space (DOLGINOV, GNEDIN and SILANTYEV [1979]). The equation for $\tilde{F}$ (more accurately, the system of equations) has the form

$$\tilde{F}_{\alpha\beta;\,\alpha'\beta'}(\boldsymbol{q}; z, z') = \tilde{F}^{(0)}_{\alpha\beta;\,\alpha'\beta'}(\boldsymbol{q}; z - z') + \int_0^\infty dz''\, \tilde{F}^{(0)}_{\alpha\beta;\,\alpha''\beta''}(\boldsymbol{q}; z - z'')\tilde{F}_{\alpha''\beta'';\,\alpha'\beta'}(\boldsymbol{q}; z'', z'), \tag{3.73}$$

where

$$\tilde{F}^{(0)}_{\alpha\beta;\,\alpha'\beta'}(\boldsymbol{q}, z) = \tfrac{3}{2}\int d^2\rho\, P_{\alpha\alpha'}(\boldsymbol{s})\, P_{\beta\beta'}(\boldsymbol{s})\, \frac{\exp(i\boldsymbol{q}\cdot\boldsymbol{\rho} - r)}{4\pi r}, \tag{3.74}$$

with $r = \sqrt{\rho^2 + z^2}$, and $\boldsymbol{s} = \boldsymbol{r}/r$.

From eq. (3.73) it follows that we generalized relationship (3.38), which after the Laplace transformation (3.72) becomes

$$F_{\alpha\beta;\,\alpha'\beta'}(\boldsymbol{q}; p, p') = \frac{i}{p + p'}\,[F_{\alpha\beta;\,\alpha'\beta'}(\boldsymbol{q}, p) + F_{\alpha'\beta';\,\alpha\beta}(-\boldsymbol{q}, p') + F_{\alpha\beta;\,\alpha''\beta''}(\boldsymbol{q}, p)\, F_{\alpha'\beta';\,\alpha''\beta''}(-\boldsymbol{q}, p')], \tag{3.75}$$

where $F_{\alpha\beta;\,\alpha'\beta'}(\boldsymbol{q}, p)$ is the Laplace transform of $\tilde{F}_{\alpha\beta;\,\alpha'\beta'}(\boldsymbol{q}; z, 0)$.

For functions $\tilde{F}_{\alpha\beta;\,\alpha'\beta'}(q, p)$, analytic in the upper half-plane of $\mathrm{Im}\{p\} > 0$ and falling off as $|p|^{-1}$ as $|p| \to \infty$, eqs. (3.73) transform to a system of Wiener–Hopf equations, namely,

$$\begin{aligned} &\Lambda_{\alpha\beta;\,\alpha''\beta''}(q, p)\, F_{\alpha''\beta'';\,\alpha'\beta'}(q, p) \\ &\quad = L^{+}_{\alpha\beta;\,\alpha'\beta'}(q, p) + F^{-}_{\alpha\beta;\,\alpha'\beta'}(q, p)\,, \end{aligned} \tag{3.76}$$

where

$$\begin{aligned} &\Lambda_{\alpha\beta;\,\alpha'\beta'}(q, p) = \delta_{\alpha\alpha'}\,\delta_{\beta\beta'} - L_{\alpha\beta;\,\alpha'\beta'}(q, p)\,, \\ &L_{\alpha\beta;\,\alpha'\beta'}(q, p) = \int_{-\infty}^{\infty} \mathrm{d}z\, \mathrm{e}^{\mathrm{i}pz}\, \tilde{F}^{(0)}_{\alpha\beta;\,\alpha'\beta'}(q, z) \\ &\qquad = \frac{3}{8\pi} \int \mathrm{d}^2 s\, \frac{P_{\alpha\alpha'}(s)\, P_{\beta\beta'}(s)}{1 - \mathrm{i}ps_z - \mathrm{i}q \cdot s_\perp}\,, \end{aligned} \tag{3.77}$$

and L^{+} is the Laplace transform of $\tilde{F}^{(0)}$. We shall assume that the values 1, 2, and 3, through which α and β run, correspond to the x, y, and z projections of the vectors.

As in the preceding section, we are willing to elicit as many analytical corollaries as possible from the derived system (3.76) of Wiener–Hopf equations. Specifically, we wish to analyze the angular dependence of enhanced backscattering predicted by the solution of this system. We intend also to investigate the results of a diffusion approximation constructed by STEPHEN and CWILICH [1986].

At $q = 0$ the matrix $\{\Lambda(q, p)\}$ and the matrix $\{F(q, p)\}$ become sparse and exhibit a block structure: an entry is nonzero provided that its index pair belongs to one of the following four groups

$$(\alpha, \beta), (\alpha', \beta') = \begin{cases} (1, 1), (2, 2), (3, 3), & \text{(i)}\,, \\ (1, 2), (2, 1) & \text{(ii)}\,, \\ (1, 3), (3, 1) & \text{(iii)}\,, \\ (2, 3), (3, 2) & \text{(iv)}\,. \end{cases} \tag{3.78}$$

As a consequence, system (3.76) can be partitioned into four systems. In view of the symmetry $\Lambda_{\alpha\beta;\,\alpha'\beta'} = \Lambda_{\beta\alpha;\,\beta'\alpha'}$ which is true for functions $F_{\alpha\beta;\,\alpha'\beta'}(0, p)$ as well, the solutions to systems (ii)–(iv) can be obtained in an explicit form. As an example, for index group (ii) we have

$$\begin{aligned} &F_{12;\,12}(0, p) = \tfrac{1}{2}[H_{+}(\mathrm{i}/p) + H_{-}(\mathrm{i}/p)] - 1\,, \\ &F_{12;\,21}(0, p) = \tfrac{1}{2}[H_{-}(\mathrm{i}/p) - H_{-}(\mathrm{i}/p)]\,, \end{aligned} \tag{3.79}$$

where $H_+(w)$ and $H_-(w)$ are Chandrasekhar's functions which are constructed according to the principle used for $H(0, w)$ of eq. (3.42) and, which for $\mathrm{Re}\{w\} > 0$, have the form

$$H_\pm(w) = \exp\left[-\frac{w}{\pi} \int_0^\infty \frac{\mathrm{d}\xi}{1 + w^2\xi^2} \ln \Lambda_\pm(0, \xi) \right]. \tag{3.80}$$

It is essential that the functions

$$\Lambda_\pm(0, p) = 1 - [L_{12;12}(0, p) \pm L_{12;21}(0, p)] \tag{3.81}$$

are analytic on the p-plane except the imaginary axis $\mathrm{Re}\{p\} = 0$, $|\mathrm{Im}\{p\}| > 1$, and have simple zeros within the intervals $\frac{1}{2} < |\mathrm{Im}\{p\}| < 1$. Therefore, solutions (3.79) have the respective poles and cuts in the lower half-plane $\mathrm{Im}\{p\} < 0$, and their inverse Laplace transforms $\tilde{F}_{\alpha\beta;\,\alpha'\beta'}(0; z, 0)$ decay exponentially as $z \to \infty$.

Instead of the functions $F_{\alpha\beta;\,\alpha'\beta'}$ with group (i) indices of eq. (3.78) it is convenient to introduce linear combinations,

$$\begin{aligned} \Phi_1 &= F_{\alpha\alpha;\,11}\,, \\ \Psi_1 &= \tfrac{1}{2}(F_{11;11} + F_{22;11}) - F_{33;11}\,, \\ X_1 &= F_{11;11} - F_{22;11}\,. \end{aligned} \tag{3.82}$$

The counterparts Φ_2, Ψ_2, X_2, and Φ_3, Ψ_3, X_3 are constructed by replacing on the right-hand sides of eq. (3.82) the second pair of indices (1, 1) with (2, 2) and (3, 3), respectively. Recognizing that these functions are symmetrical with respect to transposing the index pairs (1, 1) and (2, 2), i.e., x and y at $\boldsymbol{q} = 0$, we obtain

$$\begin{aligned} \Phi_1(0, p) &= \Phi_2(0, p)\,, \\ \Psi_1(0, p) &= \Psi_2(0, p)\,, \\ X_1(0, p) &= -X_2(0, p)\,, \\ X_3(0, p) &= 0\,. \end{aligned} \tag{3.83}$$

The system of equations for functions (3.82) derived from eq. (3.76) separates into a pair of equations for Φ_a and Ψ_a and an independent equation for X_a. Solving the latter yields

$$X_1(0, p) = F_{12;12}(0, p) + F_{12;21}(0, p)\,, \tag{3.84}$$

which can be expressed by means of H_+ and H_- with the aid of eq. (3.79).

Unfortunately, an explicit solution for the remaining three pairs of equations for functions Φ_a and Ψ_a, $a = 1, 2, 3$, defies evaluation. Nevertheless, a straightforward analysis indicates that the solutions of these equations may be represented in the form

$$\begin{aligned} \Phi_a(0,p) &= H(0, \mathrm{i}/p)\,[1 + \chi_a(p)] - 1\,, \\ \Psi_1(0,p) &= \tfrac{1}{2} H_1(\mathrm{i}/p)\,[1 + \chi_1'(p)] - \tfrac{1}{2}\,, \\ \Psi_3(0,p) &= 1 - H_1(\mathrm{i}/p)\,[1 + \chi_3'(p)]\,, \end{aligned} \tag{3.85}$$

where $a = 1, 2, 3$; $H(0, w)$ is the Chandrasekhar function (3.42) with $\omega = 1$; and the expression for $H_1(w)$ may be obtained from eq. (3.80), where $\Lambda_{\pm}(0,p)$ should be replaced with

$$\begin{aligned} \Lambda_1(0,p) = 1 - \tfrac{1}{3}[&L_{11;11}(0,p) + L_{11;22}(0,p) \\ &+ 2L_{33;33}(0,p) - 4L_{11;33}(0,p)]\,. \end{aligned} \tag{3.86}$$

It can be established that $\chi_a(p)$ and $\chi_a'(p)$ are analytic in the p plane except the imaginary axis in the interval $\mathrm{Im}\{p\} < -\frac{1}{2}$ and as $|p| \to \infty$ fall off as $|p|^{-1}$. $H_1(\mathrm{i}/p)$ exhibits similar properties. Consequently, the inverse Laplace transform for $\Psi_a(0,p)$, $a = 1, 2, 3$, decays exponentially as $z \to \infty$. At the same time the Chandrasekhar function $H(0, \mathrm{i}/p)$ has a simple pole at $p = 0$, and the inverse Laplace transform of $\Phi_a(0,p)$ demonstrates a "diffusive" behavior. Therefore, we should expect that the behavior of the intensity near the direction of backscatter will be defined by the components $F_{\alpha\beta;\,\alpha'\beta'}$ diagonal in the indices α, β, and α', β'.

In the general case of an arbitrary $q \neq 0$ the system of eqs. (3.76) has a rather complicated structure. It defies an explicit solution but lends itself to an analysis of the behavior of the solution at large and small values of q. First, we look at the range of $q \ll 1$ to evaluate the peak line shape in backscattering. If we differentiate the right- and left-hand sides of eq. (3.76) with respect to q at $q = 0$, it is not hard to verify that for the derivatives

$$\frac{\partial}{\partial q} F_{\alpha\beta;\,\alpha'\beta'}(\boldsymbol{q}, p)\,|_{q=0} \equiv \dot{F}_{\alpha\beta;\,\alpha'\beta'}(0,p)$$

with the indices from eq. (3.78) we obtain four closed systems of equations, which differ from their counterparts for $F_{\alpha\beta;\,\alpha'\beta'}(0,p)$ in their homogeneous form only.

The systems (ii)–(iv) for $\dot{F}_{\alpha\beta;\,\alpha'\beta'}(0,p)$ have a trivial solution only, $\dot{F}_{\alpha\beta;\,\alpha'\beta'}(0,p) = 0$. For system (i) we again introduce the linear combinations

$\dot{\Phi}_a$, $\dot{\Psi}_a$, and $\dot{X}_a$, composed of $\dot{F}_{\alpha\beta;\,\alpha'\beta'}$ according to the scheme of eq. (3.83). The solution of the equation for $\dot{X}_a$ also yields $\dot{X}_a(0,p) = 0$. However, the system for $\dot{\Phi}_a$ and $\dot{\Psi}_a$ has a nontrivial solution, since $\Lambda(0,p) = [H(0,\mathrm{i}/p)\,H(0,-\mathrm{i}/p)]^{-1}$ has at $p = 0$ a (diffusion) zero of second order, namely

$$\begin{aligned}\dot{\Phi}_a(0,p) &= -\frac{\mathrm{i}}{p}\,H\left(0,\frac{\mathrm{i}}{p}\right)[1+\psi_a(p)]\,,\\ \dot{\Psi}_a(0,p) &= H_1(\mathrm{i}/p)\,\psi_a'(p)\,,\end{aligned} \tag{3.87}$$

where ψ_a and ψ_a' possess properties similar to those of χ_a and χ_a'.

Now we return to the formulas (3.69)–(3.71) for the albedo, Consider the case of a normal incidence where $s_{0z} = 1$ and the vector $\boldsymbol{e}_0$ of polarization of the incident wave lies in the xy-plane; for clarity we let $e_{0y} = 1$ (fig. 3.9). For small angles of backscattering $\theta \ll 1$, for which $s_z \approx -1$, $p \approx \mathrm{i}$, and $q \approx k_0 l\theta$, we may neglect in (3.70) and (3.71) the contribution of terms that contain the z-projection of the polarization vector $\boldsymbol{e}$, which is proportional to $\sin\theta$, and assume that $e_x^2 + e_y^2 \approx 1$. Then

$$\begin{aligned}a(\boldsymbol{s},\boldsymbol{s}_0,\boldsymbol{e},\boldsymbol{e}_0) &= a(\theta,\varphi)\\ &= \frac{3}{16\pi}\cos^2\varphi + \frac{3}{8\pi}[\cos^2\varphi F_{11;11}(0,\mathrm{i},\mathrm{i}) + \sin^2\varphi F_{22;11}(0,\mathrm{i},\mathrm{i})]\\ &\quad + \frac{3}{8\pi}[\cos^2\varphi F_{11;11}(\boldsymbol{q};\mathrm{i},\mathrm{i}) + \sin^2\varphi F_{21;12}(\boldsymbol{q},\mathrm{i},\mathrm{i})]\,,\end{aligned} \tag{3.88}$$

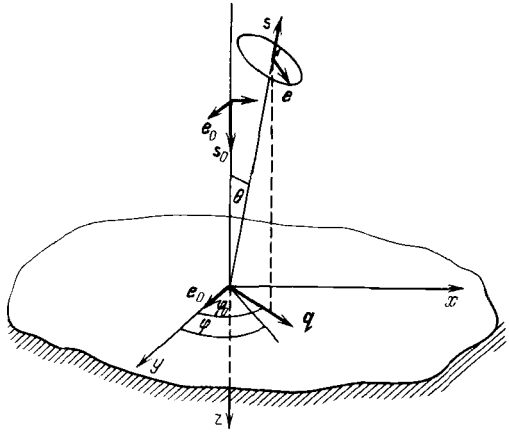

Fig. 3.9. Geometry of the normal-incidence scattering problem: $\boldsymbol{s}_0$ and $\boldsymbol{s}$ represent the directions of the incident and detected fields, $\boldsymbol{e}_0$ and $\boldsymbol{e}$ represent the corresponding polarization vectors, and $\boldsymbol{q}z$ represents the plane of scanning with $\boldsymbol{q} = k_0 l(\boldsymbol{s}_{0\perp} + \boldsymbol{s}_\perp)$.

where $\cos\varphi = \boldsymbol{e}\cdot\boldsymbol{e}_0$. The first term in this expression corresponds to single scattering, the second to the contribution of the ladder diagrams, and the third to the contribution of the maximally crossed diagrams. It suggests that for the parallel configuration when the polarizations of the incident and detected radiation are identical and $\varphi = 0$, the contributions due to the ladder and maximally crossed diagrams in the backscattered intensity coincide, and the enhancement factor $K(0, \varphi) = a(0, \phi)/a_{\mathrm{cl}}(0, \varphi)$ deviates from two, resulting from the contribution due to the single scattering only.

For the orthogonal configuration of $\varphi = \frac{1}{2}\pi$, no doubling of the intensity is observed any longer. Making use of the results of an analysis of the exact solution, we may establish that

$$\begin{aligned} &a^{(\mathrm{L})}(0, \tfrac{1}{2}\pi) > a^{(\mathrm{C})}(0, \tfrac{1}{2}\pi)\,, \\ &2a^{(\mathrm{L})}(0, 0) > a^{(\mathrm{L})}(0, \tfrac{1}{2}\pi) + a^{(\mathrm{C})}(0, \tfrac{1}{2}\pi)\,. \end{aligned} \tag{3.89}$$

These inequalities indicate that at $\varphi = \frac{1}{2}\pi$, the peak of enhancement factor ($\theta = 0$) is below 2 and lower than that of the parallel configuration,

$$1 < K(0, \tfrac{1}{2}\pi) < K(0, 0) \lesssim 2\,.$$

The behavior of albedo as a function of θ in the range of $q \ll 1$ is appreciably dependent on the mutual orientation of the polarization vectors. Observing the structure of the solutions for functions $F_{\alpha\beta;\,\alpha'\beta'}(0, p)$ and $\dot{F}_{\alpha\beta;\,\alpha'\beta'}(0, p)$ and using eq. (3.75), one can easily verify that differentiation of the functions $F_{\alpha\beta;\,\alpha'\beta'}(\boldsymbol{q}, p, p')$ with respect to q at $q = 0$ leads to a nonzero result for the functions diagonal in α, β, and α', β'. Therefore, from eq. (3.88) it follows

$$a(\theta, \varphi) - a(0, \varphi) \approx -\frac{3}{8\pi}\, hq\cos^2\varphi + 0(q^2)\,, \tag{3.90}$$

where h is derived from eqs. (3.75), (3.82), and (3.83) as

$$\begin{aligned} h = &-\tfrac{2}{9}\,[\dot{\Phi}_1(0, \mathrm{i}) + \dot{\Psi}_1(0, \mathrm{i})]\,[\Phi_1(0, \mathrm{i}) + \Psi_1(0, \mathrm{i}) + \tfrac{3}{2}] \\ &-\tfrac{1}{9}\,[\dot{\Phi}_3(0, \mathrm{i}) + \dot{\Psi}_3(0, \mathrm{i})]\,[\Phi_3(0, \mathrm{i}) + \Psi_3(0, \mathrm{i})]\,. \end{aligned} \tag{3.91}$$

Resorting to eq. (3.89), we can demonstrate that $h > 0$.

Thus, for the parallel configuration, the angular profile of the albedo $a(\theta, \varphi)$ is a symmetrical triangular peak centered at $\theta = 0$ (fig. 3.10). When φ increases, the included angle at the vertex of the peak widens, and the peak albedo decreases in magnitude to be a minimum at the perpendicular configuration, $\varphi = \frac{1}{2}\pi$, when the peak rounds off and the curve becomes smooth. The curve of the enhancement factor $K(\theta, \varphi)$ parallels these variations.

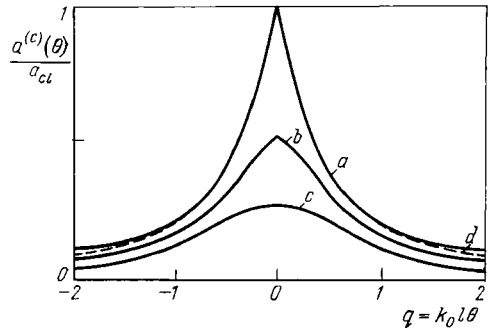

Fig. 3.10. Enhancement factor $K(\theta, \varphi)$ for normal incidence of linearly polarized light and various angles between the polarization vectors of incident $\boldsymbol{e}_0$ and detected $\boldsymbol{e}$ light ($\cos\varphi = \boldsymbol{e}\cdot\boldsymbol{e}_0$). Curves (a), (b), and (c) correspond to $\varphi = 0, \frac{1}{4}\pi$, and $\frac{1}{2}\pi$, respectively, with $\boldsymbol{e}_0$ lying in the plane of scanning; i.e., $\boldsymbol{q}\cdot\boldsymbol{e}_0 = q, \boldsymbol{q} = k_0 l(\boldsymbol{s}_{0\perp} + \boldsymbol{s}_\perp)$. Curve (d) corresponds to the case of parallel configuration ($\varphi = 0$) and scanning in a plane orthogonal to $\boldsymbol{e}_0$, i.e., with $\boldsymbol{q}\cdot\boldsymbol{e}_0 = 0$.

The origin of these results can be evaluated with the aid of the diffusion approximation, which in the case of a vector field is applicable, of course, for small q. As in the scalar problem, now the behavior of $a(\theta, \varphi)$ is governed by the behavior of the Green function of the transfer equation, $\mathscr{F}_{\alpha\beta;\,\alpha'\beta'}(\boldsymbol{r}, \boldsymbol{r}')$, at far transverse distances $|\boldsymbol{\rho} - \boldsymbol{\rho}'|$. To be more specific, the diffusion law $|\boldsymbol{\rho} - \boldsymbol{\rho}'|^{-3}$ leads to a linear dependence of θ, to a triangular peak line shape, and at a faster, say power-exponential decay we find ourselves with a rounded peak.

Consider the integrals of Green functions $\mathscr{F}_{\alpha\beta;\,\alpha'\beta'}(\boldsymbol{r}, \boldsymbol{r}')$ of the transfer equation with a concentrated isotropic source. These integrals describe the averages of field component products $\langle E_\alpha(\boldsymbol{r}) E^*_\beta(\boldsymbol{r}')\rangle$. In an unconfined scattering medium, at distances r from the source greater than the mean free path or extinction length l, the averages $\langle E_x E_y^*\rangle$ are factorized and fall off as $\exp(-\beta r/l)$ with a constant β. In view of the isotropic property the averages of type $\langle |E_x|^2 - |E_y|^2\rangle$ or $\langle \frac{1}{2}(|E_x|^2 + |E_y|^2) - |E_z|^2\rangle$, related respectively with the functions X_a and Ψ_a of eq. (3.82), exhibit the same behavior. An exception is the diagonal combination $\langle |E_x|^2 + |E_y|^2 + |E_z|^2\rangle$, which can be expressed through the function Φ_a of eq. (3.82), which is proportional to the energy density and falls off as r^{-1}.

In the case of a half-space, as $\rho \to \infty$ the averages $\langle E_x E_y^*\rangle$ and $\langle |E_x|^2 - |E_y|^2\rangle$ decay, as before, exponentially fast at a fixed z, and the energy density law of r^{-1} gives way to ρ^{-3}. However, now that the isotropic property is broken by the medium boundary, at finite distances z from this

boundary the average $\langle \frac{1}{2}(|E_x|^2 + |E_y|^2) - |E_z|^2 \rangle$ decays as $\rho \to \infty$, according to the same law as $\langle E_\alpha E_\alpha^* \rangle$. This is the reason why the coefficient of the linear term in eq. (3.91) is expressed by means of the derivatives $\dot{\Psi}_a$ and $\dot{\Phi}_a$. It is worth noting that the relation of these two "modes" manifests itself at finite distances from the interface, in that the pairs of Wiener–Hopf equations for Φ_a and Ψ_a defy separation into independent equations. If we neglect this relationship, i.e., let $\chi_a = \chi_a' = \psi_a = \psi_a' = 0$ in eqs. (3.87) and (3.85), the coefficient h in eq. (3.91) assumes the form it had in the scalar problem, namely, $h \approx \frac{1}{3}H^2(0, 1)$.

Although the evaluation of estimates of $a(0, \varphi)$, $K(0, \phi)$, and h in the exact-solution approach needs a rather cumbersome computational procedure associated with the solution of the system of integral equations for Φ_a and Ψ_a, the diffusion approximation of STEPHEN and CWILICH [1986] yields these estimates in a rather straightforward manner. If we take for each function $\tilde{F}_{\alpha\beta;\,\alpha'\beta'}(\boldsymbol{q}, z, z')$ the boundary condition (3.57b) of the absorbing plane type, then in the diffusion approximation

$$F_{\alpha\beta;\,\alpha'\beta'}(\boldsymbol{q}, p, p') \approx \int\int_0^\infty dz\, dz'\, \exp(ipz + ip'z')$$

$$\times \int_{-\infty}^{\infty} \frac{dp_1}{2\pi} \Big\{ \exp[-ip_1(z - z')] - \exp[-ip_1(z + z' + 2z_0)] \Big\} G^{(\mathrm{dif})}_{\alpha\beta;\,\alpha'\beta'}(\boldsymbol{q}, p_1)\,. \tag{3.92}$$

Here, $G^{(\mathrm{dif})}_{\alpha\beta;\,\alpha'\beta'}$ stands for the diffusion asymptotic expansion obtained for the Fourier transform $G_{\alpha\beta;\,\alpha'\beta'}(\boldsymbol{q}, p)$ of the Green function of the transfer equation derived for an infinite scattering medium. Unlike eq. (3.73), in the equation for this function the integral term is a convolution over the entire z-axis. The equation is solvable with the aid of Fourier transformation resulting in

$$G_{\alpha\beta;\,\alpha'\beta'}(\boldsymbol{q}, p) = \frac{M_{\alpha\beta;\,\alpha'\beta'}(\boldsymbol{q}, p)}{\det\{\Lambda(k)\}} - \delta_{\alpha\alpha'}\,\delta_{\beta\beta'}\,, \tag{3.93}$$

where $\Lambda(k)$ is a matrix with elements $\Lambda_{\alpha\beta;\,\alpha'\beta'}(\boldsymbol{q}, p)$ given in eq. (3.77), and $M_{\alpha\beta;\,\alpha'\beta'}(\boldsymbol{q}, p)$ is the cofactor of $\Lambda_{\alpha'\beta';\,\alpha\beta}(\boldsymbol{q}, p)$. By virtue of the invariance of the determinant, the function $\det \Lambda(k)$ depends only on the magnitude of $\boldsymbol{k}$ with components $k_z = p$, $\boldsymbol{k} = \boldsymbol{q}$. A simple algebraic calculation yields

$$\det\{\Lambda(k)\} = [\Lambda_+(0, k)\,\Lambda'_+(0, k)\,\Lambda'_-(0, k)]^2\,\Lambda_-(0, k) \times [\Lambda(0, k)\Lambda_1(0, k) - B^2(k)]\,,$$

where the functions $\Lambda'_{\pm}$ differ from the functions $\Lambda_{\pm}$ defined in eq. (3.81) by having $L_{13;13} \pm L_{13;31}$ in place of $L_{12;12} \pm L_{12;21}$. The function $B(k)$ can also be expressed in terms of $L_{\alpha\beta;\,\alpha'\beta'}(0, k)$ which for k tending to zero, falls off as k^2. Note also that the Wiener–Hopf equations for Φ_a and Ψ_a are combined into a system resulting from $B \neq 0$.

In order to construct the diffusion asymptotics we solve the problem and obtain the eigenvalues $\lambda_i(k)$ and eigenvectors $f^{(i)}_{\beta}(q, p)$ of the matrix $\{\Lambda_{\alpha\beta;\,\alpha'\beta'}(q, p)\}$. Seven in the nine eigenvalues coincide with the functions $\Lambda_{\pm}(0, k)$ and $\Lambda'_{\pm}(0, k)$, whereas the respective eigenvectors are independent of k at $q = 0$. The remaining two eigenvalues are the solution of the equation

$$(\Lambda - \lambda)(\Lambda_1 - \lambda) - B^2 = 0\,,$$

and for k tending to zero they coincide, accurate to k^2, with $\Lambda(0, k)$ and $\Lambda_1(0, k)$.

The function $G_{\alpha\beta;\,\alpha'\beta'}(q, p)$ is written as an expansion in eigenmodes; i.e., the ratio $M_{\alpha\beta;\,\alpha'\beta'}/\det\Lambda$ in eq. (3.93) is replaced with the sum $\Sigma_i f^{(i)}_{\alpha\beta} f^{(i)}_{\alpha'\beta'}/\lambda_i$. If we keep only the leading terms of the expansion for $k \to 0$ in the numerator and denominator of these fractions, we obtain precisely $G^{(\mathrm{dif})}_{\alpha\beta;\,\alpha'\beta'}(q, p)$.

It should be noted that only one of these eigenvalues exhibits a purely diffusive behavior, namely, $\Lambda(0, k) \approx \frac{1}{3}k^2$ as $k \to 0$. The expansion of the other eigenvalues has the form $\Lambda_i(0, k) \approx C_i(1 + \alpha_i^2 k^2)$. For example, for the diagonal components of the Green function we have

$$G^{(\mathrm{dif})}_{\substack{11,11\\(22,11)}}(q, p) \approx \frac{1}{k^2} + \frac{5}{9(1 + \alpha_1^2 k^2)} \pm \frac{5}{3(1 + \alpha_+^2 k^2)}\,, \tag{3.94}$$

where $k^2 = p^2 + q^2$, $\alpha_1^2 = \frac{29}{63}$, and $\alpha_+ = \frac{23}{21}$, and the minus sign of the last term relates to $G^{(\mathrm{diff})}_{22,11}$.

Substituting this expression into eq. (3.92) yields

$$F_{\substack{11;11\\(22;11)}}(q, i, i) \approx \frac{1}{2}\left[\frac{1}{(1+q)^2} + \frac{5}{9(\alpha_1 + \sqrt{\alpha_1^2 + q^2})^2} \pm \frac{5}{3(\alpha_+ + \sqrt{\alpha_+^2 + q^2})^2}\right], \tag{3.95}$$

where, for the sake of simplicity, we put $z_0 = 0$. It will be useful to emphasize that in deriving this expression we diagonalized the exact matrix $\{\Lambda_{\alpha\beta;\,\alpha'\beta'}\}$; therefore, eq. (3.95) refines the results that STEPHEN and CWILICH [1986] have obtained with perturbation theory.

The first term on the right-hand side of (3.95) is related to the pole of $G^{(\mathrm{dif})}_{11;11}$ at $k = 0$. For the parallel configuration this term gives a contribution to the albedo, which coincides with the solution of the scalar problem. The second

and third terms are associated with the poles of non-diffusion modes. Expressions of this type enter the function $F_{21;12}(\boldsymbol{q}; i, i)$. Therefore, the angular profile of $a(\theta, \varphi)$ and $K(\theta, \varphi)$ is an approximately Lorentzian shape at $\varphi = \frac{1}{2}\pi$.

STEPHEN and CWILICH [1986] have performed an albedo calculation, also taking into account the contribution of single scattering events. The experimental estimates are $K(0, 0) \approx 1.9$ and $K(0, \frac{1}{2}\pi) \approx 1.2$.

The estimates obtained with the diffusion approximations agree well with the experimental evidence for the enhancement factor $K(\theta, 0)$, for the parallel configuration, and $q \lesssim 1$ (see fig. 3.7). For the perpendicular configuration ROSENBLUH, EDREI, KAVEH and FREUND [1987] noted that the diffusion approximation yields no satisfactory agreement with experiment although it predicts a correct qualitative behavior of $K(\theta, \frac{1}{2}\pi)$. Comparison of an exact solution with the experimental evidence is yet to be done. Characteristic experimental plots for $\varphi = \frac{1}{2}\pi$ are given in fig. 3.11.

For large values of q where the diffusion approximation is no longer applicable, $a(\theta, \varphi)$ falls off as q^{-1} and levels off to a plateau. In this range the albedo is formed basically by double-scattering events, the contribution of which in eq. (3.71) corresponds to the first term in eq. (3.73). Straightforward calculation gives for $q \gg 1$

$$a(\theta, \varphi) - a_{\mathrm{cl}}(\varphi) \approx \frac{9}{64q}\left[\cos(\varphi + \varphi_0)\cos\varphi\cos\varphi_0 + \tfrac{3}{8}\sin^2(\varphi + \varphi_0)\sin^2\varphi_0\right], \tag{3.96}$$

where $\cos\varphi_0 = \boldsymbol{e}_0 \cdot \boldsymbol{q}/q$. This expression indicates that at sufficiently large q, in

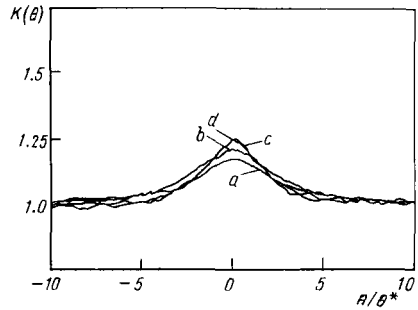

Fig. 3.11. Enhancement factor $K(\theta, \varphi)$ for perpendicular configuration of $\varphi = \frac{1}{2}\pi$ measured for the scattering of light in a 10% water suspension of polystyrene spheres 0.109, 0.305, 0.46, and 0.797 μm in diameter. Corresponding curves are (a) through (d); θ^* is defined from $K(\theta^*, 0) = 1.4$ and is dependent on the size of scatterers.

contrast to the range of $q \ll 1$, backscattering exhibits the anisotropy noted by VAN ALBADA and LAGENDIJK [1987]. To be more precise, the backscattered intensity begins to depend not only on the angle between the polarization vectors $\boldsymbol{e}$ and $\boldsymbol{e}_0$, but also on the orientation of the plane of scanning with respect to the polarization of the incident radiation, on $\boldsymbol{e}_0 \cdot \boldsymbol{q}$. By way of an example for the parallel configuration $\varphi = 0$, and given q, the backscattering intensity is a maximum when the scanning plane is parallel to $\boldsymbol{e}_0$ and $\varphi_0 = 0$. This effect was observed by VAN ALBADA, VAN DER MARK and LAGENDIJK [1987].

Results obtained for linearly polarized light show how the angular dependence of the albedo looks for various polarizations of the incident and detected light. We focus on the case of circular polarization (MACKINTOSH and JOHN [1988]). In this case the products $e_\alpha e_\beta$ and $e_{0\alpha'}\, e_{0\beta'}$ in eqs. (3.69)–(3.71) should be replaced with the tensors $P^{\sigma}_{\alpha'\beta'}(\boldsymbol{s})$ and $P^{\sigma_0}_{\alpha'\beta'}(\boldsymbol{s}_0)$ having components

$$P^{\sigma}_{\alpha\beta}(\boldsymbol{s}) = \delta_{\alpha\beta} - s_\alpha s_\beta + \mathrm{i}\sigma e_{\alpha\beta\gamma} s_\gamma \,, \tag{3.97}$$

where $e_{\alpha\beta\gamma}$ is an absolutely antisymmetrical unit tensor, and σ is plus or minus unity, depending on the direction of rotation of the polarization vector. Given $s_{0z} = 1$ and $\theta \ll 1$, the components of $P^{\sigma}_{\alpha\beta}(\boldsymbol{s})$ with $\alpha = 3$ or $\beta = 3$ may be deemed equal to zero.

Let $\sigma = \sigma_0$, i.e., the directions of the circular polarization of the incident (with respect to $\boldsymbol{s}_0$) and detected (with respect to $\boldsymbol{s}$) rotation are identical. It is not hard to verify that the contributions of the ladder and maximally crossed diagrams for $\boldsymbol{s} = -\boldsymbol{s}_0$ coincide, and at small q we have for the albedo $a(\theta, \sigma_0, \sigma_0)$

$$\begin{aligned} &a(\theta, \sigma_0, \sigma_0) - a(0, \sigma_0, \sigma_0) \approx (-\tfrac{3}{8}\pi) hq \,, \\ &a(0, \sigma_0, \sigma_0) = (\tfrac{3}{8}\pi)\,[F_{11;11}(0, i, i) - F_{12;12}(0, i, i)] \,, \end{aligned} \tag{3.98}$$

where h is the same as in eqs. (3.90) and (3.91).

The profile of $K(\theta; \sigma_0, \sigma_0)$ differs only insignificantly from the case of a parallel configuration of linear polarizations. It is essential, however, that for circular polarizations with $\sigma = \sigma_0$, in contrast to the case of linear polarizations with $\boldsymbol{e} \cdot \boldsymbol{e}_0 = \pm 1$, single-scattering events do not affect the intensity at small backscattering angles θ. Therefore, such a configuration is convenient to test experimentally if the enhancement is 2 at the maximum (ETEMAD, THOMPSON, ANDREJCO, JOHN and MACKINTOSH [1987]).

If the incident and detected waves are circularly polarized in opposite directions $\sigma = -\sigma_0$, the contribution of the maximally crossed diagrams to the

albedo is smaller than that resulting from the ladder diagrams. Thus, $K(0; -\sigma_0, \sigma_0) < 2$ and its dependence on θ are almost the same as in the case of perpendicular linear polarizations $e \cdot e_0 = 0$, the difference being that single-scattering events contribute to circular polarizations and do not affect the intensity of linear polarizations. A detailed investigation of backscattering for circular polarizations has been conducted by MACKINTOSH and JOHN [1988] on the basis of the diffusion approximation.

The model of a medium constituted by point-like isotropic scatterers occupying a half-space describes the main features of the polarization effects pertinent to backscattering. STEPHEN and CWILICH [1986] have demonstrated that the anisotropy and polarizability of the particles do not qualitatively affect the results. These authors and CWILICH and STEPHEN [1987], ETEMAD, THOMSON, ANDREJCO, JOHN and MACKINTOSH [1987], MACKINTOSH and JOHN [1988], and AKKERMANS, WOLF, MAYNARD and MARET [1988] have analyzed the effect of absorption and finite thickness of the scattering layer on the angular distribution of the intensity of polarized light. These factors manifest themselves significantly for the parallel linear and identical circular (helicity-preserving channel) polarizations of the incident and detected radiation. In these situations they cause a rounding off of the coherent backscattering peak, and so qualitatively the pattern does not differ from the case of scalar waves. The situation appears the same for a medium of large-scale scatterers, where polarization effects have been poorly documented thus far.

3.7. COHERENT BACKSCATTERING IN THE PRESENCE OF TIME-REVERSAL NONINVARIANT MEDIA

In §§ 3.4 and 3.5 we have demonstrated that absorption and confined geometry of the scattering medium round off the backscatter intensity peak and reduce its magnitude at $\theta = 0$. Nevertheless, the property of reversibility of the scattering operator and the Green function remain invariant under these conditions and the coherence is preserved. Therefore, in the case of a scalar field or linear parallel or circular identical polarizations, the enhancement factor at $\theta = 0$ (maximum) is, as before, equal (or almost equal) to 2 due to the coincidence of the contributions of the ladder and maximally crossed diagrams. In the following subsection we intend to sketch the factors that do not affect the classical (ladder) part of the backscatter peak practically but suppress the interference processes described by maximally crossed (cyclical) diagrams. This suppression is effected through the mechanisms destroying the time-reversal invariance.

3.7.1. *A weakly gyrotropic medium in a magnetic field*

Consider an electromagnetic wave scattering in a nonabsorbing, weakly gyrotropic medium constituted by point-like scatterers (MACKINTOSH and JOHN [1988]). If we put such a medium into a magnetic field $\boldsymbol{B}$, its permittivity becomes a tensor

$$\varepsilon_{\alpha\beta}(r) = [1 + \tilde{\varepsilon}(r)]\,\delta_{\alpha\beta} + \mathrm{i}e_{\alpha\beta\gamma}g_{\gamma}\,, \tag{3.99}$$

and the refractive index depends on the direction of propagation $\boldsymbol{s}$ and helicity of the polarization vector as

$$n_{\sigma} \simeq n - \sigma \boldsymbol{g}\cdot\boldsymbol{s}/2n\,,$$

where $\sigma = \pm 1$, $\boldsymbol{g} = f\boldsymbol{B}$ is the gyration vector such that $g \ll 1$, and f is the Faraday constant.

To understand what changes in the pattern of coherent backscattering when the medium is brought in a magnetic field, we resort to the qualitative argument of § 3.2 with one essential addition. Now, to each step $\boldsymbol{R}_{j+1} - \boldsymbol{R}_j$ of path γ we put a corresponding a wave vector $\boldsymbol{k}_j$ and parameter $\phi_j = \pm 1$, indicating the helicity of the polarization vector. For $\boldsymbol{B} \neq 0$ the propagation velocities of radiation with right-hand and left-hand helicities differ from one another. Therefore, the product of u_{γ} and $u^{*}_{-\gamma}$ corresponding to the contributions of the path γ and the time-reversed path $-\gamma$ in the field has the form

$$u_{\gamma}u^{*}_{-\gamma} = |u_{\gamma}|^2 \exp(\mathrm{i}\Delta\varphi)\,.$$

The phase difference $\Delta\varphi$ is the sum of the phase increments in individual steps $\boldsymbol{R}_{j+1} - \boldsymbol{R}_j$, and it does not vanish even at $\boldsymbol{s} = \boldsymbol{s}_0$.

Assume that in the path $-\gamma$ described by the set $\boldsymbol{k}_0, \sigma_0; -\boldsymbol{k}_{N-1}, \sigma'_{N-1}; \ldots; -\boldsymbol{k}_1, \sigma'_1; \boldsymbol{k}_N, \sigma$, we have for the helicity $\sigma'_j = \sigma_{N-j}$. Then, $\Delta\varphi$ may be represented in the form

$$\Delta\varphi \simeq \tfrac{1}{2}ck_0 \sum_j \tau_j[\sigma_j \boldsymbol{g}\cdot\boldsymbol{k}_j - \sigma_j \boldsymbol{g}(-\boldsymbol{k}_j)]\,. \tag{3.100}$$

Let $c\tau_j \simeq 1$ and $\boldsymbol{g}\cdot\boldsymbol{k}_j \simeq gk_0\cos\theta_j$, and assume that σ_j and $\cos\theta_j$ are uncorrelated random variables so that $(\Delta\varphi)_{\mathrm{rms}} \simeq k_0 l_g \sqrt{S_N/3l}$, where $S_N = Nl$. Since for constructive interference $(\Delta\varphi)_{\mathrm{rms}} < 1$, then a helicity-preserving magnetic field will not destroy coherence if the path length $S_N < S_{\max} \sim 1/l(k_0 g)^2$. At the same time the contribution of events with higher multiplicity of scattering having $S_N > S_{\max}$, which determine the backscattering intensity for angles $\theta < \theta_{\max} \sim 1/k_0\sqrt{lS_{\max}}$, will be suppressed. Hence, the magnetic field rounds off the backscattering peak for angles $\theta < g$.

The pattern for the albedo (not for the enhancement factor) appears to be almost the same as in the absorption case if we choose the parameter $\xi = 1/k_0 l\theta_{\max}$ in the form $\xi = 1/k_0 lg$ (see fig. 3.8). We note that when on the time-reversed path $-\gamma$ the helicity meets the condition $\sigma_j' = -\sigma_{N-j}$, the phase difference $\Delta\varphi$ vanishes. Hence, Faraday rotation does not affect, or affects only insignificantly, the backscattered intensity in opposite helicity channels.

In addition to gyrotropy, MACKINTOSH and JOHN [1988] have considered the effect of the natural optical activity on coherent backscattering. In optically active materials the dielectric constant assumes different values for right-hand and left-hand helicity states of light and is independent of the direction of light propagation, the refractive index being $n_\sigma = n - \sigma f/2n$. In this case the parity is not conserved, but the invariance to time-reversed paths remains. Therefore, natural activity does not manifest itself in helicity-preserving channels (in estimates like eq. (3.100), $\Delta\varphi \simeq 0$) and does not affect the backscatter intensity peak line shape.

A quantitative theory describing the effect of Faraday rotation on coherent backscattering of circularly polarized light is developed in a scheme which differs in some details from that outlined in § 3.6. The equation for E_α is derived by adding the term $ik_0 e_{\alpha\beta\gamma} g_\gamma$, connected with the off-diagonal part of the dielectric tensor (3.99), to the expression in the brackets in eq. (3.62). Therefore, in the far zone the averaged Green function of the Maxwell equation in the medium, calculated for $\varepsilon \ll 1$ in the effective-wavenumber approximation, has the form

$$\langle G_{\alpha\alpha'}(\boldsymbol{r}, \boldsymbol{r}') \rangle \simeq -(4\pi R)^{-1} \sum_{\sigma = \pm 1} P^{\sigma}_{\alpha\alpha'}(\boldsymbol{s}) \exp\left[ik_0 R(1 + \tfrac{1}{2}\boldsymbol{g}\cdot\boldsymbol{s}) - \frac{R}{2l} \right], \tag{3.101}$$

where $\boldsymbol{r} - \boldsymbol{r}' = \boldsymbol{R} = s\boldsymbol{R}$, and $P^{\sigma}_{\alpha\beta}$ is the polarization matrix defined by eq. (3.97).

We note that in the presence of a constant magnetic field $\boldsymbol{B}$ the Green function, like the approximate expression, eq. (3.101) for its average, obeys the reversibility condition in the form

$$G_{\alpha\alpha'}(\boldsymbol{r}, \boldsymbol{r}', \boldsymbol{B}) = G_{\alpha'\alpha}(\boldsymbol{r}', \boldsymbol{r}, -\boldsymbol{B}), \tag{3.102}$$

which follows from the time-reversal symmetry in the system "medium + light + magnetic field". Hence, for the subsystem of a medium and light we may speak of the breakdown of this symmetry (GOLUBENTSEV [1984b]), which manifests itself in that at $\boldsymbol{B} \neq 0$ the equality (3.67) for the contributions of ladder and maximally crossed diagrams in the vertex function is no longer valid.

At $\boldsymbol{B} = 0$ and circular polarizations of the incident and detected light, the formulas for the albedo $a(\boldsymbol{s}, \boldsymbol{s}_0; \sigma, \sigma_0)$ can be derived from eqs. (3.69)–(3.71) with the substitution $e_\alpha e_\beta$ for $P^{\sigma}_{\beta\alpha}(\boldsymbol{s})$ and $e_{0\alpha'} e_{0\beta'}$ for $P^{\sigma_0}_{\alpha'\beta'}$. Now, if $\boldsymbol{B} \neq 0$, the expressions for the ladder part $a^{(\mathrm{L})}$ and cyclic part $a^{(\mathrm{C})}$ of the albedo involve different functions $F^{(\mathrm{L})}_{\alpha\beta;\,\alpha'\beta'}(\boldsymbol{q}, p, p')$ and $F^{(\mathrm{C})}_{\alpha\beta;\,\alpha'\beta'}(\boldsymbol{q}, p, p')$. With the aid of eq. (3.75) the calculation of either of these functions is reduced to solving the system of the Wiener–Hopf equation of the type (3.76) and (3.77), where the coefficients $L_{\alpha\beta;\,\alpha'\beta'}$ for $F^{(\mathrm{L})}$ and the coefficients $L'_{\alpha\beta;\,\alpha'\beta'}$ for $F^{(\mathrm{C})}$ are expressed through the Fourier transforms of the products $\langle G_{\alpha\alpha'}(\boldsymbol{r}, 0)\rangle \langle G^{*}_{\beta\beta'}(\boldsymbol{r}, 0)\rangle$ and $\langle G_{\alpha\alpha'}(\boldsymbol{r}, 0)\rangle \langle G^{*}_{\beta'\beta}(0, \boldsymbol{r}')\rangle$. Using eq. (3.101), we find

$$
\begin{aligned}
L_{\alpha\beta;\,\alpha'\beta'} &= \sum_{\sigma,\,\sigma' = \pm 1} L^{\sigma,\sigma'}_{\alpha\beta;\,\alpha'\beta'}\,, \\
L'_{\alpha\beta;\,\alpha'\beta'} &= \sum_{\sigma,\,\sigma' = \pm 1} L^{\sigma,\sigma'}_{\alpha\beta';\,\alpha'\beta}\,, \\
L^{\sigma,\sigma'}_{\alpha\beta;\,\alpha'\beta'}(\boldsymbol{q}, p, g) &= \frac{3}{8\pi} \int \mathrm{d}^2 s\, \frac{P^{\sigma}_{\alpha\alpha'}(\boldsymbol{s})\, P^{\sigma}_{\beta\beta'}(\boldsymbol{s})}{1 - \mathrm{i}\boldsymbol{k}\cdot\boldsymbol{s} - \frac{1}{2}\mathrm{i}k_0 l \boldsymbol{g}\cdot\boldsymbol{s}(\sigma + \sigma')}\,,
\end{aligned}
\tag{3.103}
$$

where the components of $\boldsymbol{k}$ are $k_z = p$ and $\boldsymbol{k}_\perp = \boldsymbol{q}$.

These coefficients satisfy the conditions

$$
\begin{aligned}
L^{\sigma,\sigma}_{\alpha\beta;\,\alpha'\beta'}(\boldsymbol{k}, \boldsymbol{g}) &= L^{\sigma,\sigma}_{\alpha\beta;\,\alpha'\beta'}(\boldsymbol{k} + k_0 l \boldsymbol{g}, 0)\,, \\
L^{\sigma,-\sigma}_{\alpha\beta;\,\alpha'\beta'}(\boldsymbol{k}, \boldsymbol{g}) &= L^{\sigma,-\sigma}_{\alpha\beta;\,\alpha'\beta'}(\boldsymbol{k}, 0)\,, \\
L^{\sigma,\sigma'}_{\alpha\beta;\,\alpha'\beta'}(\boldsymbol{k}, 0) &= L^{\sigma,-\sigma'}_{\alpha\beta';\,\alpha'\beta}(\boldsymbol{k}, 0)\,.
\end{aligned}
\tag{3.104}
$$

The solution of the system for $F^{(\mathrm{C})}_{\alpha\beta;\,\alpha'\beta'}$ and for $F^{(\mathrm{L})}_{\alpha\beta;\,\alpha'\beta'}$ has a more complicated structure than in the case of $\boldsymbol{B} = 0$, although the technique of its construction for $g \ll 1$ remains almost the same. We only consider those salient features of the solution that control the behavior of the albedo near the zero angle, $\theta = 0$. This is the case of normal incidence with $s_{0z} \simeq 1$, $\theta \ll 1$, $q \approx k_0 l\theta$, and $p \approx \mathrm{i}$.

As indicated in the preceding section, at $\sigma = \sigma_0$ the linear dependence of $a(\theta, \sigma, \sigma_0)$, i.e., a triangular line shape, is associated with a diffusion pole at $p = 0$ exhibited by functions $F_{\alpha\beta;\,\alpha'\beta'}(0, p)$ diagonal in α, β, and α', β'. In turn, this pole occurs because one of the eigenvalues of matrix $\{\Lambda(0, p)\}$ behaves as $\lambda_1(p) \approx \frac{1}{3}p^2$ as $p \to 0$, whereas for the others $\lambda_j(0) \neq 0$.

At $\boldsymbol{B} = 0$ (or $\boldsymbol{g} = 0$) the matrix $\{\Lambda'(0, p, \boldsymbol{g})\}$ coincides with $\{\Lambda(0, p)\}$. Corrections to its eigenvalues due to a magnetic field can be computed with the use of perturbation theory. A simple calculation based on symmetry conditions

(3.104) yields

$$\lambda_1(p) \approx \tfrac{1}{3}[p^2 + (k_0 lg)^2],$$

where both p and $k_0 lg \ll 1$. Thus, the solution has no diffusion pole, and the dependence of the albedo on $q = k_0 l\theta$ is devoid of a linear term.

A more detailed analysis indicates that for $\boldsymbol{B} \neq 0$ and $q, k_0 lg \ll 1$, the quantity q on the right-hand side of (3.98) should be replaced with $\sqrt{q^2 + (k_0 lg)^2}$. This bears out the preceding qualitative estimates of peak rounding in the helicity-preserving channel. A thorough analysis of the albedo based on the diffusion approximation has been performed by MACKINTOSH and JOHN [1988].

3.7.2. *Brownian motion of scatterers*

Time-reversal noninvariance also takes place for light scattered by a system of moving particles. Examples of such media may be water suspensions of spherical particles of latex or polystyrene frequently employed in coherent backscattering experiments. Because of collisions with water molecules, these particles of 0.1–1.0 μm typical diameter are in constant Brownian movement. Clearly, the system consisting of a radiation and water suspension is invariant with respect to time inversion, since it also assumes the inversion of velocity of all particles. However, in a given medium, for a subsystem of light and scatterers, such a symmetry is no longer present and the Green function $G(r, t; r', t') \neq G(r', t; r, t')$ while the coherence of the forward and reverse paths is destroyed.

The effect of Brownian motion has been analyzed by GOLUBENTSEV [1984a], and similar reasoning has been explored by MARET and WOLF [1987] and AKKERMANS, WOLF, MAYNARD and MARET [1988].

Consider a path γ of length $S_N \simeq Nl$. Light travels this distance in time $t \sim Nl/c$, and the distance between every pair of scatterers alters in this time on average by $(\Delta R_j)_{\text{rms}} \sim \sqrt{D_B t}$, where D_B is the diffusion coefficient of Brownian motion. Since the increments ΔR_j are uncorrelated, the length of the entire path can change by $\Delta S_N \sim \sqrt{N D_B t}$. For interference between paths γ and $-\gamma$ to occur it is required that $\Delta S_N < \lambda$. Therefore, for paths $S_N > \sqrt{cl/D_B k_0^2}$, the Brownian motion destroys coherence, suppresses the contribution of scattering events of higher multiplicity, and for angles $\theta < (D_B/cl^3 k_0^2)^{1/4}$ the backscattering intensity peak is rounded off.

In experiments on coherent backscattering in solid disordered media, KAVEH, ROSENBLUH, EDREI and FREUND [1986] observed considerable jumps of intensity as a function of angle θ (speckle noise) associated with the

fixed disorder in the placement of scatterers. A common backscattering intensity peak at $\theta = 0$ is obtained by rotating the specimen to attain averaging over positions of scatterers. In experiments with suspensions the role of the averaging factor is played by Brownian motion. Therefore, the observation time in such systems is chosen to be sufficiently large (or the scanning speed over angle θ sufficiently small, see, e.g., WOLF, MARET, AKKERMANS and MAYNARD [1988]). This time exceeds the characteristic time to destroy the time-invariance $t_m \sim \sqrt{1/ck_0^2 D_B}$. Under ordinary experimental circumstances t_m is in the order of 10^{-8} s, and the characteristic angle is $\theta_m \sim 10^{-2}(k_0 l)^{-1}$.

3.8. COHERENT EFFECTS IN THE AVERAGE FIELD: INFLUENCE ON BACKSCATTER INTENSITY ENVELOPE

When scattering particles are embedded in a medium of effective dielectric constant $\tilde{\varepsilon} > 1$ (which is usually the case in backscattering experiments), the effects of coherent interaction of waves with the medium–vacuum interface may become significant. These effects affect the refraction of the incident and backscattered waves and the process of multiple scattering of this intensity in the medium.

If $|\tilde{\varepsilon} - 1| \ll 1$, then for grazing propagation of incident and scattered waves the coherent effects in the average field will be significant only at shallow depths (GORODNICHEV, DUDAREV, ROGOZKIN and RYAZANOV [1987]). Therefore, we may conclude that the effects of refraction and coherent scattering affect only the transmission of waves through the interface and do not affect the scattering in the medium. Corrections for the energy density due to the interaction with the interface are small, of the order of the angular size of the region where there is internal scattering from the interface related to the entire span of the scattering angles.

The results of GORODNICHEV, DUDAREV and ROGOZKIN [1989] enable us to analyze how coherent effects in the average field $\langle u(r) \rangle$ affect enhancement. Specifically, the dependence of the enhancement factor $K(-s_0, s_0)$ on the angle of incidence θ_0, $s_{0z} = \cos\theta$, is monotonic. In an optically dense medium of $\tilde{\varepsilon} > 1$, the grazing angle of an incident wave is larger than in vacuum. This leads to a higher effective multiplicity of scattering in the medium and accordingly to a higher enhancement factor.

If the medium permittivity is significantly different from unity ($\tilde{\varepsilon} - 1 \gtrsim 1$), the total internal reflection from the interface becomes significant and may alter the character of the multiple scattering and interference of waves in the medium.

A phenomenological treatment by LAGENDIJK, VREEKER and DE VRIES [1989] on the basis of the diffusion approximation with the boundary conditions involving almost total internal reflection resulted in the following conclusions. As the reflection from the medium–vacuum interface increases, the effective multiplicity of scattering in the medium also increases, producing a sharper peak of coherent backscatter intensity. This effect may be described with the aid of a renormalized diffusion coefficient, i.e., by substituting for D the quantity $D^* = D(1 + \varepsilon')^{-4/3}$, where $\varepsilon' = R/(1 - R)$, and R is the coefficient of coherent reflection from the interface.

§ 4. Multipath Coherent Effects in Scattering From a Limited Cluster of Scatterers

4.1. ENHANCED BACKSCATTERING FROM A PARTICLE

4.1.1. *Single particle near an interface*

In his early model WATSON [1969] interpreted scatterers as centers of elementary volumes of the scattering medium. However, situations exist where scatterers are centers of actual small bodies randomly distributed in space. In the preceding section we discussed the scattering from a very large number of scatterers that paved the way for an approximation of a continuous scattering medium. In this section we consider the opposite case of a small number of scatterers in which summation cannot be replaced with integration.

The possibility of enhanced backscattering due to multi-path coherent effects was recognized by KRAVTSOV and NAMAZOV [1979, 1980] who studied the single scattering of radio waves reflected from the ionosphere. However, the pure effect of enhanced backscattering from a *single* scatterer was evaluated by AKHUNOV and KRAVTSOV [1983b] somewhat later for acoustic waves. The reasoning of this paper relates to all types of waves and may be readily extended to optical phenomena.

Consider a point-like scatterer placed near the interface between two media. A wave from a source O travels to the scatterer S by way of two paths, as shown in fig. 4.1a; the direct path is labelled 1, and the path involving a reflection from the interface is labelled 2. Likewise there are two paths, 1′ and 2′, that propagate the scattered field to the point of observation O′. Hence, there are four channels of single scattering, namely, 11′, 12′, 21′, and 22′. Correspondingly the total scattered field at point O′ is represented by the sum of four

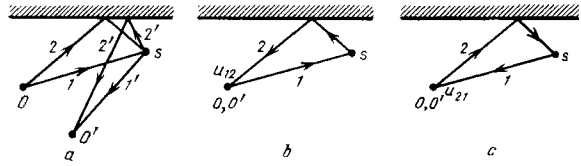

Fig. 4.1. Ray geometry of (a) scattered transmitter O and receiver O′ for a scatterer S near the interface. When the locations of the transmitter and receiver coincide, the cross channels (b) 1–2 and (c) 2–1 becomes coherent.

contributions

$$u_s = u_{11'} + u_{12'} + u_{21'} + u_{22'}\,, \tag{4.1}$$

and the total intensity is

$$I_s = |u_s|^2 = |u_{11'} + u_{12'} + u_{21'} + u_{22'}|^2\,. \tag{4.2}$$

Let us assume that the scatterer S is placed at random in a volume V_s embracing many interference fringes of the prime field. Averaging the intensity I_s over the possible positions of the scatterer r_s, i.e., integration of eq. (4.2) with the weight function $w(\boldsymbol{r}_s)$ being the probability density of $\boldsymbol{r}_s$, eliminates all the interference terms in eq. (4.2) except the contributions characterizing the interference between the channels 12′ and 21′. The point is that for O′ = O, i.e., for the location of the receiver to coincide with the transmitter's location, paths 12′ and 21′ become identical and the respective fields become completely coherent, as illustrated in fig. 4.1b and 4.1c,

$$u_{12} = u_{21}\,. \tag{4.3}$$

Thus, in the particular case of backscattering with $r' = r_t$,

$$\langle I_{bsc} \rangle = \langle I_{11} \rangle + \langle I_{22} \rangle + 4\langle I_{12} \rangle\,, \tag{4.4}$$

whereas in the general case

$$\langle I_s \rangle = \langle I_{11} \rangle + \langle I_{22} \rangle + \langle |u_{12'} + u_{21'}|^2 \rangle\,, \tag{4.5}$$

where the angular brackets imply averaging over the ensemble of positions of scatterer r_s. Thus

$$\langle I_{jk} \rangle = \langle |u_{jk}|^2 \rangle = \int_{V_s} |u_{jk}|^2\, w(\boldsymbol{r}_s)\, \mathrm{d}^3 r_s\,,$$

and by virtue of eq. (4.3), $\langle |u_{12} + u_{21}|^2 \rangle = 4\langle I_{12} \rangle$.

When the transmitter and receiver are separated by a sufficiently large

distance for the interference between channels 12′ and 21′ to vanish, we obtain instead of eq. (4.5)

$$\langle I_{\text{sep}} \rangle = \langle I_{11} \rangle + \langle I_{22} \rangle + 2 \langle I_{12} \rangle . \tag{4.6}$$

This intensity corresponds to an incoherent addition of the fields $u_{12'}$ and $u_{21'}$. If we introduce the backscatter factor as the ratio of $\langle I_{\text{bsc}} \rangle$ to $\langle I_{\text{sep}} \rangle$, then

$$K = \frac{\langle I_{11} \rangle + \langle I_{22} \rangle + 4 \langle I_{12} \rangle}{\langle I_{11} \rangle + \langle I_{22} \rangle + 2 \langle I_{12} \rangle} . \tag{4.7}$$

For a perfectly reflecting interface and about equal path lengths traversed by the wave in channels 11, 22, 12, and 21, eq. (4.7) yields the estimate $K \approx 1.5$. This figure suggests that the effective cross section of scattering of a small body placed near the interface is about 1.5 times as large as in bistatic observation and about 6 times as large as in free space. This simple and somewhat unexpected effect is directly related to the existence of coherent channels of the Watson–Ruffine type.

It is useful to note that one may average over a finite band of frequencies $(\omega_1, \omega_2 + \Delta\omega)$ rather than over the realizations of the body in (4.4–4.7). It is required only that a sufficiently large number of interference fringes ΔN should pass through the scatterer as the frequency sweeps the band. Where the condition $\Delta N \gg 1$ is satisfied, one can observe enhancement in a single measurement employing a wideband signal. Essentially, under the circumstances a self-averaging over the frequency band is realized.

4.1.2. *Combined action of a rough surface, turbulence, and multipath coherent effects*

If the interface is rough, strong focusing, as for a random phase screen, is possible in path 22, and in eq. (4.4) I_{22} acquires a factor K_{surf} to describe the backscatter enhancement in double reflection from the surface (ZAVOROTNYI and TATARSKII [1982]). If the incoming and scattered waves pass through a turbulent medium, all terms in eq. (4.4) should be multiplied by a factor K_{turb}. If we take, for the purpose of estimation, $K_{\text{turb}} \approx 2$, as for saturated fluctuations, and $K_{\text{surf}} \approx 2$ (moderate focusing), then for $\langle I_{\text{bsc}} \rangle$ we obtain $(2 + 2 \times 2 + 2 \times 4) I_{11} = 14 I_{11}$. This implies that, given the preceding circumstances, the effective backscatter cross section may be 14 times as strong as the scattering of a body in free space (AKHUNOV and KRAVTSOV [1983a]).

4.1.3. *Existence of backscatter enhancement under time-varying conditions*

In situations where the parameters of the medium or interface vary in time, the coherence of paths 12 and 21 breaks down, and we cross over from eq. (4.4) for coherent addition of fields u_{12} and u_{21} to formula (4.6) for incoherent addition. The transition from eq. (4.4) to eq. (4.6) actually occurs once the phase difference of paths 12 and 21 exceeds $\frac{1}{2}\pi$. From this condition we may derive a requirement imposed on the velocity v_t of vertical motion of the surface that would not destroy the coherence of fields u_{12} and u_{21}. If t' is the time for u_{12} to travel from source to surface and t'' is the similar time for u_{21}, then in time $t' - t''$ the surface should not go further than $\frac{1}{4}\lambda$ (AKHUNOV and KRAVTSOV [1982]); i.e.,

$$v_t(t' - t'') \lesssim \tfrac{1}{4}\lambda . \tag{4.8}$$

4.1.4. *Kettler effect*

The class of phenomena under consideration includes the Kettler effect, which was already known to Newton. It consists of observing iridescent rings on a dusty mirror viewed from a point close to a source of light. This effect can be explained as follows. If the distance ρ between the source r_t and the observer r' is comparatively small (fig. 4.2), at a frequency ω, waves 1′ and 2′ add up at a certain angle θ, which depends on the frequency and glass thickness h. In this case, averaging occurs due to the wide band of common sources of light and to the summation over numerous dust particles occupying the outer surface of the glass.

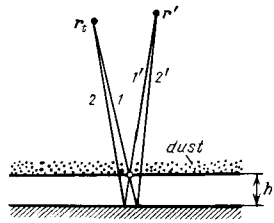

Fig. 4.2. In Kettler's experiment, coherent scattering channels occur when the point of observation r' approaches the point of transmission r_t.

4.1.5. *Particle in a waveguide*

For a waveguide we may expect higher values of the enhancement factor than for a particle near the interface, because the waveguide sharply increases the number of coherent channels. If m rays are incident on a scatterer, the total number of backscatter paths is m^2, of which $m(m-1)$ paths make $\frac{1}{2}m(m-1) = M_{\text{coh}}$ coherent pairs (ray j induces a scattered ray p, and vice versa), and m paths have no coherent counterparts (ray j reproduces itself, i.e., also ray j). Therefore, after averaging over all the realizations of the scatterer (the domain of averaging should embrace sufficiently many interference maxima of the prime field), the detected intensity in monostatic reception is estimated as

$$I_{\text{bsc}} \approx mI_{11} + M_{\text{coh}} 4I_{11} = m(2m-1)I_{11},$$

and in separated (bistatic) reception as

$$I_{\text{sep}} \approx mI_{11} + M_{\text{coh}} 2I_{11} = m^2 I_{11}.$$

Hence, an estimate for the backscatter enhancement factor is (AKHUNOV, KRAVTSOV and KUZKIN [1984])

$$K_{\text{bsc}} = I_{\text{bsc}}/I_{\text{sep}} \approx 2 - 1/m. \tag{4.9}$$

One may arrive at this estimate from the mode consideration, where the transformation of rays in scattering is treated as the transformation of the modes and m is treated as the number of propagating modes. The mode analysis suggests that the maximum number of distinct rays in a waveguide m equals the number of propagating normal waves. Hence, eq. (4.9) allows dual interpretation.

According to eq. (4.9), in a single-mode waveguide ($m = 1$) no enhancement of the backscattered intensity is evident ($K = 1$). In a two-mode waveguide ($m = 2$), $K = 1.5$, as for the case of a scatterer near an interface. This coincidence is not by chance: both situations involve four scattering channels, of which two are single (11 and 22) and the other two form a coherent pair. Finally, for many propagating modes ($m \gg 1$) we have $K \to 2$. The effect of doubling the effective scattering cross section should be taken into account when interpreting the backscattering data gathered in fiber multimode light guides.

If the waveguide possesses a clearcut property of focusing the field of a point source, which is the case with a parabolic index waveguide, then for a scatterer placed in a focal spot the scattered field increases by a factor of f^2, where

f is the focusing factor indicating how many times the field at the scatterer exceeds that produced by the source in free space.

For a waveguide the backscatter enhancement factor is

$$K = I_{bsc}/I_{sep} = \langle |G(r_t, r_s)|^4 \rangle / \langle |G(r_t, r_s)\, G(r, r_s)|^2 \rangle ,$$

where, as before, the angular brackets indicate that the ensemble average has been performed over positions of the scatterer. If the domain of averaging is limited by a focal spot, then K is rather high, $K \sim f^2 \gg 1$. When the averaging domain exceeds the distance between adjacent focal spots, then $K \to 2$, since this follows from eq. (4.9) for $m \gg 1$. For a single-mode propagation the Green function is devoid of interference structure, hence $K = 1$.

4.2. ENHANCED BACKSCATTERING BY A SYSTEM OF TWO SCATTERERS

4.2.1. *Watson equations (scalar problem)*

The system of two small scatterers is interesting since it enables an exact solution of the wave problem to any desired order of multiple scattering. First, we consider the scattering problem in the scalar formulation. Let u_1 and u_2 be the field of an external source at the locations of the first and the second scatterer, and let α_1 and α_2 be the "polarizabilities" of the scatterers. The moments induced on the scatterers, p_1 and p_2, combine from those due to the external field $\alpha_{1,2} u_{1,2}$ and those due to adjacent particles $\alpha_1 g_{12} p_2$ and $\alpha_2 g_{21} p_1$, where $g_{12} = g_{21} = -\exp(ikl)/4\pi l$ are the Green functions corresponding to the distance l between the particles.

This simple argument leads to the following system of equations

$$\begin{aligned} p_1 &= \alpha_1 (u_1 + g_{12} p_2) , \\ p_2 &= \alpha_2 (u_2 + g_{21} p_1) , \end{aligned} \tag{4.10}$$

which is an example of the equations derived by WATSON [1969]. Having determined the "moments" p_1 and p_2 from eq. (4.10), the scattered field is

$$u_s(r) = p_1 g(r_1, r) + p_2 g(r_2, r) , \tag{4.11}$$

so that p_1 and p_2 have the meaning of the scattering amplitudes.

For identical particles ($\alpha_1 = \alpha_2 = \alpha$) the solution to eq. (4.10) has the form

$$\begin{aligned} p_1 &= \alpha \frac{u_1 + \alpha g_{12} u_2}{1 - (\alpha g_{12})^2} , \\ p_2 &= \alpha \frac{u_2 + \alpha g_{12} u_1}{1 - (\alpha g_{12})^2} . \end{aligned} \tag{4.12}$$

If we expand the denominator in a series in the powers of the parameter $(\alpha g_{12})^2$, we obtain an expansion of moments $p_{1,2}$ into orders of multiple scattering. When the parameter αg_{12} is small, we can only retain in eq. (4.12) the numerator that corresponds to the double-scattering approximation.

We formulate the main results without going into great detail. Let us assume that the direction of the axis connecting the centers of the particles is uniformly distributed over a unit sphere and the distance between the particles, l assumes random values with probability density $w_l(l)$. If the source of the prime field is at a considerable distance from the system of particles ($r \gg \bar{l}$, where $\bar{l}$ is the mean distance between the scatterers), eqs. (4.11) and (4.12) may be used to calculate the averaged (over l and axis orientations) cross section of scattering $\sigma(\theta)$, which is a function of the angle θ between the directions to the source and the detector.

If $\sigma_0 = (\alpha/4\pi)^2$ is the cross section for a single particle, the plot of the angular dependence for the normalized cross section of scattering $\sigma(\theta)/2\sigma_0$ may be viewed as the profile of the enhancement factor (fig. 4.3)

$$K(\theta) = \frac{\sigma(\theta)}{2\sigma_0} . \tag{4.13}$$

In the forward direction ($\theta = \pi$) there is always a maximum of $K(\theta) = 2$ corresponding to the in-phase addition of single scattered fields $\sigma(\pi) \approx 4\sigma_0$. Another maximum of considerably lower height

$$K_{\text{bsc}} - 1 = K(0) - 1 \sim (\alpha g_{12})^2 \sim \sigma_0/\bar{l}^2 \tag{4.14}$$

is evident in the backscatter direction.

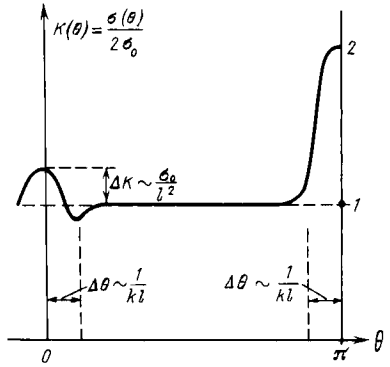

Fig. 4.3. Enhancement factor $K(\theta)$ for two identical, randomly located scatterers.

Thus, the averaged cross section of backscattering $\sigma_{bsc} = \sigma(0)$ always exceeds the sum of single cross sections $2\sigma_0$. This small enhancement is observed in a comparatively narrow cone of halfwidth $\Delta\theta \sim 1/k\bar{l}$. Despite its small magnitude the effect is of major significance because a maximum in $K(\theta)$ suggests that the scatterer should have an internal structure which is often hard to reveal by other methods.

4.2.2. *Polarization effects*

For an electromagnetic field the system of Watson equations takes the form

$$\begin{aligned} \boldsymbol{p}_1 &= \alpha_1(\boldsymbol{E}_1 + \hat{g}_{12}\boldsymbol{E}_2), \\ \boldsymbol{p}_2 &= \alpha_2(\boldsymbol{E}_2 + \hat{g}_{21}\boldsymbol{E}_1), \end{aligned} \tag{4.15}$$

where this time $\alpha_{1,2}$ are the "true" polarizabilities, $\boldsymbol{p}_{1,2}$ have the meaning of induced dipole moments, and the tensor operators $\hat{g}_{12}$ and $\hat{g}_{21}$ yield the field due to the dipole moments $\boldsymbol{p}_1$ and $\boldsymbol{p}_2$ at the adjacent particles.

Because of the random orientation of vector $\boldsymbol{l} = \boldsymbol{r}_2 - \boldsymbol{r}_1$ connecting the particle centers, the polarization of the scattered field $\boldsymbol{E}_s = \hat{g}(r, r_1)\boldsymbol{p}_1 + \hat{g}(r, r_2)\boldsymbol{p}_2$ differs from the polarization of the prime wave. Let the center of the system of two particles lie at the origin, and the source at a distance $L \gg \bar{l}$ from this center along the z-axis radiates an intensity polarized along the x-axis. For a detector receiving the co-polarized component of the scattered field, E_{sx}, we introduce the angular dependences of the enhancement factor K_{xx} on angles θ_{yz} and θ_{xz} lying in the mutually orthogonal planes yz and xz (fig. 4.4a).

Figure 4.4b illustrates an analysis of such dependences for the case where

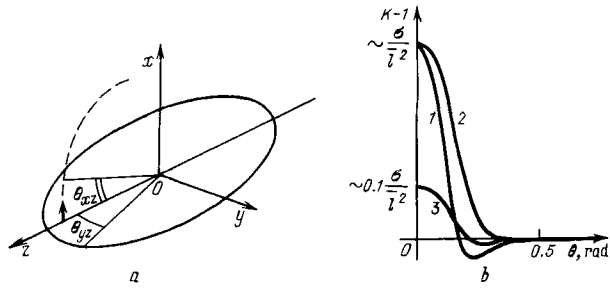

Fig. 4.4. (a) System of coordinates and (b) angular profiles of $K(\theta)$ for the different measurement schemes: (1) $K_{xx}(\theta_{yz})$, (2) $K_{xx}(\theta_{xz})$, and (3) $K_{xy}(\theta)$.

the interparticle distance l is distributed uniformly in the interval $(\lambda, 10\lambda)$. The enhancement factor in the backscatter direction, K_{xx}, differs from unity by a value of about $\sigma_0/\bar{l}^2$, i.e., of the same magnitude as in the scalar problem. In the xz plane the peak is 1.5 times as wide as in the yz plane (which may be attributed to the different interference pattern of secondary electromagnetic waves), but for both cases $\Delta\theta \sim 1/k\bar{l}$ (curves 1 and 2). For the orthogonal y-polarization difference $K_{xy}(\theta) - 1$, curve 3, is one tenth as high as $K_{xx} - 1$.

It is hoped that the polarization features of backscattering from a system of two particles will take place in the case of many particles if double scattering is the dominant mechanism. A proof of this hypothesis can be obtained by comparing the experimental data of VAN ALBADA and LAGENDIJK [1987], who established that the intensity of a depolarized scattered field is about one tenth as strong as the intensity of the polarized component.

It should be noted that the considered model of two scatterers yields very small enhancement as compared with the many-particle experiment, namely, $K - 1 \sim |\alpha g|^2 \sim \sigma_0/\bar{l}^2 \ll 1$. For N scatterers, there will be about $\frac{1}{2}N$ pairs, and $K - 1$ will increase many times.

4.3. MORE INVOLVED SCATTERER SYSTEMS AND GEOMETRIES

4.3.1. *Cluster of N scatterers: Paired and single scattering channels*

For a system consisting of more than two scatterers, it would be reasonable to evaluate the classes of paired and single scatterings from the entire family of multiple scatterings (BUTKOVSKII, KRAVTSOV and RYABYKIN [1987]). Consider N scatterers that are more or less uniformly distributed within a volume V. The scattered field u_s can be represented as a series into the orders of multiple scattering

$$u_s = u_s^{(1)} + u_s^{(2)} + \cdots = \sum_{n=1} u_s^{(n)}, \tag{4.16}$$

where in turn, every term may be written as a sum of the fields that have experienced scattering by certain scatterers.

Let us consider a specific path $Os_i s_j \ldots s_p O'$ of scattering of order n along with the corresponding field $u_{Oij\ldots pO'}$. Clearly the number of partners in such a path can be less than n, due to repeated scattering, but all adjacent indices in the series $i, j, \ldots, p$ must be different in order to prevent self-scattering from

entering into consideration. In other words, a field scattered by one particle will have another scattering event at a different particle. The single, double, and triple scattered fields are represented, respectively, by the sums

$$u_s^{(1)} = \sum_{i=1}^{N} u_{OiO'},$$

$$u_s^{(2)} = \sum_{i,j=1}^{N} u_{OijO'},$$

$$u_s^{(3)} = \sum_{i,j,k=1}^{N} u_{OijkO'},$$

where the primes correspond to the requirement that two adjacent indices should not coincide. All in all there are N terms for a single scattered field, $N(N-1)$ terms for double scattering, $N(N-1)^2$ for triple scattering, etc.

When the locations of the transmitter and receiver coincide (O = O'), expansion (4.16) acquires coherent Watson–Ruffine pairs; specifically, the field $u_{Oij\ldots pO}$ equals the field corresponding to the reverse sequence of scatterers

$$u_{Oij\ldots pO} = u_{Op\ldots jiO}. \tag{4.17}$$

Some sequences, however, remain without a coherent partner. These are primarily single scattered fields u_{OiO} and the fields of multiplicity $2m+1$ that have been scattered m times in the forward direction, say, via an index series $j_1, \ldots, j_m$, and $m+1$ times in the reverse direction via a series $j_{m+1}, j_m, \ldots, j_1$. For such fields a reversed row of indices $p, \ldots, j, i$ coincides with the forward row $i, j, \ldots, p$, so that the fields $u_{Oij\ldots pO}$ and $u_{Op\ldots jiO}$ are identical, as is, for example, $u_{O12321O}$ or $u_{O76567O}$. A typical scattering pattern corresponding to such unpaired, or single, channels is shown in fig. 4.5. Single channels of an even order of scattering ($n = 2m$) are absent.

Let us use the sum of coherent pair fields (denoted by $2\tilde{u}$) and the sum of

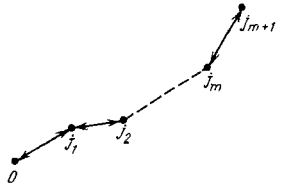

Fig. 4.5. Example of a simple scattering channel $Oj_1j_2\ldots j_{m+1}\ldots j_2j_1O$, for which the forward and reversed sequence of symbols coincide.

single fields $\tilde{u}$, including the single-scattered fields

$$u = \tilde{u} + 2\tilde{\tilde{u}}$$

$$= \sum_{m=0}^{\infty} \tilde{u}^{(2m+1)} + 2 \sum_{m=1}^{\infty} (\tilde{\tilde{u}}^{(2m)} + \tilde{\tilde{u}}^{(2m+1)}) . \tag{4.18}$$

All cross terms in these sums vanish because of the averaging over the positions of the scatterers (or over the frequencies), so that the intensity of the back-scattered field may be written as

$$I_{\mathrm{bsc}} = \tilde{I} + 4\tilde{\tilde{I}}, \tag{4.19}$$

where

$$\tilde{I} = \sum_{m=0}^{\infty} |\tilde{u}^{(2m+1)}|^2 ,$$

$$\tilde{\tilde{I}} = \sum_{m=0}^{\infty} (|\tilde{\tilde{u}}^{(2m)}|^2 + |\tilde{\tilde{u}}^{(2m+1)}|^2) ,$$

and the average is implied but not indicated.

When the point of observation O′ moves away from the source O, the fields $u_{\mathrm{O}ij\ldots p\mathrm{O}'}$ and $u_{\mathrm{O}p\ldots ji\mathrm{O}'}$ are no longer in phase, although the intensities of these fields remain almost unchanged. As a result, the coherent effects manifest themselves only within a certain coherence zone surrounding the source.

Let a cloud of scatterers of diameter L be seen from a source at a distance R at an angle $\theta \sim L/R$. If the source is in the near zone with respect to the cloud ($R < L^2/\lambda$), the longitudinal dimension of the coherence zone $l_{\parallel}$ (along the line from the source to the center of the cloud) is estimated as λ/θ^2 and the transverse dimension as $l_{\perp} \sim \lambda/\theta$ (fig. 4.6a). (These estimates are similar to those given in the monograph of RYTOV, KRAVTSOV and TATARSKII [1989a].) If the source is in the far (Fraunhofer) zone of $R > L^2/\lambda$, the transverse dimension of the coherence zone is given by the previous formula

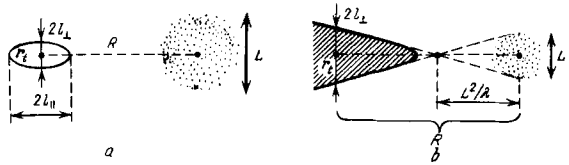

Fig. 4.6. Region of enhanced backscatter intensity in the vicinity of the transmitter $\boldsymbol{r}_t$ for many-scatterer cases with the source (a) in the near zone ($R < L^2/\lambda$) and (b) in the far zone ($R > L^2/\lambda$).

$l_\perp \sim \lambda/\theta \sim \lambda R/L$, but in the longitudinal direction the coherence zone extends from the Fresnel length $R \sim L^2/\lambda$ to infinity, as shown in fig. 4.6b.

Outside the coherence zone the coherent addition of paired channels gives way to an incoherent addition, so that instead of eq. (4.19) we have

$$I_{\text{sep}} = \tilde{I} + 2\tilde{\tilde{I}}. \tag{4.20}$$

The ratio of I_{bsc} to I_{sep} yields the enhancement factor

$$K_{\text{bsc}} = \frac{\tilde{I} + 4\tilde{\tilde{I}}}{\tilde{I} + 2\tilde{\tilde{I}}} = 1 + \frac{2\tilde{\tilde{I}}}{\tilde{I} + 2\tilde{\tilde{I}}} = 1 + \frac{2M}{1 + 2M}, \tag{4.21}$$

where $M = 2\tilde{\tilde{I}}/\tilde{I}$ characterizes the contribution of paired channels with respect to single channels,

$$M = 2\tilde{\tilde{I}}/\tilde{I} = (K - 1)/(2 - K). \tag{4.22}$$

Values of K close to unity imply that single scattering predominates and $M \ll 1$. Conversely, when $K \to 2$, multiple scattering prevails. In this case the contribution of unpaired channels, the principle of which is single scattering, tends to zero, hence $M \to \infty$. Thus the magnitude of an enhancement factor conveys information about the ratio of the contribution of paired channels to that of single scattering channels.

Let us estimate the contribution of paired channels on the assumption that in expansion (4.16) we may limit ourselves to single and double scattering only. Let σ_0 be the scattering cross section of a single scatterer and l_t be the characteristic distance for most events of double scattering. If $w(l)$ is the probability density of interparticle spacing l, then

$$\frac{1}{l_t^2} \approx \left\langle \frac{1}{l^2} \right\rangle = \int \frac{w(l)}{l^2}\, \mathrm{d}l.$$

This distance l compares in the order of magnitude, with the diameter of the scatterer cluster, L.

If a prime field of intensity I_0 is incident upon a scatterer, an individual single scattering event produces a field of intensity $I' \sim I_0 \sigma_0/R^2$, in the neighborhood of the source, where R is the distance from the source to the center of the cluster. All N scatterers of the cluster give the intensity $I^{(1)} \sim NI'$. Likewise, a single event of double scattering produces the intensity $I'' \sim I_0 \sigma_0^2/R^2 l_t^2$ near the source, and the total number of such events is $N(N-1) \approx N^2$. As a result, the total intensity of double scattering is $I^{(2)} \sim N^2 I'' \sim I_0 + N^2 \sigma_0^2/R^2 l_t^2$.

The total intensity of a scattered field outside the coherence zone may be

written as

$$I_{\text{sep}} \simeq I^{(1)} + I^{(2)} = I^{(1)}(1 + \mu), \tag{4.23}$$

where the correction $\mu \sim N\sigma_0/l_t^2$ is considered to be small. Continuing this argument, we may think of the triple scattered field as being of the order of $\mu^2 I^{(1)}$, etc. As long as μ is small compared with unity $\mu \ll 1$, we can neglect the contribution of triple scattering; then, $M \sim \mu$ and

$$K_{\text{bsc}} - 1 \approx \frac{2\tilde{\tilde{I}}}{\tilde{I}} \approx \frac{2I^{(2)}}{I^{(1)}} \sim 2\mu \sim 2N\sigma_0/l_t^2 . \tag{4.24}$$

Thus, by the backscatter enhancement data, we can judge the magnitude of the ratio $N\sigma_0/l_t^2$.

It should be stressed that the evaluation of N by the preceding method does not require that the magnitudes of intensities be measured and, consequently, eliminates the need for calibration of the transmitter and receiver. Therefore, the method suggested to estimate $\mu = N\sigma_0/l_t^2$ can be an addition to the traditional techniques of scattering media analysis. It can be used either by measuring the intensity of the scattered field, which is proportional to $N\sigma_0$ when single scattering predominates, or by measuring the extinction coefficient, which is proportional to $N\sigma_0/V$.

4.3.2. *Scattering by bodies of intricate geometry*

We say that a scattering body has an intricate geometry if the intensity scattered from this body exhibits a number of spatially separated light spots due to specular reflections and scattering from edges, vertices, and such. The Fresnel criterion for physical independence of these light spots has been outlined by KRAVTSOV [1988]. The multipath coherent effects leading to enhanced backscattering in this case stem from the fact that the incident wave suffers sequential scattering (diffraction) on a complex envelope as is the case with multiple scattering by a cluster of N individual scatterers.

There exists, however, an important distinction between such a body and a system of independent scatterers; namely, some light spots are tightly associated with the characteristic elements of diffraction on the surface of the body (bosses, vertices, and sharp peaks). Accordingly, the averaging to reveal backscatter enhancement in this case is performed over the orientations of the body, rather than over the locations of the scatterer.

Despite this difference, many features of backscattering for a body of intricate

geometry are essentially the same as those for a cluster of scatterers. These include, e.g., the envelope of the coherence zone and relationships (4.21) and (4.22) between the enhancement factor K and factor of multiple scattering M. The importance of eqs. (4.21) and (4.22) is that they qualitatively characterize the intricacy of the shape of a body, e.g., in laser detection and ranging. Specifically, the value of $M = (K - 1)/(2 - K)$ can be viewed as a criterion in target identification.

4.3.3. *Coherent effects in diffraction by large bodies*

In the systematic analysis of scattering by bodies of regular shape (e.g., discs, spheres, cylinders, bodies of revolution) the multipath coherent effects are automatically incorporated into consideration. However, their contribution to the total scattering cross section has not been treated separately, perhaps because it has not occurred to anyone to break down symmetrical bodies into individual elements that alone are capable of inducing the multipath transverse effects. The "elementary" approach to scattering may be of methodological and practical significance in much the same way as the approximate methods of diffraction theory, which were tried out initially for elementary solids, have been extended to bodies of more intricate geometry. In fact, the method of edge waves due to UFIMTSEV [1971] and the geometrical theory of diffraction due to J. B. KELLER [1958], along with their generalizations, have been developed precisely in this manner.

As an example, consider the scattering by a conducting sphere and focus attention on the Keller diffraction rays returning toward the source (fig. 4.7a). All such rays represent mutually coherent fields, with a forward and reverse channel corresponding to each ray. Therefore, the axis connecting the source to the sphere is the focus where focusing of the Keller diffraction rays will occur. Depending on the phase difference between the Keller rays and a ray secularly reflected from the sphere, the corresponding fields will be added or subtracted. This explains the noteworthy oscillating behavior of the cross section of the

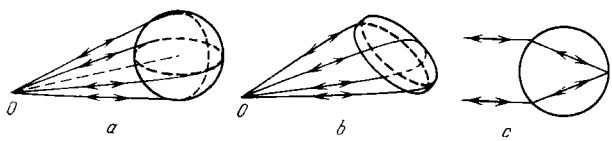

Fig. 4.7. Coherent paths formed by rays diffracted on (a) a large conducting sphere and (b) on a large conducting ellipsoid. (c) In dielectric bodies, coherent paths can form due to total internal reflection.

sphere as a function of frequency when the sphere perimeter $2\pi a$ is several wavelengths long.

Although the amplitude of the Keller rays is markedly attenuated on traversing around the sphere, this attenuation is compensated to a large degree by the "number" of rays taking part in the constructive interference. If we supply each ray with the Fresnel width $\Delta l \sim 2\sqrt{\lambda a}$ in a fairly natural manner, the sphere perimeter will accommodate about $N = \pi a/2\sqrt{\lambda a}$ rays. Accordingly, the focused field will be about $N^2 \sim \pi^2 a/4\lambda = \frac{1}{8}\pi ka$ times stronger than the field of one ray; e.g., for $a = 4\lambda$, $N^2 \sim 10$.

For a deformed sphere the number of the Keller rays whose fields add coherently in backscattering drops sharply. For example, only two pairs of coherent rays survive in the scattering by an ellipsoid, as shown in fig. 4.7b.

For a dielectric sphere the coherent effects can be associated not only with the Keller grazing diffraction rays, but also with the rays that suffered internal reflection (fig. 4.7c). Such rays occurring in small water droplets help to explain the phenomenon of a halo when sunlight incident from the observer's back to a cloud or a mist gives rise to a light nimbus around the head of the shadow. A dark ring around the nimbus corresponds to the subtraction of the diffracted waves. This phenomenon can be observed high in the mountains, above the clouds, or in an airplane for a certain position with respect to the sun. In the latter situation a halo is observed around the airplane shadow. A diffraction theory for this phenomenon (without evaluation of coherent channels) has been proposed by NUSSENZVEIG [1977].

Similar effects take place in an optical phenomenon observed when automobile headlights illuminate modern road signs. An enhanced backscattering is achieved here with the aid of tiny glass spheres added in the coating of the road sign. These balls scatter the light in a backward direction as in the case of a water droplet. A similar effect occurs with the reflection of light from retroreflectors, specifically those mounted on the moon for laser ranging.

It is useful to note the difference in the action of cat's eyes and the effect of backscatter enhancement. Cat's eye devices are usually arranged as sets of retroreflecting studs that concentrate the reflected rays toward the radiant source. The action of these devices is underlaid by the incoherent addition of the fields from all elements of the device. Accurate measurements of reflected fields near the source may reveal the coherent addition of the fields corresponding to coherent pairs of rays. As far as we know, no coherent experiments with cat's eye devices have been reported. The coherent effects may manifest themselves as a very narrow peak of angular width in the order of λ/D, where D is the cat's eye diameter, with the intensity in the close neighborhood of the source being twice that of the background.

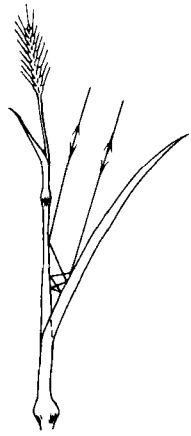

Fig. 4.8. Typical ray pattern in laser sounding of grain crops. The laser return to the source gives rise to the hot-spot effect.

The double magnitude of the backscattered intensity peak will be observed on the average over the various positions (orientations) of the device. Certain realizations may exhibit both enhancement by a factor N of the number of reflecting studs in the device, and attenuation of the intensity down to zero, which corresponds to an equal number of elements in phase and out of phase; but on the average the quantity $K = \langle I_{\text{bsc}} \rangle / \langle I_{\text{sep}} \rangle$ will be around two.

The analogy with the cat's eye is useful in considering another interesting effect, referred to as the hot-spot (GERSTL, SIMMER and POWERS [1986] and ROSS and MARSHAK [1988]). This effect is observed in the laser scanning of grain crops when a considerable proportion of the beam energy is reflected from the plant stem and blade almost in the backscatter direction (fig. 4.8), giving rise to the name of this phenomenon. In general, in the circumstances one may also expect an enhanced backscattering due to coherent scattering channels, but actually this is hardly feasible for in-flight laser scanning of grain crops from an airplane or helicopter.

§ 5. Enhanced Backscattering from Rough Surfaces

5.1. TREND TO INTENSITY PEAKING IN THE ANTISPECULAR DIRECTION

An early indication of enhanced backscattering from randomly rough surfaces seems to have been given by KRAVTSOV and SAICHEV [1982b] for very rough, steep surfaces that reflect the rays back to the source with a high probability (fig. 5.1a), and by ZAVOROTNYI and OSTASHEV [1982] for rough

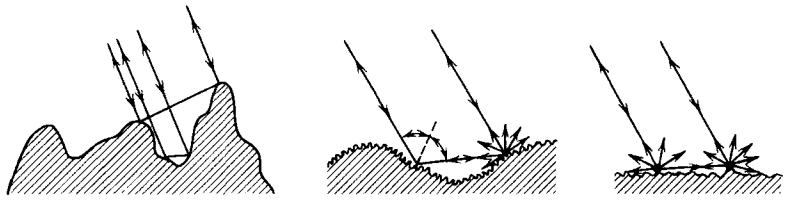

Fig. 5.1. Coherent channels arising in scattering from statistically rough surfaces, specifically due to double scattering by small inhomogeneities.

surface areas illuminating one another. ZAVOROTNYI [1984] extended these considerations on a two-scale surface (fig. 5.1b).

In the treatment of ZAVOROTNYI and OSTASHEV [1982] and ZAVOROTNYI [1984], one of the reflections in fig. 5.1b, say, at point A, is specular (the field is reflected from the large-scale component of the surface roughness profile), and the other reflection at B is diffusive. The latter is due to the small-scale component and does not obey the laws of geometrical optics. Hence, the relevant coherence scattering channels occur because of single Bragg scattering and single specular reflection. For large and steep roughness heights as in fig. 5.1a, coherence channels occur due to multiple (at least double) scattering of the rays.

One more mechanism is capable of producing coherent channels, namely, that due to double scattering from small surface inhomogeneities (fig. 5.1c). It is weaker than its counterparts, but it does not involve specular channels and, in this respect, is a more universal mechanism; weak effects of double scattering always co-exist with the stronger mechanisms.

Of the theories developed thus far to describe backscatter enhancement, the full-wave approach of BAHAR and FITZWATER [1987, 1989] is worth mentioning. According to the authors' terminology, it deals with single scattering, but actually represents a second-order iterative solution. In fact, the enhancement effect is "hidden" in the ordinary theory of double scattering, but it has avoided an explicit elucidation as far as we know. On the other hand, computer simulations performed with great ingenuity by NIETO-VESPERINAS and SOTO-CRESPO [1987], MACASKILL and KACHOYAN [1988], and SOTO-CRESPO and NIETO-VESPERINAS [1989] have revealed a backscatter intensity peak and certain polarization effects.

Neither analytical nor numerical methods, however, have been able to produce an effect that compares with the experimental data of MENDEZ and O'DONNELL [1987], O'DONNELL and MENDEZ [1987], SANT, DAINTY and KIM [1989], KIM, DAINTY, FRIBERG and SANT [1990]. These workers studied

scattering from a specially prepared, very rough surface, i.e., an aluminium coated rough surface of a photoresist resulted after speckle-field irradiation. These experiments revealed a sizeable maximum in the antispecular direction and a very strong depolarization – the intensity of the depolarized back-scattered component was almost 50%.

The qualitative interpretation of the backscatter intensity peak given by these authors bears on the ray optics representations and essentially parallels the arguments of KRAVTSOV and SAICHEV [1982b]. The ray optics interpretation provides an explanation for certain features of the polarization, specifically for the absence of axial symmetry of the scattered field. A reasonable explanation of the polarization characteristics has been given in the full-wave theory of BAHAR and FITZWATER [1987, 1989].

As long as a well-developed theory of scattering from large, steep, and rough heights is unavailable, it is logical to resort to a model description of antispecular scattering. A simple model of a unipolar, very rough surface has been devised by KRAVTSOV and RYABYKIN [1988]. This model does not pretend to explain polarization phenomena and has been constructed as a collection of upright waveguides of random depth and width, as illustrated in fig. 5.2a. A beam launched at an angle θ_0 with the axis of the waveguides excites in them eigenwaves of different types. If the waveguides are sufficiently wide and deep compared to the wavelength, the reflection of the incident wave from the side walls and bottom of the waveguides may be described in the framework of geometrical optics. In this approximation the incident beam is split into two parts – one portion of the energy is reflected in the specular direction, as shown in fig. 5.2b, and the other portion is reflected backwards, i.e., in the antispecular direction, as illustrated in fig. 5.2c.

Averaged over all the waveguides, one half of the energy is reflected in the mirror direction, and the other half in the antispecular direction, so that the angular distribution of intensity will exhibit two sharp maxima of equal magnitudes. If we observe the diffraction nature of the reflection, these peaks acquire a finite angular width.

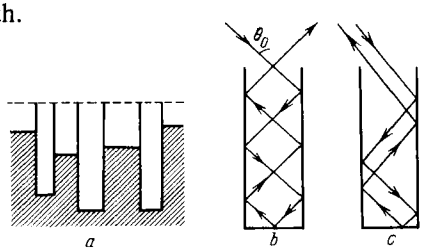

Fig. 5.2. (a) Model of a very rough surface made of open waveguide sections of random depth and width; (b) and (c) specular and antispecular ray paths.

5.2. BACKSCATTER ENHANCEMENT INVOLVING SURFACE WAVES

A well-known method of exciting electromagnetic surface waves by light involves diffraction gratings that launch one of the diffraction spectra along the metallic surface. These surface waves can suffer multiple scattering in view of the imperfections of the grating and roughness of the metal surface. Among other directions the scattered waves will emerge from the grating in the specular or antispecular direction. In the presence of paired coherent channels for surface waves one can expect enhanced backscattering for spatial light waves.

These types of effect have been the focus of theoretical and numerical considerations of CELLI, MARADUDIN, MARVIN and MCGURN [1985], MCGURN, MARADUDIN and CELLI [1985], ARYA, SU and BIRMAN [1985], MCGURN and MARADUDIN [1987], TRAN and CELLI [1988], and MARADUDIN, MENDEZ and MICHEL [1989]. An important event was the experimental observation of enhanced backscattering for spatial light waves by GU, DUMMER, MARADUDIN and MCGURN [1989].

The effects involving surface waves (polaritons) are interesting because they are accompanied by wave-type transformation: light → polariton → light, the enhancement occurring in the transformed wave. It is likely that this is not the only example of scattering in the transformed wave process. Specifically, the scattering after a nonlinear transformation of a wave type or frequency seems feasible as a result of a parametric interaction.

§ 6. Related Effects in Allied Fields of Physics

6.1. ENHANCED BACKSCATTERING IN ACOUSTICS

In acoustics, enhanced backscatter effects are almost as diverse as in optics. At the same time there are some specific acoustic manifestations caused by the small value of the velocity of sound.

We note the possibility of the multipath coherent phenomena in a confined volume. A beam launched in a confined space by a transmitter t (fig. 6.1) gives rise to paired channels like tabcdt and tdcbat, as well as single channels like tAt. In measuring pulse signals the different reflections from the walls may be resolved in time to discover that the amplitudes in the paired channels have been doubled and the intensities quadrupled.

When the transmitter and receiver locations are separated, the transverse effect vanishes. This explains why we hear our own voices differently from our

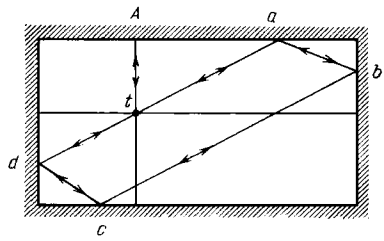

Fig. 6.1. Single (tAt) and paired (tabcdt) scattering channels in a confined space of rectangular cross section.

roommates, but alas fails to explain the origin of misunderstanding. A theory of coherent effects in confined geometries is outlined by BUTKOVSKII, KRAVTSOV and RYABYKIN [1986] and the relevant experimental evidence by GINDLER, KRAVTSOV and RYABYKIN [1986].

In view of the small velocity of sound the acoustic coherent effects find themselves destroyed faster than their optical counterparts. This circumstance can be utilized to monitor the stationary status of a medium by recording the front where the enhancement effect vanishes (AKHUNOV and KRAVTSOV [1984]). The variety of acoustical manifestations of this effect has been examined by KRAVTSOV and RYABYKIN [1988].

6.2. EFFECTS IN THE RADIO WAVE BAND

An early indication of the important role of backscatter enhancement in radio sounding of the ionosphere can be found in the work of VINOGRADOV and KRAVTSOV [1973]. It is devoted to the evaluation of the concentration of electrons in the upper ionosphere by the method of incoherent scattering that has been incapable of determining the electronic concentration by the power of the scattered field. The backscatter enhancement increases this power (in monostatic observations), thus leading to concentration estimates K times higher than the true concentration values. Similar problems have been addressed by YEH [1983] and YANG and YEH [1985] for scatterers of other physical origin.

Multi-channel coherent effects can also be observed in the scattering of radio waves from the ionosphere. These effects occur when the inhomogeneities are irradiated simultaneously by a direct wave from the transmitter and a wave reflected from the ionosphere (KRAVTSOV and NAMAZOV [1979, 1980]).

In microwave scattering from vegetation, coherent channels occur due to the reflection of the wave from the earth's surface (LANG [1981] and LANG and SIDHU [1983]). If the coefficient of reflection of microwaves from the earth's surface is close to unity, then, on average, one may expect a growth of the effective cross section of scattering from leaves, branches, blades, and stems by a factor of 1.5 compared with the value in free space. The estimate of vegetable biomass will increase accordingly.

6.3. OTHER EFFECTS OF DOUBLE PASSAGE THROUGH RANDOM MEDIA

In addition to the intensity the backscattered wave has its other parameter altered, specifically, the phase. Let $\sigma_s^2(L)$ be the variance of phase for a single passage of distance L in a random medium. As has been shown, in backscattering the variance of phase increases four times over $\sigma_s^2(L)$ rather than twice, as might be expected from a common-sense consideration.

For a rather large separation of the transmitter and receiver when the forward and reverse paths propagate through different inhomogeneities of the medium, the relevant variance exceeds $\sigma_s^2(L)$ only twice. These and other features of phase fluctuations have been investigated in the review paper of KRAVTSOV and SAICHEV [1982b].

The growth of the variance of the phase leads to an additional widening of the partial spectrum because the fluctuations of frequency occur as the derivative of the fluctuation of phase. Such a broadening of the spectrum has been observed experimentally in radio communications with the Venera space probe (EFIMOV, YAKOVLEV, VYSHILOV, NABATOV, RUBTSOV and SHEVERDYAEV [1989]), when the fluctuations of phase were caused by the motion of inhomogeneities in space plasma (solar wind).

6.4. COHERENT BACKSCATTERING OF PARTICLES FROM DISORDERED MEDIA

The coherent backscattering of particles other than photons has been approached only from the theoretical standpoint. IGARASHI [1987] has considered the effect of backscattering for isotopic and spin incoherent scattering of neutrons in the framework of the double-collision model. When the predominant channel of incoherent scattering is by spin–spin (magnetic) interactions, the enhancement may give way to the attenuation of backscattering.

The backscattering of electrons of middle energy (in the order of several hundred eV) and an unusual behavior of the enhancement factor as a function of the cross section of spin–orbital interaction have been discussed qualitatively by BERKOVITS and KAVEH [1988]. They have noted that the spin–orbital interaction can bring about a coherent antienhancement of backscattering and a sharp minimum in the angular distribution of the backscattered intensity.

GORODNICHEV, DUDAREV and ROGOZKIN [1990a] have obtained an exact solution to the problem of scattering of spin-$\frac{1}{2}$ particles, which participate in magnetic and spin–orbital interactions with a disordered medium and with a medium with an Anderson's type of disorder. These authors have also developed a theory of coherent enhancement of the backscattering process.

The effect of enhancement for neutrons scattered backwards and in certain other directions has been taken up by DUDAREV [1988] for neutrons diffracted in imperfect crystals, i.e., in crystals with isotopic and spin disorder, which corresponds to an Anderson model of disorder. The sharp resonance peaks revealed in the angular spectrum of reflected particles is associated with the diffraction of the particles at a regular part of the crystal potential. Moreover, resonance peaks occur when the periods of oscillations of the coherent field density in the nodes of the crystal lattice coincide as the particle is approaching a scatterer and returns to the surface of the crystal.

DUDAREV [1988] and GORODNICHEV, DUDAREV, ROGOZKIN and RYAZANOV [1989] noted in their studies of scattering in ordered periodic structures with fluctuating potentials that the effect of an additional enhancement of incoherent intensity owes its existence to the fact that the system of scattering centers possesses translational symmetry. The coherent enhancement of backscattering is caused by the effect of weak localization of particles in multiple scattering in the medium.

We have avoided discussing the problem of weak localization of electrons in metals and semiconductors in this review, since it is too large a topic to be addressed in the space allotted to this article. The interested reader is referred to the review paper by BERGMANN [1984].

§ 7. Conclusion

It is not uncommon in the history of physics that a chance remark, trivial at first glance, has been a seedling for an entire branch of new physical phenomena, giving birth (not immediately but in 15 or 20 years) to a developed system of theoretical representations and experimental evidence. This is exactly

what happened with the private communication between Ruffine and Watson about coherent channels in 1969. It is high time to reconsider the evolution of this beautiful physical idea. Has it been completely exhausted, or will new and interesting facets be revealed to researchers? Whatever happens, we admit that we have been completely satisfied by our participation in the solution of problems associated with enhanced backscattering and weak localization phenomena.

Acknowledgement

We are indebted to Prof. E. Wolf for the interest shown in our work. We want to thank M. S. Belenkii, A. S. Gurvich, V. L. Mironov and D. V. Vlasov for communicating their results to us and A. I. Fedulov and F. I. Ismagilov for their assistance in computations.

References*

ABRAHAMS, E., P. W. ANDERSON, D. C. LICCARDELLO and T. V. RAMAKRISHNAN, 1979, Scaling theory of localization: absence of quantum diffusion in two dimensions, Phys. Rev. Lett. **42**(10), 673–676.

AGROVSKII, B. S., A. N. BOGATOV, A. S. GURVICH, S. V. KIREEV and V. A. MYAKININ, 1991, Enhanced backscattering from a plane mirror viewed through turbulent phase screen, J. Opt. Soc. Am. A **8** (in press).

AKHUNOV, KH. G., and YU. A. KRAVTSOV, 1982, Coherent effects accompanying backscattering of sound from bodies near rough sea surface, Akust. Zh. **28**(4), 438–440.

AKHUNOV, KH. G., and YU. A. KRAVTSOV, 1983a, Development of the enhanced backscatter effect in reflection from a phase conjugated mirror, Izv. VUZ Radiofiz. **26**(5), 635–638.

AKHUNOV, KH. G., and YU. A. KRAVTSOV, 1983b, Effective cross section of a small body placed near the interface between two random media, Kratk. Soobshch. Fiz. FIAN 8, 8–11.

AKHUNOV, KH. G., and YU. A. KRAVTSOV, 1984, Conditions for coherent addition of back-scattered sound waves under multipath propagation, Akust. Zh. **30**(2), 145–148.

AKHUNOV, KH. G., F. V. BUNKIN, D. V. VLASOV and YU. A. KRAVTSOV, 1982, Efficiency of wavefront inversion in media with time-varying fluctuations, Kvant. Elektron. **9**(6), 1287–1289.

AKHUNOV, KH. G., YU. A. KRAVTSOV and V. M. KUZKIN, 1984, Effect of enhanced back-scattering from a body in a regular multimode waveguide, Izv. VUZ Radiofiz. **27**(3), 319–323.

AKHUNOV, KH. G., F. V. BUNKIN, D. V. VLASOV and YU. A. KRAVTSOV, 1984, On the efficiency of phase conjugated focusing of waves in turbulent media, Radiotekh. Elektron. **29**(1), 1–4.

* The titles of Russian papers have been translated for convenience. We note also that some Soviet journals are translated into English on a cover-to-cover basis, e.g., Akust. Zh. [Sov. Phys.–Acoust.], Dokl. Akad. Nauk SSSR [Sov. Phys.–Dokl.], Izv. VUZ Radiofiz. [Radiophys. & Quantum Electron.], Radiotekh. & Elektron. [Radio Eng. & Electron. Phys.], Kvant Elektron. [Sov. J. Quant. Electronics], Zh. Eksp. & Teor. Fiz. [Sov. Phys.–JETP], Kratk. Soobsh. Fiz. [Sov. Phys. Lebedev Inst. Reports].

AKKERMANS, E., and R. MAYNARD, 1985, Weak localization of waves, J. Phys. (France) Lett. **46**(22), L1045-L1053.

AKKERMANS, E., P. E. WOLF and R. MAYNARD, 1986, Coherent backscattering of light by disordered media: analysis of the peak line shape, Phys. Rev. Lett. **56**(14), 1471–1474.

AKKERMANS, E., P. E. WOLF, R. MAYNARD and G. MARET, 1988, Theoretical study of the coherent backscattering of light by disordered media, J. Phys. (France) **49**(1), 77–98.

AKSENOV, V. P., and V. L. MIRONOV, 1979, Phase approximation of the Huygens-Kirchhoff method in problems of reflections of optical waves in the turbulent atmosphere, J. Opt. Soc. Am. **69**(11), 1609–1614.

AKSENOV, V. P., V. A. BANAKH and V. L. MIRONOV, 1984, Fluctuations of retroreflected laser radiation in a turbulent atmosphere, J. Opt. Soc. Am. A **1**(3), 263–274.

ALIMOV, V. A., and L. M. ERUKHIMOV, 1973, Distribution of SW-signal fluctuations, Izv. Vuz Radiofiz. **16**(10), 1540–1551.

ALTSHULER, B. L., A. G. ARONOV, D. E. KHMELNITSKII and A. I. LARKIN, 1982, Coherent effects in disordered conductors, in: Quantum Theory of Solids, ed. I. M. Lifshits (Mir, Moscow) pp. 130–237.

ANDERSON, P. W., 1958, Absence of diffusion in certain random lattices, Phys. Rev. **109**, 1492–1505.

APRESYAN, L. A., and D. V. VLASOV, 1988, On the role of large-scale focusing inhomogeneities in remote experiments, Izv. Vuz Radiofiz. **31**(7), 823–833.

ARYA, K., Z. B. SU and J. L. BIRMAN, 1985, Localization of the surface plasmon-polariton caused by random roughness and its role in surface-enhanced optical phenomena, Phys. Rev. Lett. **54**, 1559–1562.

BAHAR, E., and M. A. FITZWATER, 1987, Full wave theory and controlled optical experiments for enhanced scattering and depolarization by random rough surfaces, Opt. Commun. **63**(6), 355–360.

BAHAR, E., and M. A. FITZWATER, 1989, Depolarization and backscatter enhancement in light scattering from random rough surfaces: comparison of full wave theory with experiment, J. Opt. Soc. Am. A **6**(1), 33–43.

BANAKH, V. A., and V. L. MIRONOV, 1987, Laser light ranging in turbulent atmosphere (Artech House, Boston).

BARABANENKOV, YU. N., 1969, On the spectral theory of radiation transport equation, Zh. Eksp. Teor. Fiz. **56**(6), 1262–1270.

BARABANENKOV, YU. N., 1973, Wave corrections to the transport equation for backscattering, Izv. VUZ Radiofiz. **16**(1), 88–96.

BARABANENKOV, YU. N., 1975, Multiple scattering of waves in an ensemble of particles and a theory of radiation transfer, Usp. Fiz. Nauk **117**(1), 49–78.

BARABANENKOV, YU. N., and V. M. FINKELBERG, 1967, Radiation transport equation for correlated scatterers, Zh. Eksp. Teor. Fiz. **53**(5), 978.

BARABANENKOV, YU. N., and V. D. OZRIN, 1988, Diffusion approximation in the theory of coherent backscatter enhancement for randomly inhomogeneous media, Zh. Eksp. Teor. Fiz. **94**(6), 56–64.

BELENKII, M. S., and V. L. MIRONOV, 1972, Diffraction of optical radiation on a mirror disc in a turbulent atmosphere, Kvant. Elektron. **5**(11), 38–45.

BELENKII, M. S., and V. L. MIRONOV, 1974, Evaluation of the profile of C_n^2 parameter from optical radar measurements in the atmosphere, Kvant. Elektron. **1**(10), 2253–2262.

BELENKII, M. S., A. A. MAKAROV, V. L. MIRONOV and V. V. POKASOV, 1978, The effect of saturation of receiver averaging on the fluctuation of the reflected intensity, Izv. VUZ Radiofiz. **21**(2), 299–300.

BERGMANN, G., 1984, Weak localization in thin films: time-of-flight experiment with conduction electrons, Phys. Rep. **107**, 1–58.

BERKOVITS, R., and M. KAVEH, 1988, Backscattering of high-energy electrons from disordered media: antienhancement due to spin–orbit interaction, Phys. Rev. B **37**(1), 584–587.

BOGATOV, A. N., A. S. GURVICH, S. S. KASHKAROV and V. Z. MYAKININ, 1991, Backscattering from different objects in turbulent media, Waves in Random Media **1** (in press).

BUNKIN, A. F., D. V. VLASOV and D. M. MIRKAMILOV, 1987, Fizicheskie osnovy lazernogo aerozondirovaniya (Physical foundations of laser surveying of earth's surface) (Fan, Tashkent).

BUTKOVSKII, O. YA., YU. A. KRAVTSOV and V. V. RYABYKIN, 1986, Multipath coherent effects and enhanced backscattering of sound in a confined space, Akust. Zh. **32**(5), 666–667.

BUTKOVSKII, O. YA., YU. A. KRAVTSOV and V. V. RYABYKIN, 1987, Multichannel coherent effects in backscattering from a collection of small scatterers, Izv. VUZ Radiofiz. **30**(5), 609–612.

CASE, K. M., and P. F. ZWEIFEL, 1967, Linear Transport Theory (Addison-Wesley, Reading, MA).

CELLI, V., A. A. MARADUDIN, A. M. MARVIN and A. R. MCGURN, 1985, Some aspects of light scattering from a randomly rough metal surface, J. Opt. Soc. Am. A **2**(12), 2225–2239.

CHANDRASEKHAR, S., 1960, Radiative Transfer (Dover, New York).

CWILICH, G., and M. J. STEPHEN, 1987, Rayleigh scattering and weak localization: geometric effects and fluctuations, Phys. Rev. B **35**(13), 6517–6520.

DAINTY, J. C., D. N. QU and S. XU, 1988, Statistical properties of enhanced backscattering produced by dense collections of latex spheres, Proc. SPIE **976**, Stat. Opt. 178–184.

DASHEN, R., 1979, Path integrals for waves in random media, J. Math Phys. **20**(5), 894–920.

DE WOLF, D. A., 1971, Electromagnetic reflection from an extended turbulent medium: cumulative forward-scatter single-backscatter approximation, IEEE Trans. Anten. Propag. **AP-19**, 254–262.

DOLGINOV, A. Z., YU. N. GNEDIN and N. A. SILANTYEV, 1979, Propagation and polarization of radiation in space (in Russian) (Nauka, Moscow).

DUDAREV, S. L., 1988, Quantum kinetic equation for inelastic scattering of particles in crystals: extension beyond the Born approximation, Zh. Eksp. & Theor. Fiz. **94**(11), 189–306.

EDREI, I., and M. KAVEH, 1987, Weak localization of photons and backscattering from finite systems, Phys. Rev. B **35**(12), 6461–6463.

EFIMOV, A., O. I. YAKOVLEV, A. S. VYSHILOV, A. S. NABATOV, S. N. RUBTSOV and A. D. SHEVERDYAEV, 1989, Dm–cm-radiowave line broadening in communications with the Venera 15, 16 space probes through the near solar corona, Radiotekh. Elektron. **34**(8), 1596–1603.

ETEMAD, S., 1988, Coherent backscattering of light by disordered media: the vector nature of a photon, Phys. Rev. **37**(7), 3652–3653.

ETEMAD, S., R. THOMPSON and M. J. ANDREJCO, 1986, Weak localization of photons: universal fluctuations and ensemble averaging, Phys. Rev. Lett. **57**(16), 575–578.

ETEMAD, S., R. THOMPSON, M. J. ANDREJCO, S. JOHN and F. C. MACKINTOSH, 1987, Weak localization of photons: termination of coherent random walks by absorption and confined geometry, Phys. Rev. Lett. **59**(13), 1420–1423.

FINKELBERG, V. M., 1967, Propagation of waves in random media. The correlated group method, Zh. Eksp. & Teor. Fiz. **53**, 401.

FOLDY, L. L., 1945, The multiple scattering of waves. I. General theory of isotropic scattering by randomly distributed scatterers, Phys. Rev. **67**, 107.

FREUND, I., M. ROSENBLUH, R. BERKOVITS and M. KAVEH, 1988, Coherent backscattering of light in a quasi-two-dimensional system, Phys. Rev. Lett. **61**(10), 1214–1217.

FRISCH, U., 1965, Wave Propagation in Random Media. II. Multiple Scattering by n Bodies (Institut d'Astrophysique, Paris).

GAZARYAN, YU. L., 1969, Propagation of a one-dimensional wave through a medium with random inhomogeneities, Zh. Eksp. & Teor. Fiz. **56**(8), 1856–1862.

GEHLHEAR, U., 1982, Computer simulations and theory of oceanographic fluorescence lidar signals: effect of sea surface structure, Appl. Opt. **21**, 3743–3755.

GELFGAT, V. I., 1976, Reflection in diffusive media, Akust. Zh. **22**(1), 123–124.

GELFGAT, V. I., 1981, Compensation of phase distortions by wave front reversal in random single-mode and multi-mode acoustic waveguides, Akust. Zh. **27**(2), 194–201.

GERSTL, S. A. W., C. SIMMER and B. J. POWERS, 1986, The canopy hotspot as crop identifier, in: Remote Sensing for Resource Development and Environmental Management, Proc. 7th Int. Symp. Enschede, 25–29 Aug. 1986 (Rotterdam, Boston).

GINDLER, I. V., YU. A. KRAVTSOV and V. V. RYABYKIN, 1986, Experimental investigation of enhanced backscattering of sound in a closed tank, Sov. Phys.-Lebedev Inst. Reports No. 11, pp. 42–43.

GOCHELASHVILI, K. S., and V. I. SHISHOV, 1981, Propagation of reflected radiation through a randomly inhomogeneous medium, Kvantovaya Elektron. **8**(9), 1953–1956.

GOLDBERGER, M. L., and K. M. WATSON, 1964, Collision Theory (Wiley, New York).

GOLUBENTSEV, A. A., 1984a, Suppression of interference effects in multiple scattering, Zh. Eksp. & Teor. Fiz. **86**(1), 47–59.

GOLUBENTSEV, A. A., 1984b, Contribution of interference into albedo of strong gyrotropic medium with random inhomogeneities, Izv. VUZ Radiofiz. **127**, 734–738.

GORKOV, L. P., A. I. LARKIN and D. E. KHMELNITSKII, 1979, Conductivity of a particle in a two-dimensional potential, Pis'ma Zh. Eksp. & Teor. Fiz. **30**(4), 248–252.

GORODNICHEV, E. E., S. L. DUDAREV, D. B. ROGOZKIN and M. I. RYAZANOV, 1987, Coherent effects in backscattering of waves from a medium with random inhomogeneities, Zh. Eksp. & Teor. Fiz. **93**(5), 1642–1650.

GORODNICHEV, E. E., S. L. DUDAREV, D. B. ROGOZKIN and M. I. RYAZANOV, 1989, Weak localization of waves in incoherent scattering in crystals, Zh. Eksp. & Teor. Fiz. **96**(5), 1801–1807.

GORODNICHEV, E. E., S. L. DUDAREV and D. B. ROGOZKIN, 1989, Coherent backscatter enhancement under weak localization in two- and three-dimensional systems, Zh. Eksp. & Teor. Fiz. **96**(3), 847–864.

GORODNICHEV, E. E., S. L. DUDAREV and D. B. ROGOZKIN, 1990a, Polarization phenomena in coherent backscattering of waves by random media, Zh. Eksp. Theor. Fiz. **97**(5), 1511–1529.

GORODNICHEV, E. E., S. L. DUDAREV and D. B. ROGOZKIN, 1990b, Coherent wave back-scattering by random media. Exact solution of the albedo problem, Phys. Lett. A **144**(1), 48–54.

GU, Z.-H., R. S. DUMMER, A. A. MARADUDIN and A. R. MCGURN, 1989, Experimental study of the opposition effect in the scattering of light from a randomly rough metal surface, Appl. Opt. **28**(3), 537–543.

GURBATOV, S. N., A. N. MALAKHOV and A. I. SAICHEV, 1991, Nonlinear Random Waves in Nondispersive Media (Manchester University Press, Manchester).

GURVICH, A. S., and S. S. KASHKAROV, 1977, Enhancement of backscattering in a turbulent medium, Izv. VUZ Radiofiz. **20**(5), 794–796.

HOGE, F. E., and R. N. SWIFT, 1983a, Airborne detection of oceanic turbidity cell structure using depth-resolved laser-induced water Raman backscatter, Appl. Opt. **22**(23), 3778–3786.

HOGE, F. E., and R. N. SWIFT, 1983b, Experimental feasibility of the airborne measurement of absolute oil fluorescence spectral conversion efficiency, Appl. Opt. **22**(1), 37–47.

IGARASHI, J., 1987, Coherent backscattering of neutrons, Phys. Rev. B **35**(16), 8894–8897.

ISHIMARU, A., 1978, Wave Propagation and Scattering in Random Media (Academic Press, New York).

ISHIMARU, A., and L. TSANG, 1988, Backscattering enhancement of random discrete scatterers of moderate sizes, J. Opt. Soc. Am. A **5**(2), 228–235.

JAKEMAN, E., 1988, Enhanced backscattering through a deep random phase screen, J. Opt. Soc. Am. A **5**(10), 1638–1648.

JOHN, S., 1988, The localization of light and classical waves in disordered media, Comments Cond. Mat. Phys. **14**(4), 193–230.

JOHN, S., and M. J. STEPHEN, 1983, Wave propagation and localization in a long-range correlated random potential, Phys. Rev. B **28**(11), 6358–6368.

KASHKAROV, S. S., 1983, Enhancement of the average backscattered intensity in a turbulent atmosphere, Izv. VUZ Radiofiz. **26**(1), 44–48.

KASHKAROV, S. S., T. N. NESTEROVA and A. S. SMIRNOV, 1984, Fluctuations of backscattered light intensity in turbulent media, Izv. VUZ Radiofiz. **27**(10), 1272–1278.

KAVEH, M., 1987, Localization of photons in disordered systems, Philos. Mag. B **56**(6), 693–703.

KAVEH, M., M. ROSENBLUH, I. EDREI and I. FREUND, 1986, Weak localization and light scattering from disordered solids, Phys. Rev. Lett. **57**(16), 2049–2052.

KELLER, J. B., 1958, A geometrical theory of diffraction, in: Calculus of Variations and its Applications (McGraw-Hill, New York); Proc. Symp. Appl. Math. **8**, 27–38.

KIM, M.-J., J. C. DAINTY, A. T. FRIBERG and A. J. SANT, 1990, Experimental study of enhanced backscattering from one- and two-dimensional random rough surfaces, J. Opt. Soc. Am. A **7**(4), 569–577.

KLYATSKIN, V. I., 1975, On the statistical theory of light propagation in a medium with random inhomogeneities, Izv. VUZ Radiofiz. **18**(1), 63–68.

KLYATSKIN, V. I., 1980, Stokhasticheskie uravneniya i volny v sluchainoneodnorodnykh sredakh (Stochastic equations and waves in randomly inhomogeneous media) (Nauka, Moscow).

KRAVTSOV, YU. A., 1968, Strong fluctuations of the amplitude of a light wave and probability of formation of random caustics, Sov. Phys. JETP **28**(3), 413–414.

KRAVTSOV, YU. A., 1970, On the "geometrical" depolarization of light in a turbulent atmosphere, Izv. VUZ Radiofiz. **13**(2), 281–287.

KRAVTSOV, YU. A., 1988, Rays and caustics as physical objects, in: Progress in Optics, Vol. 26, ed. E. Wolf (North-Holland, Amsterdam) pp. 227–348.

KRAVTSOV, YU. A., and S. A. NAMAZOV, 1979, Backscatter theory for multipath propagation in random media, in: Proc. URSI Spring Meeting and USA Nat'l Rad. Sci. Meeting, Seattle, Wash. Commun. G p. 262.

KRAVTSOV, YU. A., and S. A. NAMAZOV, 1980, Scattering of radiowaves from magnetically oriented ionospheric inhomogeneities, Radiotekh. Electron. **25**(3), 459–466.

KRAVTSOV, YU. A., and V. V. RYABYKIN, 1988, Multichannel coherent effects in backscattering of waves, Preprint No. 15 (General Physics Institute, Moscow).

KRAVTSOV, YU. A., and A. I. SAICHEV, 1982a, Effects of partial wave front reversal on reflection of waves by randomly inhomogeneous media, Zh. Eksp. Teor. Fiz. **83**(2), 532–538.

KRAVTSOV, YU. A., and A. I. SAICHEV, 1982b, Effects of double passage of waves in randomly inhomogeneous media, Sov. Phys. Usp. **25**(7), 494–508.

KRAVTSOV, YU. A., and A. I. SAICHEV, 1985, Properties of coherent waves reflected in a turbulent medium, J. Opt. Soc. Am. A **2**(12), 2100–2105.

KRUPNIK, A. B., 1985, Relation of backscatter enhancement with partial wavefront reversal, Radiotekh. Electron. **30**(4), 625–629.

KRUPNIK, A. B., and A. I. SAICHEV, 1981, Coherent properties and focusing of wave beams reflected in a turbulent medium, Izv. VUZ Radiofiz. **24**(10), 1233–1239.

KUGA, Y., and A. ISHIMARU, 1984, Retroreflectance from a dense distribution of spherical particles, J. Opt. Soc. Am. A **1**(8), 831–839.

KUGA, Y., L. TSANG and A. ISHIMARU, 1985, Depolarization effects of the enhanced retroreflectance from a dense distribution of spherical particles, J. Opt. Soc. Am. A **2**(6), 616–618.

LAGENDIJK, A., M. P. VAN ALBADA and M. B. VAN DER MARK, 1986, Localization of light: the quest for the white hole, Physica A **140**, 183–190.

LAGENDIJK, A., R. VREEKER and P. DE VRIES, 1989, Influence of internal reflection on diffusive transport of strongly scattering media, Phys. Lett. A **136**(1, 2), 81–88.

LANG, R. H., 1981, Electromagnetic backscattering from a sparse distribution of lossy dielectric scatterers, Rad. Sci. **16**(1), 15–30.

LANG, R. H., and J. S. SIDHU, 1983, Electromagnetic backscattering from a layer of vegetation: a discrete approach, IEEE Trans. Geosci. Electron. **GE-21**(1), 62–71.

LAX, M., 1951, Multiple scattering of waves, Rev. Mod. Phys. **23**(4), 287–310.

LUCHININ, A. G., 1979, Wind-wave effect on characteristics of light field backscattered by bottom and water layer, Izv. Akad. Nauk SSSR Ser. Fiz. Atmos. & Okeana **15**(7), 770–775.

MACASKILL, C., and B. J. KACHOYAN, 1988, Numerical evaluation of the statistics of acoustical scattering from a rough surface, J. Acoust. Soc. Am. **84**(5), 1826–1835.

MACKINTOSH, F. C., and S. JOHN, 1988, Coherent backscattering of light in the presence of time-reversal-noninvariant and parity-nonconserving media, Phys. Rev. B **37**(4), 1884–1897.

MALAKHOV, A. N., and A. I. SAICHEV, 1979, Representation of a wave reflected from a randomly inhomogeneous slab in the form of a series satisfying the causality condition, Izv. VUZ Radiofiz. **22**(11), 1324–1333.

MALAKHOV, A. N., and A. I. SAICHEV, 1981, An effect of irregularity drift over beam propagation on efficiency of wavefront reversing systems, Izv. VUZ Radiofiz. **24**(11), 1356–1361.

MALAKHOV, A. N., A. V. POLOVINKIN and A. I. SAICHEV, 1983, Average intensity of a wave reflected by a phase-conjugated mirror in turbulent media, Izv. VUZ Radiofiz. **26**(5), 579–586.

MALAKHOV, A. N., A. V. POLOVINKIN and A. I. SAICHEV, 1987, Average intensity of a beam reflected by a wavefront reversing mirror in randomly inhomogeneous media, Izv. VUZ Radiofiz. **30**(7), 857–865.

MARADUDIN, A. A., E. R. MENDEZ and T. MICHEL, 1989, Backscattering effects in the elastic scattering of p-polarized light from a large-amplitude random metallic grating, Opt. Lett. **14**(3), 151–153.

MARET, G., and P. E. WOLF, 1987, Multiple light scattering from disordered media. The effect of Brownian motion of scatterers, Z. Phys. B **65**(4), 409–413.

MARTIN, J. M., and S. M. FLATTE, 1988, Intensity images and statistics from numerical simulation of wave propagation in 3-D random media, Appl. Opt. **27**(11), 2111–2126.

MCGURN, A. R., and A. A. MARADUDIN, 1987, Localization effects in the elastic scattering of light from a randomly rough surface, J. Opt. Soc. Am. B **4**(6), 910–926.

MCGURN, A. R., A. A. MARADUDIN and V. CELLI, 1985, Localization effects in the scattering of light from a randomly rough grating, Phys. Rev. B **31**(8), 4866–4871.

MENDEZ, E. R., and K. A. O'DONNELL, 1987, Observation of depolarization and backscattering enhancement in light scattering from Gaussian random surfaces, Opt. Commun. **61**(2), 91–95.

MIRONOV, V. L., 1981, Laser beam propagation in a turbulent atmosphere (Nauka, Novosibirsk) in Russian.

NIETO-VESPERINAS, M., and J. M. SOTO-CRESPO, 1987, Monte-Carlo simulations for scattering of electromagnetic waves from perfectly conductive random rough surfaces, Opt. Lett. **12**(12), 979–981.

NUSSENZVEIG, H. M., 1977, The theory of rainbow, Sci. Am. **236**(4), 116–145.

O'DONNELL, K. A., and E. R. MENDEZ, 1987, Experimental study of scattering from characterized random surfaces, J. Opt. Soc. Am. A **4**(7), 1194–1205.

PATRUSHEV, G.YA., A. I. PETROV and V. V. POKASOV, 1983, Intensity fluctuations of mirror-reflected optical beams in a turbulent atmosphere, Izv. VUZ Radiofiz. **26**(7), 823–831.

POLOVINKIN, A. V., and A. I. SAICHEV, 1981, Average field of a laser beam reflected with wavefront inversion, Izv. VUZ Radiofiz. **24**(4), 433–437.

POLOVINKIN, A. V., and A. I. SAICHEV, 1984, Wave reflection from a phase-conjugated mirror in a medium with moving large-scale inhomogeneities, Radiotekh. Elektron. **29**(2), 193–198.

QU, D. N., and J. C. DAINTY, 1988, Polarization dependence of dynamic light scattering by dense disordered media, Opt. Lett. **13**(12), 1066–1068.

ROSENBLUH, M., I. EDREI, M. KAVEH and I. FREUND, 1987, Precision determination of the line shape for coherently backscattered light from disordered solids: comparison of vector and scalar theories, Phys. Rev. B **35**(10), 4458–4460.

ROSS, J. K., and A. L. MARSHAK, 1988, Calculation of canopy bidirectional reflectance using the Monte-Carlo method, Remote Sens. Environ. **24**(2), 213–225.

RUFFINE, R. S., and D. A. DE WOLF, 1965, Cross-polarized electromagnetic backscatter from turbulent plasmas, J. Geophys. Res. **70**(17), 4313–4321.

RYBICKI, G. B., 1971, Searchlight problem with isotropic scattering, J. Quantum Spectros. & Rad. Trans. **11**, 827–844.

RYTOV, S. M., YU. A. KRAVTSOV and V. I. TATARSKII, 1989a, Principles of Statistical Radiophysics, Vol. 3, Random Fields (Springer, Berlin, Heidelberg).

RYTOV, S. M., YU. A. KRAVTSOV and V. I. TATARSKII, 1989b, Principles of Statistical Radiophysics, Vol. 4, Wave Propagation through Random Media (Springer, Berlin).

SAICHEV, A. I., 1978, Relation of statistical characteristics of transmitted and reflected waves in a medium with large-scale random inhomogeneities, Izv. VUZ Radiofiz, **21**(9), 1290–1293.

SAICHEV, A. I., 1980, Analysis of backscattering in turbulent medium under multiple scattering in the direction of propagation: the diffuse approximation, Izv. VUZ Radiofiz. **23**(11), 1305–1313.

SAICHEV, A. I., 1981, Reflection from a wavefront inverting mirror, Izv. VUZ Radiofiz. **24**(9), 1165–1167.

SAICHEV, A. I., 1982, Compensation of wave distortions by a phase-conjugated mirror in an inhomogeneous medium, Radiotekh. Elektron. **27**(9), 1961–1968.

SAICHEV, A. I., 1983, Ray description of waves reflected with phase conjugation, Radiotekh. Elektron. **28**(10), 1889–1894.

SALPETER, E. E., 1967, Interplanetary scintillations. I. Theory, Astrophys. J. **147**(2), 433–**XXX**.

SANT, A. J., J. C. DAINTY and M.-J. KIM, 1989, Comparison of surface scattering between identical randomly rough metal and dielectric diffusors, Opt. Lett. **14**(1), 1183–1185.

SCHMELTZER, D., and M. KAVEH, 1987, Back-scattering of electromagnetic waves in random dielectric media, J. Phys. C **20**, L175–L179.

SHISHOV, V. I., 1974, Dependence of oscillation spectrum on spectrum of refractive index inhomogeneities. I. Phase screen, Izv. VUZ Radiofiz. **17**(11), 1684–1692.

SOBOLEV, V. V., 1963, Transfer of Radiation Energy in the Atmospheres of Stars and Planets (Van Nostrand, New York).

SOTO-CRESPO, J. M., and M. NIETO-VESPERINAS, 1989, Electromagnetic scattering from very rough random surfaces and deep reflection gratings, J. Opt. Soc. Am. A **6**(3), 367–384.

STEPHEN, M. J., and G. CWILICH, 1986, Rayleigh scattering and weak localization: effects of polarization, Phys. Rev. B **34**(11), 7564–7572.

TATARSKII, V. I., 1967, Estimation of light depolarization by turbulent inhomogeneities of the armosphere, Izv. VUZ Radiofiz. **10**(12), 1762–1765.

TATARSKII, V. I., 1971, Effects of turbulent atmosphere on wave propagation, Nat. Technol. Inform. Service USA, TT-68-50464.

TRAN, P., and V. CELLI, 1988, Monte-Carlo calculation of backscattering enhancement for a randomly rough grating, J. Opt. Soc. Am. A **5**(10), 1635–1637.

TSANG, L., and A. ISHIMARU, 1984, Backscattering enhancement of random discrete scatterers, J. Opt. Am. **1**(6), 836–839.

TSANG, L., and A. ISHIMARU, 1985, Theory of backscattering enhancement of random discrete isotropic scatterers based on the summation of all ladder and cyclical terms, J. Opt. Soc. Am. A **2**(8), 1331–1338.

UFIMTSEV, P. YA., 1971, The Method of Edge Waves in the Physical Theory of Diffraction (US Air Force, Wright-Patterson AFB, OH).

VAN ALBADA, M. P., and A. LAGENDIJK, 1985, Observation of weak localization of light in a random medium, Phys. Rev. Lett. **55**(24), 2692–2695.

VAN ALBADA, M. P., and A. LAGENDIJK, 1987, Vector character of light in weak localization: spatial anisotropy in coherent backscattering from a random medium, Phys. Rev. B **36**(4), 2353–2356.

VAN ALBADA, M. P., M. B. VAN DER MARK and A. LAGENDIJK, 1987, Observation of weak localization of light in a finite slab: anisotropy effects and light-path classification, Phys. Rev. Lett. **58**(4), 361–364.

VAN DER MARK, M. B., M. P. VAN ALBADA and A. LAGENDIJK, 1988, Light scattering in strongly scattering media: multiple scattering and weak localization, Phys. Rev. B **37**(7), 3575–3592.

VINOGRADOV, A. G., 1974, Enhanced backscattering in reflection of waves from rough surfaces placed in a randomly inhomogeneous medium, Izv. VUZ Radiofiz. **17**(10), 1584–1586.

VINOGRADOV, A. G., and YU. A. KRAVTSOV, 1973, A hybrid approach to the calculation of field fluctuations in a medium with large- and small-scale random inhomogeneities, Izv. VUZ Radiofiz. **16**(7), 1055–1063.

VINOGRADOV, A. G., YU. A. KRAVTSOV and V. I. TATARSKII, 1973, Enhanced backscattering from bodies immersed in a random inhomogeneous medium, Izv. VUZ Radiofiz. **16**(7), 1064–1070.

VINOGRADOV, A. G., A. G. KOSTERIN, A. S. MEDOVIKOV and A. I. SAICHEV, 1985, Effect of refraction on the propagation of a beam in a turbulent medium, Izv. VUZ Radiofiz. **25**(10), 1227–1235.

VLASOV, D. V., 1985, Laser sounding of an upper layer of the ocean, Izv. Akad. Nauk SSSR Ser. Fiz. **49**(3), 463–472.

WATSON, K. M., 1969, Multiple scattering of electromagnetic waves in an underdense plasma, J. Math. Phys. **10**(4), 688–702.

WOLF, P. E., and G. MARET, 1985, Weak localization and coherent backscattering of photons in disordered media, Phys. Rev. Lett. **55**(24), 2696–2699.

WOLF, P. E., G. MARET, E. AKKERMANS and R. MAYNARD, 1988, Optical coherent backscattering by random media: an experimental study, J. Phys. (France) **49**(1), 63–75.

YAKUSHKIN, I. G., 1978, Moment of field intensity propagated in a randomly inhomogeneous medium in the region of saturated fluctuations, Izv. VUZ Radiofiz. **21**(8), 1194–1201.

YAKUSHKIN, I. G., 1985, Intensity fluctuations due to small-angle scattering of wave fields, Izv. VUZ Radiofiz. **28**(5), 535–565.

YANG, C. C., and K. C. YEH, 1985, The behavior of the backscattered power from an intensely turbulent ionosphere, Rad. Sci. **20**(3), 319–324.

YEH, K. C., 1983, Mutual coherence functions: intensities of backscattered signals in a turbulent medium, Rad. Sci. **18**(2), 159–165.

ZAVOROTNYI, V. U., 1984, Backscattering of waves from two-scale rough surface: account of reillumination, Izv. VUZ Radiofiz. **27**(2), 196–202.

ZAVOROTNYI, V. U., and V. E. OSTASHEV, 1982, On the enhanced backscattering of waves from rough surfaces, Izv. VUZ Radiofiz. **25**(11), 1291–1295.

ZAVOROTNYI, V. U., and V. I. TATARSKII, 1982, Backscattering enhancement of waves by a body near a random interface, Dokl. Akad. Nauk SSSR **265**(3), 608–612.

ZAVOROTNYI, V. U., V. I. KLYATSKIN and V. I. TATARSKII, 1977, Strong fluctuations of electromagnetic intensity in randomly inhomogeneous media, Zh. Eksp. & Teor. Fiz. **73**(2), 481–497.

ZUEV, V. E., V. A. BANAKH and V. V. POKASOV, 1988, Optika turbulentnoi atmosfery (Optics of a turbulent atmosphere) (Gidromet, Leningrad).